Concawe

Environmental Science for European Refining

Report

Report no. 10/23

The impact of aviation emissions to urban air quality in Europe - Detailed airport-city analysis

ISBN 978-2-87567-177-6

9 782875 671776

The impact of aviation emissions to urban air quality in Europe - Detailed airport-city analysis

G. Valastro (Concawe Science Executive)

This report was prepared by: J.P. Tokaya, J.S. Hullegie, R. Kranenburg, R. M. A. Timmermans, and P.W.H.G. Coenen

Under the supervision of: T. Megaritis (Concawe Science Associate)

At the request of:

Concawe Air Quality Management Group (AQMG)

Thanks for their contribution to:

Members of AQMG: N. Novachev, D. Steinert, S. Van Gulck

EXECUTIVE SUMMARY

Aviation causes emissions of NO_x, SO_2 and PM that have a negative impact on air quality. To investigate the extent of this impact, simulations with the chemical transport model (CTM) LOTOS-EUROS (LE) have been performed to model the atmospheric concentrations of NO_2, SO_2, PM_{10} and $PM_{2.5}$ in 2018. The concentrations of these pollutants were simulated for six cities in Europe (London, Paris, Amsterdam, Frankfurt am Main, Munich and Brussels) with large airports (Heathrow, Charles de Gaulle, Schiphol, Frankfurt am Main, Munich and Zaventem).

For LE, and CTMs in general, the quality of the input data could determine to a large extent how well modelled atmospheric pollutant concentrations reflect reality. Arguably the most important of these inputs is the emission dataset, that describes how quantities of pollutants emissions are temporally and spatially represented in the model. An initial exploration into the most suitable emission dataset led to the conclusion that the GrETA (Gridding Emission Tool for ArcGIS) and ER (Emission Registration) datasets were most equipped for 1x1 km resolution simulations so should be used whenever available (i.e., Amsterdam, Frankfurt am Main and Munich). Alternatively, when this set is not available, a CAMS-REG v5.1 1x1 km dataset could be used (London, Paris and Brussels).

The results from the simulations with the selected emission datasets show:

- An average contribution from aviation to the annual NO_2 concentration in the respective city centres of 2.5%.
- For SO_2, $PM_{2.5}$, and PM_{10} the relative contributions are respectively 1.8%, 0.5% and 0.3%.
- At the airports locations, the average relative contributions from aviation to the concentration of NO_2, SO_2, $PM_{2.5}$, and PM_{10} over the six airport that were simulated are respectively 38%, 45%, 6.0% and 4.5%.

Next to NO_2, also SO_2 receives a high relative contribution from aviation, but in absolute values the total SO_2 concentrations attributed to aviation are much lower (between 6.1 $\mu g/m^3$ and 2.0 $\mu g/m^3$) and of less concern than the respective NO_2 concentrations (between 25 $\mu g/m^3$ and 30 $\mu g/m^3$). For relatively long-lived PM, the relative contribution from aviation is lower. Hence throughout this report NO_2 will get most attention.

Most cities have a large number of inhabitants that live in the area between the airport and the city centre and hence are exposed to NO_2 concentrations with a contribution from aviation that lies between the average city centre contribution of 2.5% and the average contribution at the airport of 40%. London is the largest city with nearly 10 million inhabitants in the city centre and it was found that:

- At Heathrow (LHR) airport the NO_2 concentrations are significantly elevated with a contribution of 55% (17 $\mu g/m^3$) from aviation.
- In the city centre of London the contribution is diminished to 1.6% (0.44 $\mu g/m^3$).
- In addition, the densely populated regions between city centre and airport exposures will vary in this range.
- It was also found that the relative contribution of aviation drops off at a rate of 50% per 2.6 km distance from the airport.

Paris is the second largest city with 7.8 million inhabitants in the urban area, followed by Munich with 2.5 million residents. These cities as well as the smaller

cities (Frankfurt am Main (2.3 million), Amsterdam (1.5 million) and Brussels (1.3 million)) show a similar trend of decreasing concentrations from airport to city centre in a comparable range.

INTERNET

This report is available as an Adobe pdf file on the Concawe website (www.concawe.eu).

CONTENTS

Page

LIST OF ACRONYMS AND DEFINITIONS

ACRONYM	EXPLANATION
CAMS	Copernicus Atmosphere Monitoring Service
CAMS-REG	Copernicus Atmosphere Monitoring Service REGional emissions
CDS	Climate Data Store
CTM	Chemical Transport Model
LES	Large-Eddy Simulation
DEPAC	DEPosition of Acidifying Compounds
EEA	European Environment Agency
ECMWF	European Centre for Medium-range Weather Forecasts
EIONET	European Environment Information and Observation NETwork
ER	Emission Registration
ERA 5	ECMWF ReAnalysis (generation 5)
GRETA	Gridding Emission Tool for ArcGIS
GNFR	Gridding Nomenclature for Reporting
HR	High Resolution
LE	LOTOS-EUROS
LES	Large Eddy Simulation
LOTOS-EUROS	Long Term Ozone Simulation - EURopean Operational Smog model
LTO	Landing and Take-Off cycle (aircraft operation modes below 3000 feet of height)
NO	Nitric Oxide
NO_2	Nitrogen dioxide
NO_X	The nitrogen oxides, the combination of nitric oxide and nitrogen dioxide
NRMSE	Normalised Root Mean Square Error
PM	Particulate Matter
PM2.5	Particulate Matter with a diameter smaller than 2.5 micron
PM10	Particulate Matter with a diameter smaller than 10 micron
SA	Source Apportionment
SNAP	Selected Nomenclature for sources of Air Pollution
SO2	Sulphur dioxide
STEAM	Ship Traffic Emission Assessment Model
TNO	Toegepast-Natuurwetenschappelijk Onderzoek (Dutch organisation for applied scientific research)

Throughout this document technical terminology is used that we define in the table below for clarity.

DEFINITIONS	EXPLANATION
ATMOSPHERIC COMPONENT	A chemical constituent in the atmosphere. Not all of these constituents are modelled.
TRACER	Model equivalent to a chemical component present in the atmosphere, i.e., a modelled atmospheric component.
POLLUTANT	Atmospheric component with known harmful effects to human health and/or the environment, e.g., PM and NO_2.
ATMOSPHERIC CONCENTRATION	The concentration of an atmospheric component in mass per volume, often measured in $\mu g/m^3$.
ATMOSPHERIC SURFACE CONCENTRATION	The atmospheric concentration at 2.5 meter above ground level/earth surface.

1. INTRODUCTION

Fuels burnt by combustion engines of aircrafts result in emissions of NO_x, SO_2 and particulate matter (PM) that have a negative impact on air quality and thus harm human health and ecosystems. This work aims to provide insights and enhance Concawe's understanding on the influence of aircraft emissions on the ambient air quality in cities with or near major airports. For this purpose, the chemical transport model LOTOS-EUROS is used to assess the contribution of aviation emissions on the concentrations of major pollutants (NO_2, SO_2, $PM_{2.5}$, PM_{10}) in such cities.

1.1. AIM

The main focus of this work is to address the research question:

"How is the air quality influenced by aviation emissions over Europe and specifically in cities with large airports in comparison to other sectors?".

1.2. BACKGROUND

It is well known that elevated concentrations of atmospheric pollutants can lead to adverse effects on both human health and ecosystems. Epidemiological studies have shown that the exposure to pollutants such as fine particulate matter ($PM_{2.5}$) and nitrogen dioxide (NO_2) is associated with cardiovascular and respiratory diseases, leading to increased sickness, hospital admissions and premature death (Beelen et al., 2014). Moreover, nitrogen deposition in soils and water bodies leads to eutrophication and biodiversity loss, algae blooms and overall ecosystem damage; and sulphur dioxide is a gas that together with other sulphur oxides can contribute to acidification which can harm sensitive ecosystems.

NO_x (NO_x = NO + NO_2) is formed in the combustion process due to the high temperatures and the naturally abundant nitrogen in the atmosphere. PM emissions primarily result from carryover of non-combustible trace constituents in fuels or formation from condensable gases released during the combustion process.

Over the past decades, legislation has been introduced to reduce emissions of these harmful pollutants. The efforts to reduce emissions in several sectors have resulted in a decrease in the atmospheric concentrations of $PM_{2.5}$, PM_{10}, NO_2 and SO_2. The most recognized example of successful emission reduction is the one of SO_2. Due to abatement measures in powerplants and desulphurization of fuels the atmospheric SO_2 concentration in the European Union countries declined by around 70% between 2000 and 2017 (Colette & Rouïl, 2020) based on aggregated observations.

On average, in Europe the aviation sector is not considered a large contributor in emissions of the studied air pollutants. However, the sector has seen an increase in emissions compared to most other sectors (Kuenen et al., 2021). In particular, between 2000 and 2018, NO_x aviation emissions (GNFR sector H) showed an increase from 61 kton to 86 kton (41%) (**Figure 1**), while for most of the other sectors the emissions in general decreased. The relative contribution of the aviation sector to the total emissions is low for the whole of Europe. However, locally in cities with major nearby airports, the effect of emissions from the aviation sector on the ambient air quality is expected to be higher due to the proximity to the airports.

Emissions are not the only factor that can influence the atmospheric pollutant concentrations. Meteorological conditions, like precipitation, solar radiation, wind speed, temperature and relative humidity play an important role in atmospheric processes. Especially the height of the boundary layer, that can vary between 100 m and 2 km and in which atmospheric mixing and hence dilution of pollutants is strong, has a large effect on surface concentrations. This is a well-known phenomenon that holds for all pollutants. There is always a strong correlation between boundary layer height and concentration.

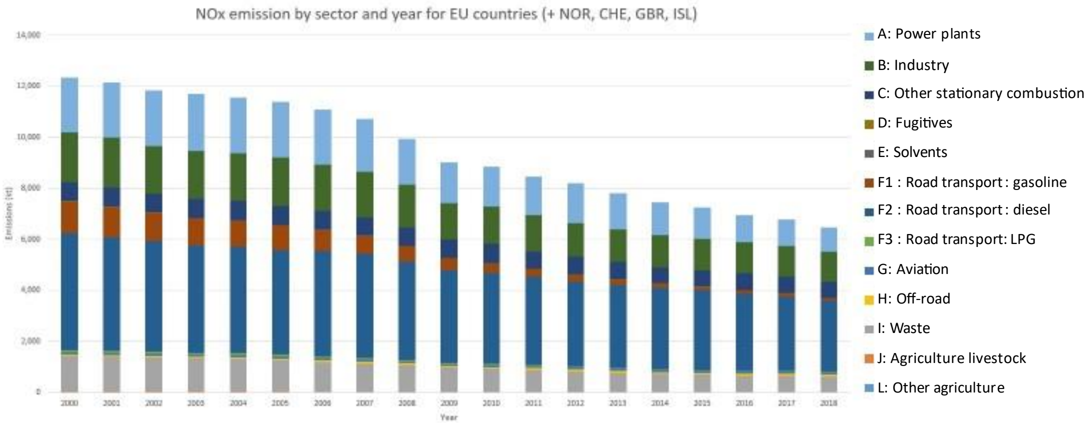

Figure 1 Total NO_x emissions (in kton) for all countries in Europe for the different GNFR sectors (A-L) (2000-2018) (Figure based on Kuenen et al., 2021)

1.3. APPROACH

In this study, insight is gained in the contribution of aviation emissions to the air quality in European cities with major airports using the chemical transport model (CTM) LOTOS-EUROS. This model computes air quality by taking into account emissions of pollutants, transport and chemistry in the atmosphere using meteorological data, land use and orographic information.

Besides the total pollutant concentrations in the atmosphere, it is relevant to assess the relative contributions from the various source sectors that cause them. Source Apportionment (SA) is applied both in the modelling and monitoring of air pollution. Various techniques exist to specify the sources that may cause the air pollution of interest. These techniques make it possible to estimate how much of an atmospheric concentration originated from a specific source (e.g., traffic, industry, etc.).

In modelling air quality with CTMs, two main approaches for source apportionment exist. A brute force approach that incrementally reduces the emissions from various source sectors that are fed as an input to the model. By extrapolating the effect on the resulting atmospheric concentrations of a certain percentage emission reduction to 0%, it is possible to derive contributions from these sectors to the concentration in a region or at a location of interest. The second method, which is used in this project, is the labelling approach. In this approach, chemical tracers receive a label based on the emission source that caused them. These labelled chemical pollutants are traced throughout the model to be able to monitor what sectors contributed to the surface concentration of that component at a region or location of interest.

The brute force approach is particularly useful to investigate the effects of emission reduction scenarios, taking into account non-linearities in modelled chemical and physical processes that make it hard to directly translate an emission reduction of a pollutant into an atmospheric concentration reduction. The brute force approach comes at the expense of more computational and memory costs in comparison to the labelling approach, because it requires the performance and storage of a large set simulations where each member of the set contains a particular reduction scenario. For every additional label the set needs to be extended with simulations of reduction scenarios for that particular label.

On the contrary, the labelling approach is less appropriate for scenario evaluations because non-linearities in the translation from emissions towards atmospheric concentrations can cause emission and concentration partitioning in various sectors to change in unanticipated ways. The labelling approach uses a single simulation, also taking into account non-linearities, and gives more accurate insight in a situation under consideration as the chemical regime remains unchanged, i.e. no changes in atmospheric concentrations are required to discern contributions from the various sectors. Since this study has a particular interest in accurately describing the current contribution from aviation emissions to the air quality in cities, the labelling methodology is considered most suitable.

1.4. OUTLINE

The methodology used in the study is described in chapter 2. This chapter provides details on the model that is used and what data is taken as input to the model to perform the simulations of the atmospheric concentrations.

Chapter 3 presents the results of the study. The CTM provides labelled atmospheric concentrations over the simulation domain. Using the simulation results, the contributions of various sectors to the air quality in cities of interest are computed.

Further discussions, implications and challenges are described in chapter 4 of the report and in chapter 5, the conclusions and recommendations from this study are given.

2. METHODS

In this chapter a detailed description of the modelling approach is given. Firstly, the used CTM and its capabilities are introduced. Secondly, focus is given on project specific simulation settings and data usage. Lastly, the strategy of evaluating model results is described.

2.1. MODEL DESCRIPTION

LOTOS-EUROS is a 3D chemistry transport model. The off-line Eulerian grid model simulates air pollution concentrations in the lower troposphere by solving the advection-diffusion equation on a regular latitude-longitude grid with variable resolution over Europe (Manders et al., 2017; Schaap et al., 2008).

The vertical transport and diffusion scheme accounts for atmospheric density variations in space and time and for all vertical flux components. The vertical grid is based on terrain following vertical coordinates and when excluding stacked boundary layer on top extends to 5 km above sea level. The model uses a multilayer approach to determine the vertical structure where the vertical layers vary in space and time. The height of the layers on top of the 25 m surface layer is determined by heights in the meteorological input data.

In the model version used in this study, 12 model layers are simulated (with 7 stacked top layers above the upper model layer), leading to a resolvent of the first km of the atmosphere in 7 layers (depending on meteorological conditions). The horizontal advection of pollutants is calculated applying a monotonic advection scheme developed by Walcek & Aleksic (1998) For the simulations at a high resolution (1x1 km), a linear advection scheme was used. Gas-phase chemistry is simulated using the TNO CBM-IV scheme, which is a condensed version of the original scheme (Whitten, 1980). Hydrolysis of N_2O_5 is explicitly described following Schaap et al. (2004). LOTOS-EUROS explicitly accounts for cloud chemistry, computing sulphate formation as a function of cloud liquid water content and cloud droplet pH as described in Banzhaf et al. (2012). For aerosol chemistry, the thermodynamic equilibrium module ISORROPIA2 is used (Fountoukis & Nenes, 2007). Dry Deposition fluxes are calculated using the resistance approach as implemented in the DEPAC (DEPosition of Acidifying Compounds) module (Zanten et al., 2010). Furthermore, a compensation point approach for ammonia is included in the dry deposition module (Wichink Kruit et al., 2012). The wet deposition module accounts for droplet saturation following Banzhaf et al. (2013).

In LOTOS-EUROS, the temporal variation of the emissions is represented by monthly, daily and hourly time factors that distribute the annual emission totals in time for each source category. This is also the case for aviation emissions which reflects daily peaks, and weekday vs weekend activity based on flight statistics. The biogenic emission routine is based on detailed information on tree species over Europe (Köble & Seufert, 2001). The emission algorithm is described in Schaap et al. (2009) and is very similar to the simultaneously developed routine by Steinbrecher et al. (2009). Sea salt emissions are described using Mårtensson et al. (2003) for the fine mode and Monahan et al. (1986) for the coarse mode. Dust emissions from agricultural activities and resuspension of particles from traffic are included following Schaap et al. (2009).

The model is part of the Copernicus Atmospheric Monitoring Service (CAMS) regional ensemble providing operational forecasts and analyses over Europe. In this context the model is regularly updated and validated using ground-level and satellite observations. The model performance is also subject to numerous peer-reviewed publications (e.g., 2015; Escudero et al., 2019; Schaap et al., 2015; Skoulidou et al., 2021; Timmermans et al., 2022). For an overview the reader is referred to the model's website: www.lotos-euros.nl.

2.2. SOURCE APPORTIONMENT

The Dutch organisation for Toegepast-Natuurwetenschappelijk Onderzoek (Applied Scientific Research), TNO, has developed a system to track the impact of emission categories within a LOTOS-EUROS simulation (source apportionment) based on a labelling technique (Kranenburg et al., 2013). This technique provides more accurate information about the source contributions than using a brute force approach with scenario runs as the chemical regime remains unchanged. Another important advantage is the reduction of computational costs with respect to the brute force approach. The source apportionment technique based on the labelling approach has been previously used to investigate the origin of particulate matter (episodes) (Pommier, 2021; Timmermans et al., 2017, 2022), nitrogen dioxide and nitrogen deposition (Curier et al., 2014; Thürkow et al., 2023).

Besides the total pollutants' concentrations, the contributions of selected sources to these concentrations are calculated. The labelling routine is implemented for primary, inert aerosol tracers as well as for chemically active tracers containing a C, N (reduced and oxidized) or S atom, as these are conserved and traceable.

The source apportionment module for LOTOS-EUROS provides a source attribution valid for current atmospheric conditions as all chemical conversions occur under the same oxidant levels. For details and validation of this source apportionment module, the reader is referred to Kranenburg et al. (2013).

The module is currently being further developed to also include source apportionment of ozone and methane.

2.3. MODEL SETUP

2.3.1. Meteorology

The LOTOS-EUROS model is run with ECMWF ERA 5 reanalysis meteorological data (2018). ERA5 provides hourly estimates of a large number of atmospheric, land and oceanic climate variables, that are necessary inputs for calculations of atmospheric concentrations. The ERA 5 data cover the Earth on a 30x30 km grid and resolve the atmosphere using 137 levels from the earth surface up to a height of 80 km. Typical inputs required by LOTOS-EUROS are for example surface and air temperature, cloud cover, windspeed and direction, precipitation and relative humidity.

Quality-assured monthly updates of ERA5 (1959 to present) are published within 3 months of real time and available through the Climate Data Store (CDS). Preliminary daily updates of the dataset are available to users within 5 days of real time.

2.3.2. Emissions

For anthropogenic trace gas emissions, the CAMS-REG inventory emission data for the year 2018 version 5.1 REF2 (Kuenen et al. 2019) is used. This is the latest available data set; an update with more recent years is expected to be published in 2023. This emission dataset stays as close as possible to the emissions as officially reported and used in policy assessment. The inventory uses the officially reported emission data by European countries (national inventories). The aviation emissions in the national inventories only include the total national emissions during the landing and take-off cycle (LTO). The LTO covers four modes of engine operation, namely idle, approach, climb out and take-off, each of which is associated with a specific engine thrust setting and a time in mode.

The emissions during cruise flights (above 3,000 feet) are not reported in the national inventories. The national aviation emissions (LTO's) in a country are distributed over the contributing airports in that country based on flight statistics per airport on an annual basis (Eurostat, 2019). All emissions from an airport are represented as a point-source at the location of the airport in the CAMS-REG inventory.

In this study, simulations are performed at a 1x1 km resolution to capture the local effects and spatial extent aviation emissions at an airport have on the air quality in its vicinity. Because the CAMS-REG inventory has a 6x6 km resolution, it is not well equipped for the usage in 1x1 km resolution simulations. For this purpose, a 1x1 km regridded dataset was used that contains CAMS-REG emissions for NO_x at a 1x1 km resolution. The regridding is done based on high-resolution proxy data, like road and rail networks and land use maps while keeping the annual total emissions per sector unchanged. For SO_2 and PM, this level of detail is not available from the CAMS-REG inventory. However, for the Netherlands and Germany, emissions for all pollutants of interest are available at this resolution from other national data sets, namely the Emission Registration (ER) in the Netherlands and GrETA (Gridding Emission Tool for ArcGIS) in Germany (Schneider et al., 2016). An overview of the emission datasets that were used in the various simulation domains (as shown in **Figure 2**, section 2.4) is given in **Table 1**.

Table 1 Overview of the emission datasets used in the various simulation domains

	Spatial Coverage	Remark
CAMS-REG v5.1 6x6	All locations	**Coarser resolution** than the resolution for the performed simulation which results in unnatural patches in the concentration fields.
CAMS-REG v5.1 1x1	All locations	Contains data for NO_x, NH_3, NMVOC. **No data for PM and SO_2.**
ER and GrETA datasets 1x1	Only for locations in NL and GE	More detailed representation of airports with runways rather than point sources.

It should be noted that even in the 1x1 km resolution dataset, the actual flight patterns, as registered at the airports (with exact location in 3 dimensions), are not fully represented. The annual emissions from all LTO cycles are projected in the 1x1 km grid aggregating any additional spatial information on individual flights to the model grid.

2.4. SIMULATION DESCRIPTION

Figure 2 shows the different domains which are part of the LOTOS-EUROS simulations. In the middle of the figure, a coarse resolution (circa 25x25 km) simulation performed over Europe (domain edge in purple) is shown. Results from this simulation are used as boundary condition for the nested simulation over Northwest Europe (domain in green) at a higher resolution (circa 6x6 km). As a next step, simulations are performed for the cities that are part of this study at higher resolution (circa 1x1 km). The chosen cities and domains are shown with orange dots in the centre figure. On the outsides of the figure, the domains of the 1x1 km high-resolution zoom runs are shown in more detail.

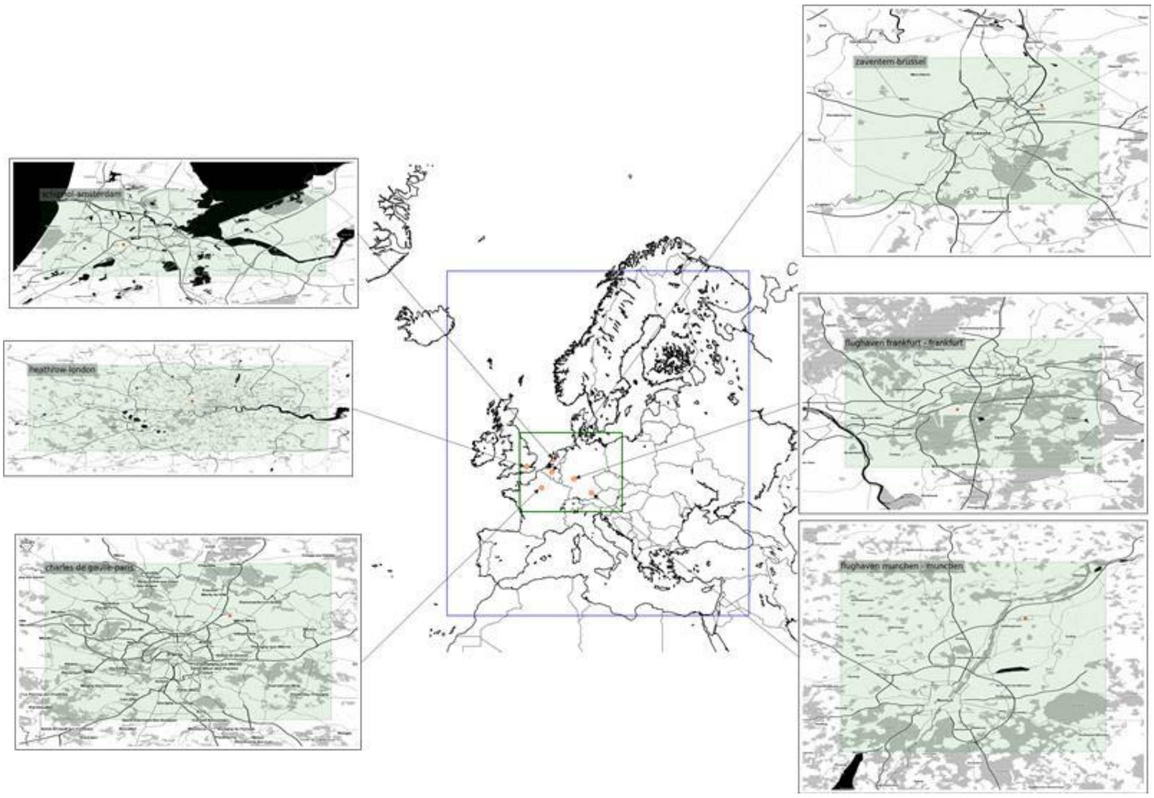

Figure 2 Display of the simulation setup domains

2.4.1. Domains and resolution

A simulation across Europe (15°W, 40°E, 31°N, 69°N) at a resolution of 0.4° longitude × 0.2° latitude (approximately 25×25 km) was performed, the results of which were used as boundary conditions for simulations at a resolution of 0.1° longitude × 0.05° latitude (approximately 6×6 km) over Northern Europe, including Germany, the Benelux and the North Sea (1.5°W, 17.5°E, 46°N, 50°N). The following major cities are studied in the high-resolution zoom runs:

1. London (UK)
2. Paris (FR)
3. Amsterdam (NL)
4. Frankfurt am Main (GE)
5. Munich (GE)
6. Brussels (BE)

These runs are performed at a 1/60° longitude × 1/120° latitude (approximately 1×1 km) resolution in small domains (depicted in green in **Figure 2**) that are nested in the Northern European simulation and use pollutant concentrations from this 6×6 km simulations as a boundary.

2.4.2. Included labels

The simulations were performed for the year 2018, since this is the most recent year for which the used emission dataset is available. Labels were applied to distinguish emissions sources from different sectors. The complete set of labels (20) used in this study is as follows:

1. Aviation
2. International shipping (all sea-going shipping)[1]
3. Inland shipping (all river-going shipping)[1]
4. Public Power /Energy
5. Residential combustion
6. Industry
    a. Solvent use[a]
    b. Fuel Production
    c. Refineries[b]
    d. Other Industry
7. Mobile machinery[c]
8. Road transport exhaust
9. Road transport non-exhaust (only contributes to PM)
10. Waste management
11. Agriculture
    a. Livestock
    b. Manure management
12. Biogenic[2]
13. Wildfires (GFAS -daily (Kaiser et al., 2012))
14. Sea salt (only contributes to PM)
15. Saharan dust (only contributes to PM)
16. Boundary[3]

[a]Even though “Solvent use” is considered a subcategory of industry here domestic solvent use is included. This is however a relatively small contribution.

[b]Oil, gas and petroleum refining is in incorporated in this label. The label “Fuel Production” contains emissions that occur during the production, distribution, exploration, venting, flaring in gas, oil and coal handling.

[c]”Mobile machinery” contains emissions from railways, small agricultural, forestry and fishing equipment, compressors, gardening, off road vehicle usage etc.

These emission sources vary strongly in their influence on surface concentrations of $PM_{2.5}$, PM_{10}, NO_2 and SO_2. In the analysis throughout this report, only significantly

[1] A detailed analysis of the contribution from shipping can be found at Concawe (2023), Report no. 2/23: “The impact of shipping emissions to urban air quality in Europe – Detailed port-city analysis”

[2] Biogenic emissions include isoprene and monoterpene from vegetation and soil NOx emissions.

[3] The label “Boundary” is used to describe contributions from the CAMS global simulation results that are used as a boundary condition to the simulation over the European domain

contributing sectors (>2%) are reported in graphs and tables for conciseness, with the exception of sectors of special interest (aviation) that are always reported if they contribute. All less contributing sectors are aggregated and labelled as “other”.

2.5. EVALUATION OF MODELLED CONCENTRATIONS

The modelled atmospheric surface concentrations of pollutants $PM_{2.5}$, PM_{10}, NO_2 and SO_2 have been compared to measured concentrations from validated stationary air quality stations near or in cities. The results for NO_2 are discussed in the main text and for the other air pollutants SO_2, $PM_{2.5}$, and PM_{10} we refer to the **Appendix**. The measurements used for verification are collected from the (CAMS Copernicus Atmospheric Monitoring Service) dataset of surface observations from the EEA/EIONET NRT database. This dataset of the European Environment Information and Observation Network (EIONET) is produced by a collaboration of the European Environment Agency (EEA) and its 38 member and cooperating countries. It contains validated surface observations for a large number of chemical tracers and pollutants, including NO_2, SO_2, $PM_{2.5}$ and PM_{10}.

3. RESULTS

Simulations with the chemical transport model LOTOS-EUROS have been performed to study the effect of aviation on air quality for the year 2018 by modelling the atmospheric concentrations of NO_2, SO_2, PM_{10} and $PM_{2.5}$. This chapter presents the results of these calculations. Firstly, the emissions of aviation compared to the emissions from other sectors will be displayed. Secondly, the results of the (Northwest) European runs are presented. Finally, we zoom in on the cities and present comparisons of the results with nearby measurements.

3.1. COMPARISON OF THE DIFFERENT EMISSION DATASETS

As discussed in **section 2.3.2**, multiple emission datasets are available and a selection has been made for the most appropriate option for each investigated city. These choices are summarized in **Table 1**. To draw this conclusion, an exploratory study into the various emission datasets has been performed for the city of Amsterdam. In total 6 simulations were performed for Amsterdam to investigate the influence of the used emission dataset. All three emission datasets (CAMS-REG v5.1 6x6, CAMS-REG v5.1 1x1 and ER datasets 1x1) are available for Amsterdam and were used as input for LOTOS-EUROS for a simulation of the pollutant concentrations in January and July 2018.

3.1.1. CAMS-REG v5.1 6x6

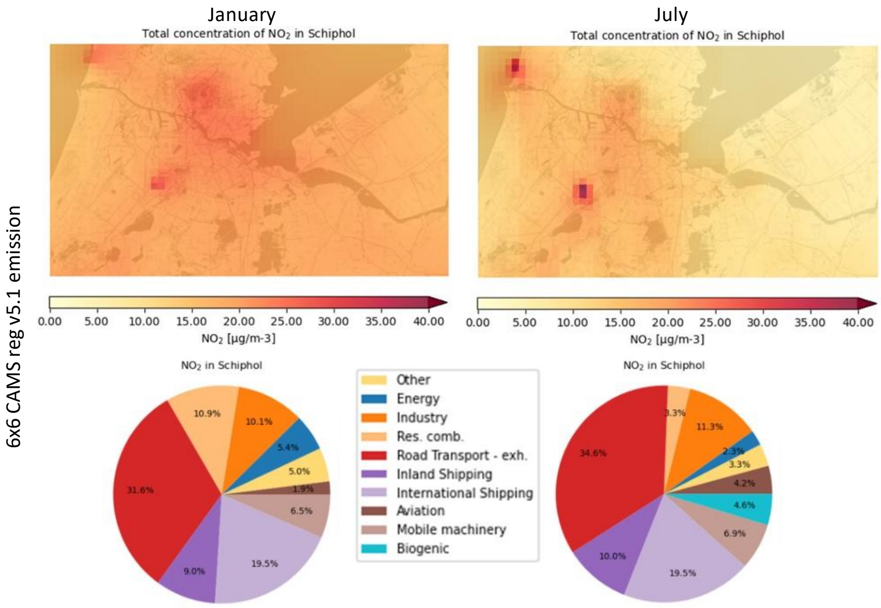

Figure 3 Total NO_2 concentrations around Amsterdam for January and July 2018 (top) and the attribution of this concentration to the different sources for the entire domain (bottom) using CAMS-REG v5.1 6x6 as emission dataset

The CAMS-REG v5.1 6x6 emission dataset contains the emissions at a ~6x6 km resolution. It is still technically possible to perform a higher resolution simulation (e.g., 1x1 km) with this dataset. The emissions will simply be up-sampled to artificially create the higher resolution (6x6 = 36 grid cells will receive the same contribution from surface sources) and higher resolution data will be used for other inputs (e.g., land use and meteorological data). In the CAMS-REG v5.1 6x6 dataset, some emissions sources (e.g., airports) are represented as point sources with a specific longitude and latitude. These sources are not gridded and are represented at their exact location. Therefore, any differences in resolution in the emission datasets will not change their representation as it will only influence surface sources (e.g., road transport) which are modelled at a ~6x6 km resolution as shown in **Figure 3**. All other inputs (meteorology, land-use, orography, etc.) and the chemical and physical processes are modelled at higher resolution. The coarse (6x6 km) resolution results in unrealistic/unphysical patches in the modelled concentration field, due to the aforementioned artificial up-sampling. This is most evidently visible in the average simulated concentration for July (top right in **Figure 3**). Here the up-sampling of the used emissions is visible in the final concentration field, because each patch of 36 cells in the 1x1 km simulation will receive for example the equal traffic emissions which causes this effect to appear.

3.1.2. CAMS-REG v5.1 1x1

The CAMS-REG v5.1 1x1 emission dataset contains the same total emissions as the CAMS-REG v5.1 6x6 emission dataset, but at a higher resolution for NOx emissions. This means that the annual totals are the same but the spatial distribution differs. Simulation results at 1x1 km resolution using the former emission set as input are shown in **Figure 4**. It is evident that the concentration fields show a more natural spatial distribution compared to **Figure 3**.

For $PM_{2.5}$, PM_{10} and SO_2 emissions the 1x1 km resolution is not available and the exact same emission data input is used as for the 6x6 set, because only 1x1 km resolution emissions for NO_x, NH_3, NMVOC are available in the dataset. The emissions for $PM_{2.5}$, PM_{10} and SO_2 will hence be artificially up-sampled. The extent of the CAMS-REG v5.1 1x1 dataset covers the six cities that are investigated in this study.

The most important downside of using this emission dataset is the fact that 1x1 km resolution emissions are not available for all pollutants. For $PM_{2.5}$, PM_{10} and SO_2 similar patchy concentration fields as shown in **Figure 3** will emerge.

In the CAMS-REG data set the shipping emission estimates are derived with STEAM (Ship Traffic Emission Assessment Model, which is independent of the national inventories) and there is only a geographic distinction between ships at sea and ships on inland waterways. The split between these categories is made based on the layout of the seaports and or the location where the river flows into the sea. Therefore, the emissions from sea going ships sailing to an inland port are (partly) accounted for in the inland shipping emissions in the CAMS-REG dataset. For more details on shipping emissions and their influence on local air quality, the reader is referred to Concawe report no 2/23 (2023).

Because the distinction between inland and international shipping is absent in the CAMS-REG v5.1 1x1 km emission dataset, comparing the attribution results in **Figure 4** with **Figure 3** one should only compare the total shipping contributions (respectively 29.3% and 38.8% for January and July for the 1x1 km simulation and 28.7% vs 29.3% for the 6x6 km simulation). The residual concentrations attributed to inland shipping in **Figure 4** results from influx through the boundaries of the simulation, because the used emission dataset does not contain this sector.

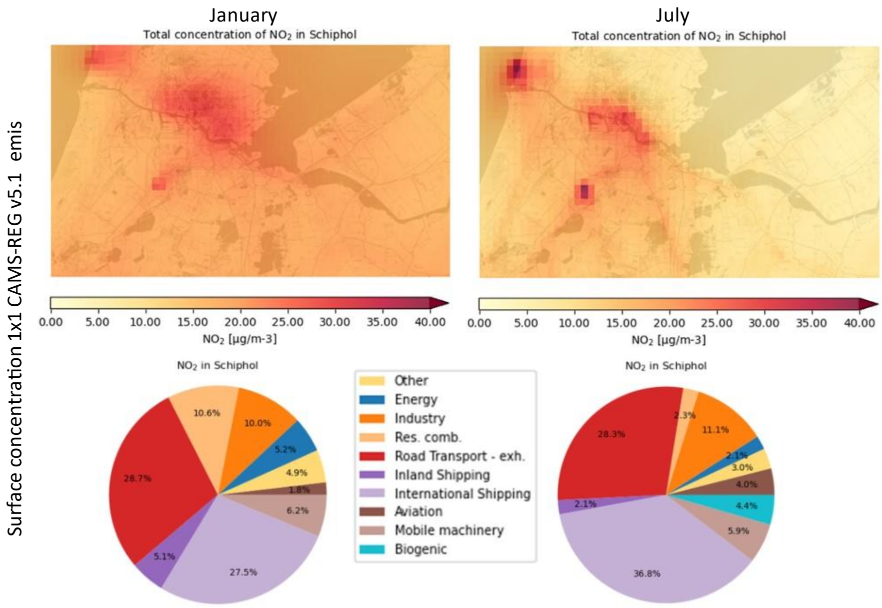

Figure 4 Total NO_2 concentrations around Amsterdam for January and July 2018 (top) and the attribution of this concentration to the different sources for the entire domain (bottom) using CAMS-REG v5.1 1x1 as emission dataset

3.1.3. GrETA and ER datasets 1x1

GrETA and ER datasets contain emissions at a 1x1 km resolution for all relevant pollutants. These datasets are dedicated emission datasets for specific countries and hence the GrETA dataset is only available over Germany and the ER dataset is only available over the Netherlands. In these sets, airports are no longer represented as point sources but the exact geometry of the runways of the given airports are taken into account. This shifts the representation of the airport from a point source to a surface source.

Results from simulations performed with the GrETA and ER dataset have been conducted for Germany and The Netherlands respectively. Since Amsterdam has been chosen as case study in this explanatory analysis, the results using the ER data (available over the Netherlands) are shown in **Figure 5**. Similar concentration patterns as found in the simulations with the other two emission datasets are clearly visible, but so is the fact that Schiphol is represented as a surface rather than a point source. In the ER dataset the actual topology of the airport is incorporated, taking into account where runways are located. Schiphol has multiple runways (six) with a total length of 19 km. The airport's total surface area is 28 km2. The surface representation in the ER emission dataset hence gives a more physically truthful description of where emissions take place than the point source representation in the CAMS-REG datasets. This becomes particularly important when simulations are performed at a high resolution (1x1 km).

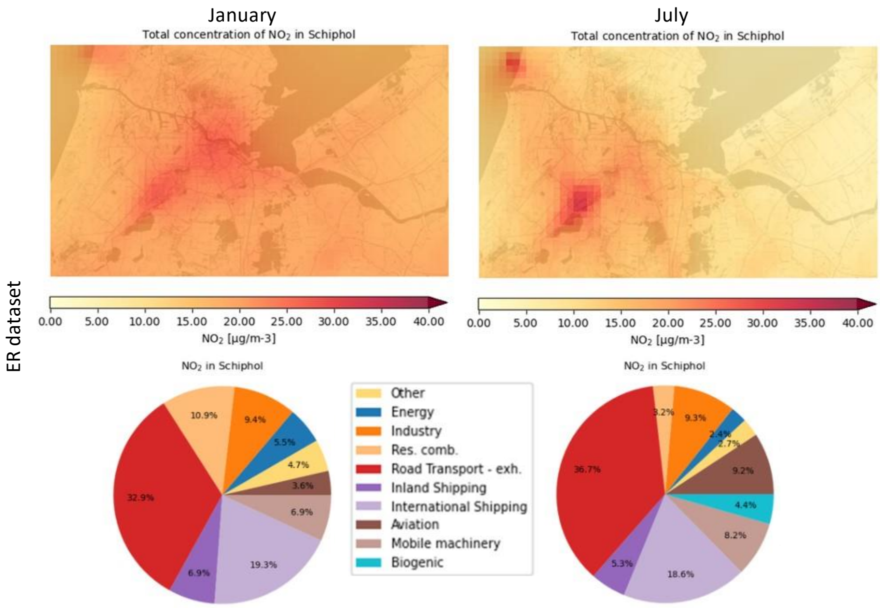

Figure 5 Total NO_2 concentrations around Amsterdam for January and July 2018 (top) and the attribution of this concentration to the different sources for the entire domain (bottom) using the ER emission dataset

The conclusion was drawn to use emissions at the highest available resolution for as many of the relevant pollutants as possible to avoid unrealistic patches in the simulated concentrations. Hence, for the Netherlands and Germany, ER and GrETA emissions are used since for all pollutants of interest high-resolution data is available. Unfortunately, this set does not cover Paris, London and Brussels. For these domains, the CAMS-REG v5.1 1x1 set was used.

3.2. EMISSIONS IN THE DOMAINS OF THE DIFFERENT AIRPORTS

In **Table 2**, the relative sectoral contributions to the total NO_x emissions as disaggregated from reported emission totals and used in the simulations for the different cities are presented. Note that emissions are provided for NO_x and in LE these are distributed into a fraction NO and NO_2. On average over the examined domains, aviation contributes 8% to the total NO_x emissions with the airports in Paris and Brussels having the largest contribution.

Table 2 The relative contributions (%) of the various sectors to the total NOx emissions in the HR simulation domains for six cities of interest. ‡Simulations performed with GrETA and ER datasets. *Simulations performed with the CAMS-REG v5.1 dataset

	London*	Paris*	Amsterdam‡	Frankfurt am Main‡	Munich‡	Brussels*	average
Total	100.0	100.0	100.0	100.0	100.0	100.0	100.0
Public Power/Energy	6.3	9.0	5.3	3.1	2.7	4.1	5.1
Refineries	0.0	0.0	0.0	0.2	0.2	0.0	0.1
Industry	7.8	4.4	11.0	3.7	1.4	5.0	5.5
Res. comb.	16.3	21.8	2.2	2.5	3.2	15.1	10.2
Fuel prod.	0.0	0.0	0.0	0.0	0.0	0.0	0.0
Solvent use	0.1	0.3	0.1	0.0	0.0	0.1	0.1
Road Transport - exhaust	46.1	44.1	65.8	82.0	87.0	57.0	63.7
Inland Shipping	0.0	0.0	1.8	0.0	0.0	0.0	0.3
International Shipping	3.3	2.2	5.4	0.3	0.0	1.7	2.1
Aviation	7.6	13.2	5.1	7.2	3.2	11.7	8.0
Mobile machinery	12.3	4.2	2.4	0.9	1.3	4.7	4.3
Waste	0.2	0.9	0.0	0.0	0.0	0.6	0.3
Manure and storage	0.0	0.0	0.0	0.1	0.8	0.0	0.1
Wildfire	0.0	0.0	0.6	0.0	0.0	0.0	0.1

The table shows that the aviation (LTO) emissions are relatively low compared to the other emission sources in the calculation domains. This is partly due to fact that the emissions during LTO (emission up to 3,000 ft) only occur during a short period for every landing or take-off. The majority of the aircraft emissions occur during the rest of the fight (cruise phase) which take place at higher altitudes and locations at a larger distance from the airport. However, the cruise emissions are not available in the national emission data sets and thus they are not included in the emission data used in this study. One of the reasons that explain this is that the cruise emissions cannot be unambiguous allocated to the countries over which every individual plane flies. For instance, how can the cruise emissions over international waters (like the Pacific or Atlantic ocean) be attributed to any country?

The cruise emissions however do not affect the air pollutant concentrations at ground level near the airports as the cruise emissions occur mainly above the mixing layer and thus the exchange to the lower parts of the atmosphere is very slow and occurs only over long distances. Thus, the concentration of an air pollutant at ground level is predominantly governed by the emissions in the mixing layer.

One other aspect to mention is the fact that the emissions in this study are projected in a 1x1 km grid. Therefore, the details on the actual flight, take-off, landing and taxiing within this grid (which take place on a finer resolution) are not available and therefore are not taken into account. If one would like to model the actual flight patterns, this would require a different (local) model. Large Eddy Simulations (LES) are required to model all the processes that are relevant at a resolution high enough to capture actual airplane trajectories.

Performing such a study is a tremendous effort and would require a different type of model with detailed information (i.e., resolutions in the order of ~10 m) for the land use, meteorology and emissions around each of the airports. Furthermore, these LES computations are generally extremely computationally demanding and hence hardly ever used in long term (~year) computations of air quality.

3.3. CONTRIBUTION OF AVIATION EMISSIONS TO AIR QUALITY IN EUROPE

3.3.1. NO_2

In **Figure 6**, the total yearly averaged surface concentration of NO_2 in 2018 for the European domain is shown (left panel) together with the source apportionment results of the whole domain (right panel). The source attributed relative contributions include aquatic areas, like the North Sea and Mediterranean Sea. It is computed by summing the total surface concentration resulting from the emissions in a certain source sector over the entirety of the simulation domain and dividing this value by the total summed surface concentration with the contributions from all the sectors.

The left side shows that the highest NO_2 concentration values are predicted in the western part of Europe (Benelux, Germany, UK) and in the Po Valley (north of Italy). The annual total average concertation for the entire domain is 2.5 µg/m^3. The largest contributions to the atmospheric NO_2 concentration in the displayed domain are “Road Transport – exhaust” and “International Shipping”. Road transport is known to be a large contributor to the NO_2 concentration over land. Because a large part of the chosen domain covers seas, it is also logical that international shipping has a relatively large contribution. Nevertheless, locally shipping can also have a significant impact on air quality (in the vicinity of large ports) (Concawe, 2023). The aviation sector contribution averaged over the whole European domain is relatively small (0.5%), which is as expected due to its local nature and the short lifetime of NO_2.

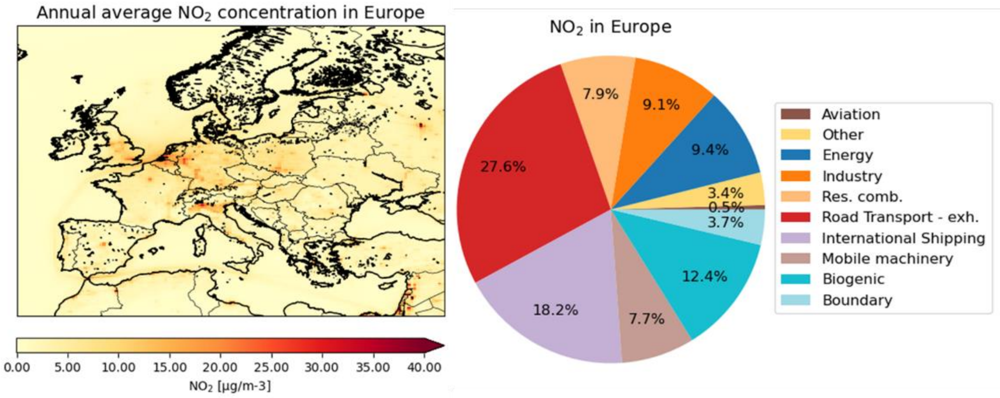

Figure 6 Annual average NO_2 surface concentration for 2018 in the simulation domain of the coarse (25x25 km) resolution LOTOS-EUROS simulation (left panel). The relative contributions from the various labelled sectors to the surface concentration of NO_2 for the entire simulation domain is also shown (right panel)

3.3.2. Other components

For the other pollutants ($PM_{2.5}$, PM_{10} and SO_2), aviation is also predicted to be a small contributor to the average surface concentrations in the European domain. The pie charts showing the contributions from the various sectors are presented in **Figure 7**. In these pie charts the aviation contribution is barely or even not at all visible. This is a consequence of the fact that for $PM_{2.5}$, PM_{10} and SO_2 the contribution is 0.14% (a 1.7 ng/m^3 contribution to an average of 1.2 µg/m^3 for the domain), 0.04% (a 2.2 ng/m^3 contribution to an average 5.5 µg/m^3 for the domain) and 0.03% (a 6.6 ng/m^3 contribution to an average 21 µg/m^3 domain average) respectively.

By looking at the surface contributions, averaged over the European domain, aviation seems to be a sector of limited significance. Aviation activities are nevertheless relevant, since these are commonly concentrated in densely populated areas. Therefore, it is worthwhile to take a closer look at the fractional contributions of the various source sectors in the vicinity of large airports which will be the topic of the next section.

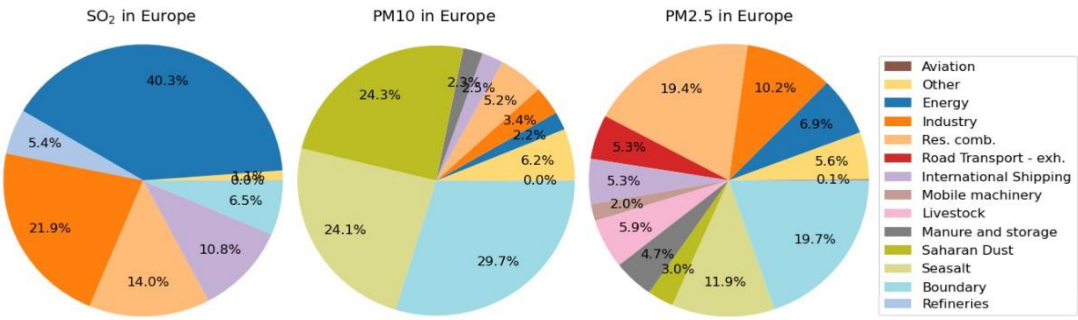

Figure 7 Relative contributions from the various labelled sectors to the surface concentration of SO_2, PM_{10} and $PM_{2.5}$ for the entire simulation domain

3.4. CONTRIBUTION OF AVIATION EMISSIONS FOR EACH CITY

In this section, the results of the calculated aviation contribution to NO_2 levels near the cities in the 1x1 km simulation will be presented and discussed. For a similar detailed (graphical) analysis for the other air pollutants of interest (i.e., SO_2, $PM_{2.5}$, and PM_{10}), we refer to the **Appendix**. For the analysis, a representative central location for the airport and the city centre were determined for the selected cities. The city centre locations are represented as blue dots and the airport locations as turquoise dots in **Figure 8** through **Figure 13**. For these locations of interest, the concentration fields were calculated as a weighted average of the 4 nearest grid points in the 1x1 km simulation domain (inversely with distance from the grid point to the coordinates of the location of interest). Note that results from the high-resolution simulations are presented and that these will differ from the simulations at coarser resolutions.

3.4.1. London

Heathrow (IATA-Code: LHR) is the busiest airport of Europe with respect to passenger throughput. More than 80 million passengers passed through Heathrow in 2018 [*UK airport data | Civil Aviation Authority (caa.co.uk) UK Civil Aviation Authority. Retrieved 11 January 2021*]. The airport is located 25 km west from the city centre (defined as the Big Ben). At Heathrow, elevated NO_2 concentrations can be largely attributed to aviation activities with a contribution of 54.9% (17.2 µg/m^3). In the city centre, the contribution from aviation diminishes to 1.6% (0.44 µg/m^3) due to dilution upon transport and the lifetime of NO_2 in the atmosphere. If an exponent is fitted to the declining contribution of aviation as function of distance from the airport it is found that a 63% reduction of the relative contribution is seen for every 2.8 km separation from the airport toward the city centre. This means that at 2.8 km from Heathrow a contribution from aviation to the NO_2 concentration of 20% is present. More details on this analysis can be found in **Appendix 7.6.2**. The declining trend as function of distance is also a result of a larger absolute contribution from other sources in the city of London (e.g., road transport and residential combustion) thereby reducing the relative contribution from aviation.

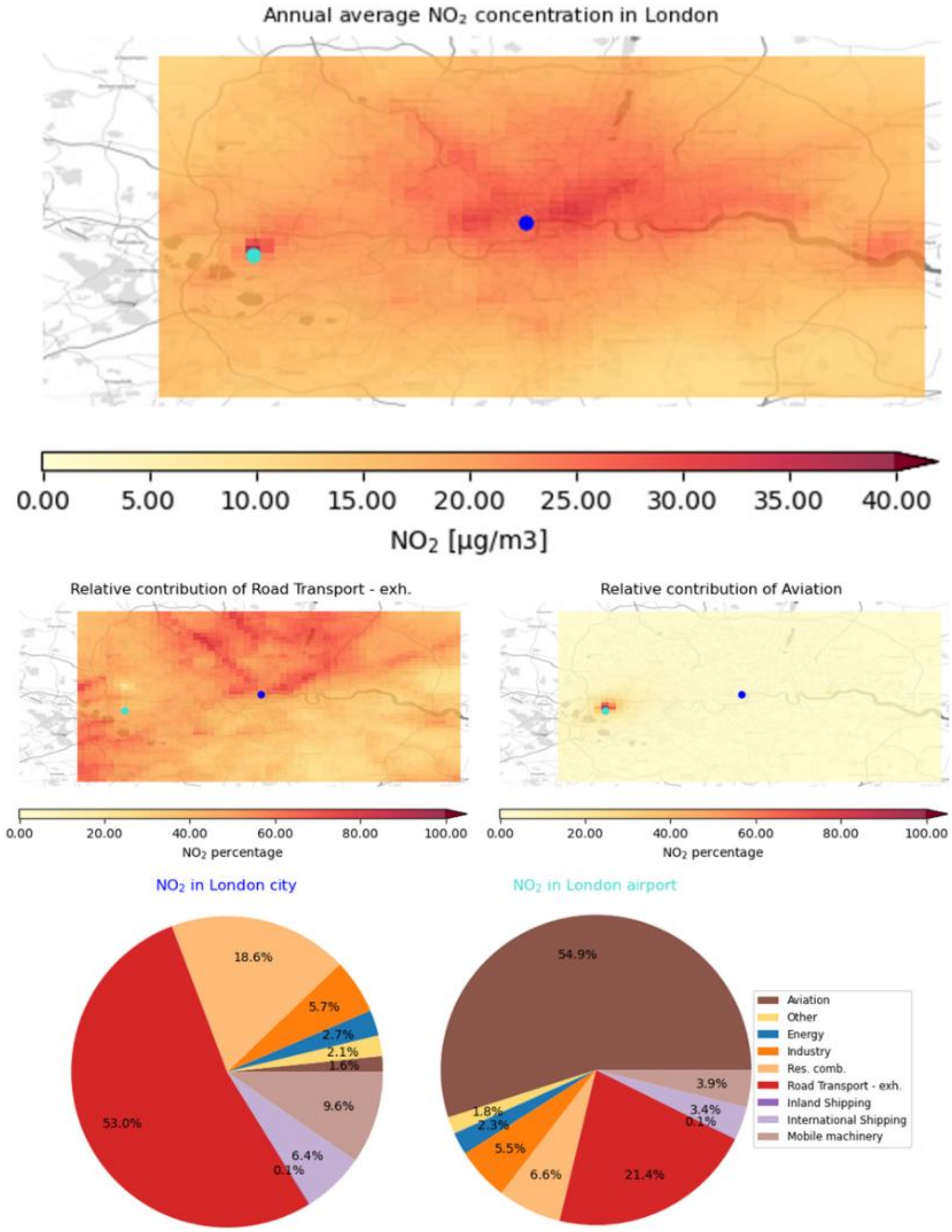

Figure 8 Predicted annual average NO_2 concentration in the vicinity of London (top panel) and the relative contributions of traffic (the largest contributor in the region) and aviation to this concentration in respectively the middle left and right panel. The bottom panel shows the contribution from various sectors to the NO_2 concentration in the city centre (left) and near the airport (right)

3.4.2. Paris

Paris has two airports in relatively close proximity to the city centre. First of all, Charles de Gaulle airport (IATA code: CDG) is located about 30 km northeast from the city centre (e.g., 31 km to the Notre dame) and is Europe's second largest airport with a throughput of 72 million passengers. To the south of Paris is the second largest French airport called Orly Airport (IATA code: ORY), where in 2018, 33 million passengers took off or landed [http://www.aeroportsdeparis.fr]. At Charles de Gaulle airport, aviation contributes for about 58% (15.5 $\mu g/m^3$) to the NO_2 surface concentration. In the city centre, both aviation activities at Orly and Charles de Gaulle airport contribute for 2.3% (0.68 $\mu g/m^3$) to the NO_2 surface concentration which is dominated by emissions from traffic and residential combustion activities which together account for ~80% of the total concentration. At 4.3 km from CDG airport the relative contribution from aviation to the NO_2 concentration is reduced with 63% (to 21%) w.r.t. the concentration at the airport. This drop-off is less steep than found for London. It can be due to a larger region of influence of the CDG airport compared to Heathrow, the presence of contributions from the Orly airport or a smaller relative contribution from other sources.

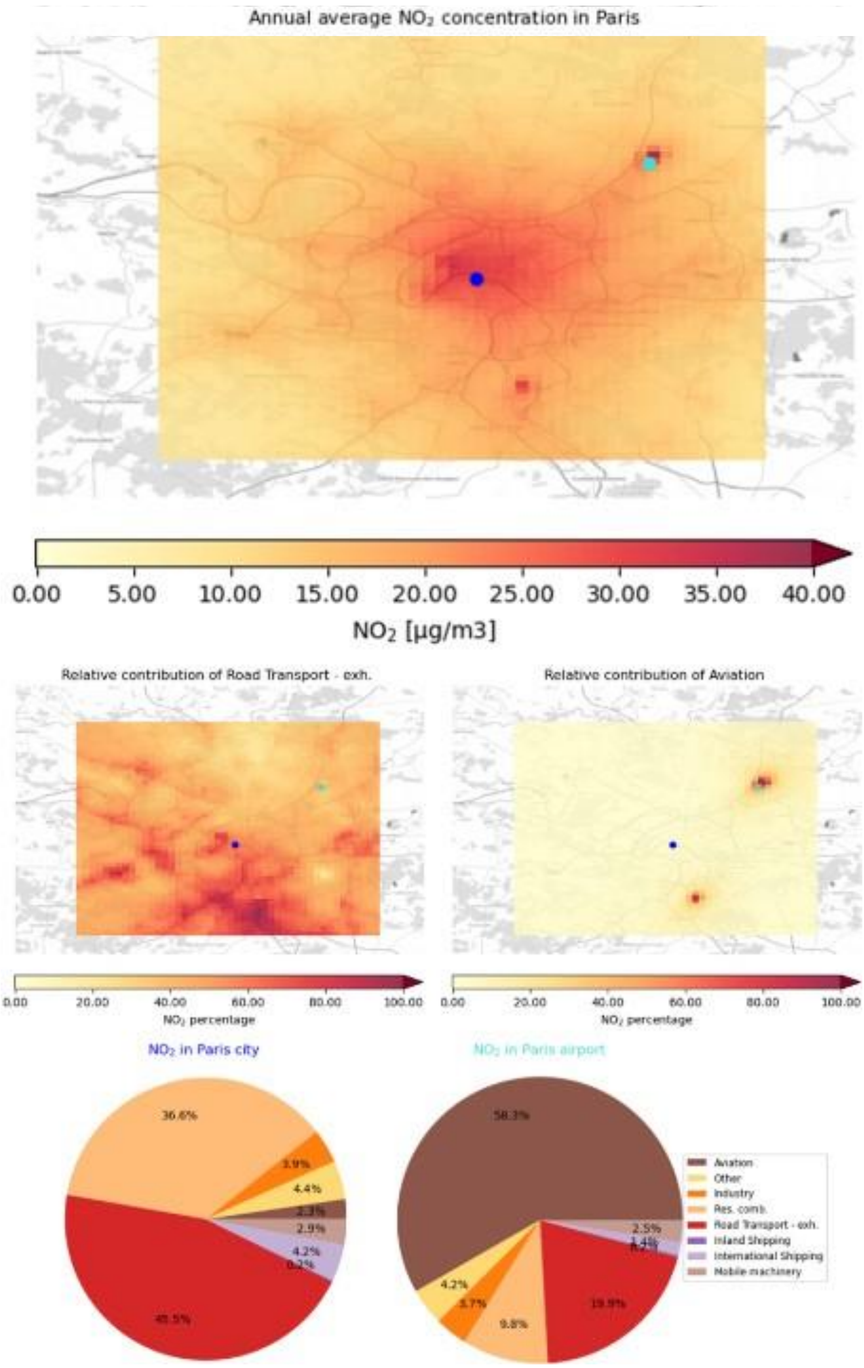

Figure 9 Predicted annual average NO_2 concentration in and around Paris (top panel) and the relative contributions of traffic (the largest contributor in the region) and aviation to this concentration in respectively the middle left and right panel. The bottom panel shows the contribution from various sectors to the NO_2 concentration in the city centre (left) and near the CDG airport (right). It should be noted that the sector aviation was labelled and hence the contribution from the Orly airport cannot be distinguished for the one from CDG meaning both contributions are incorporated in the pie charts (brown slices)

3.4.3. Amsterdam

In the vicinity of Amsterdam (15 km southwest of the city centre) lies Schiphol airport (IATA code: AMS), which is the largest airport in the Netherlands and third largest airport in Europe (after Heathrow and Charles de Gaulle). 71 million passengers passed through Schiphol in 2018 [*https://www.schiphol.nl/en/schiphol-group/page/transport-and-traffic-statistics/*]. Aviation activity at Schiphol contributes about 35% (10.9 µg/m^3) to the NO_2 concentration at the airport location and 4.6% (1.19 µg/m^3) to the concentration in the city centre. A 63% reduction of the relative contribution is seen for every 4.2 km separation from the airport toward the city centre.

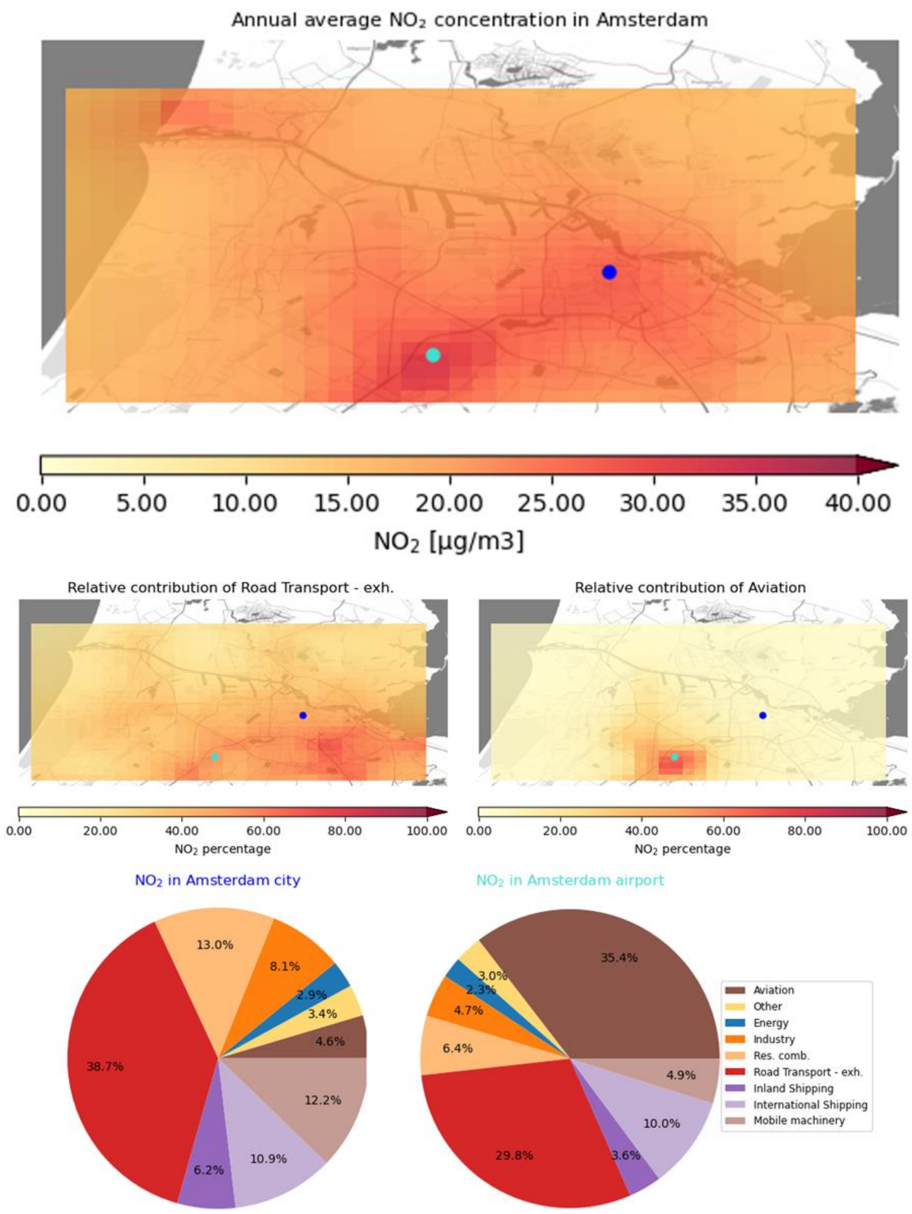

Figure 10 Predicted annual average NO_2 concentration in and around Amsterdam (top panel) and the relative contributions of traffic (the largest contributor in the region) and aviation to this concentration in respectively the middle left and right panel. The bottom panel shows the contribution from various sectors to the NO_2 concentration in the city centre (left) and near the airport (right)

3.4.4. Frankfurt am Main

The largest airport in Germany is Frankfurt am Main Airport (IATA code: FRA) with 70 million passengers in 2018 [*https://www.fraport.com/en/investors/traffic-figures.html*]. This makes it the 4th largest airport in Europe. It is located relatively close to the city centre (~12 km). Locally, the airport contributes to approximately 26% (8.3 µg/m^3) of the NO_2 concentration. In the city centre, the relative contribution from aviation decreases to 5.0% (1.4 µg/m^3). For both locations, traffic emissions form the dominant contribution to the NO_2 concentration. A 63% reduction of the relative contribution is seen for every 4.9 km separation from the airport toward the city centre.

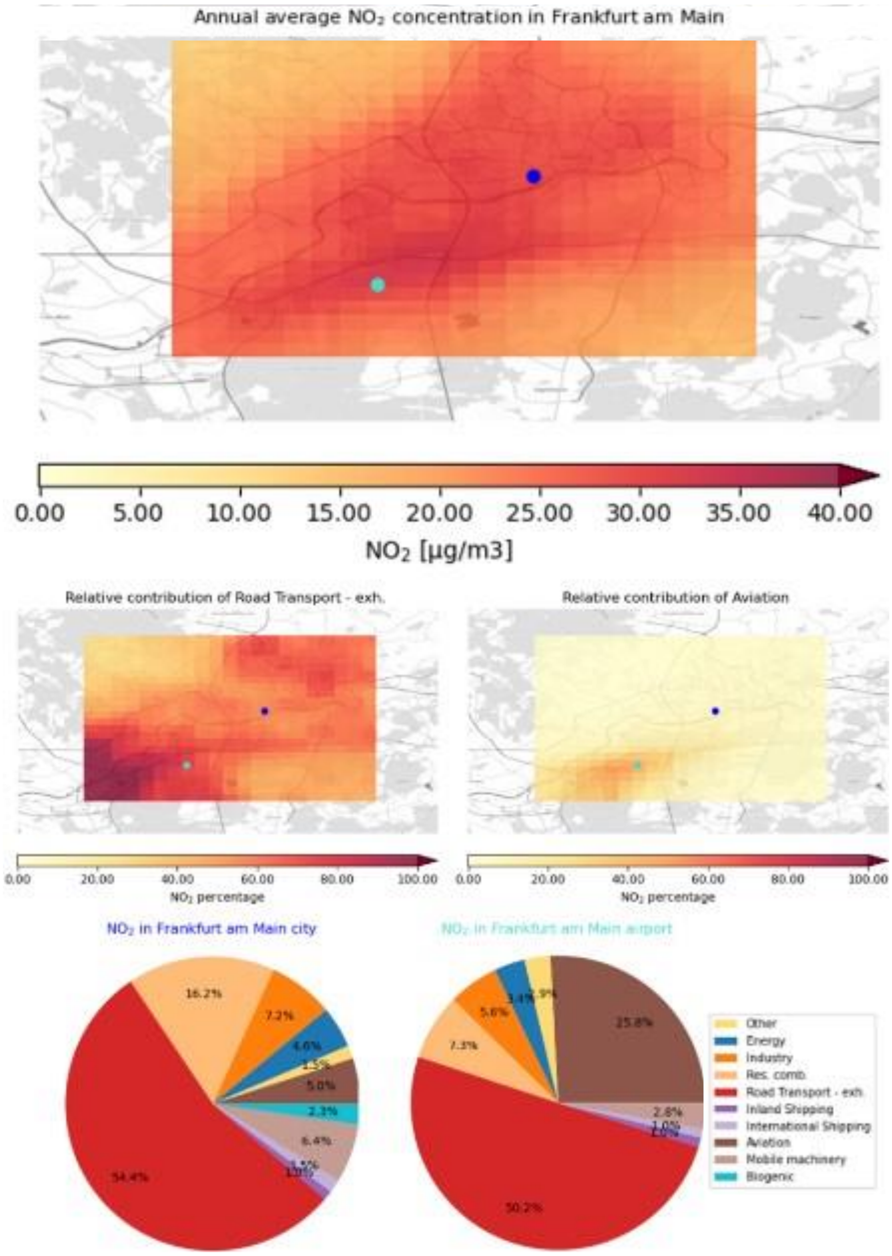

Figure 11 Predicted annual average NO_2 concentration in and around Frankfurt am Main (top panel) and the relative contributions of traffic (the largest contributor in the region) and aviation to this concentration in respectively the middle left and right panel. The bottom panel shows the contribution from various sectors to the NO_2 concentration in the city centre (left) and near the airport (right)

3.4.5. Munich

Munich Airport (IATA code: MUC) is the second largest airport in Germany and the 9th largest in Europe [*https://www.fraport.com/en/investors/traffic-figures.html Traffic Figures". Fraport. 22 December 2020*]. 48 million passengers were transported through this airport in 2018, which is located 35 km north east of the city centre. These activities cause a contribution to the annual average NO_2 concentration of 39% (8.3 µg/m^3) at the airport and 0.5% (0.12 µg/m^3) in the city centre. The latter location is heavily dominated by traffic emissions that contribute 60% (15.0 µg/m^3) to the total NO_2 concentration. A 63% reduction of the relative contribution is seen for every 4.9 km separation from the airport toward the city centre.

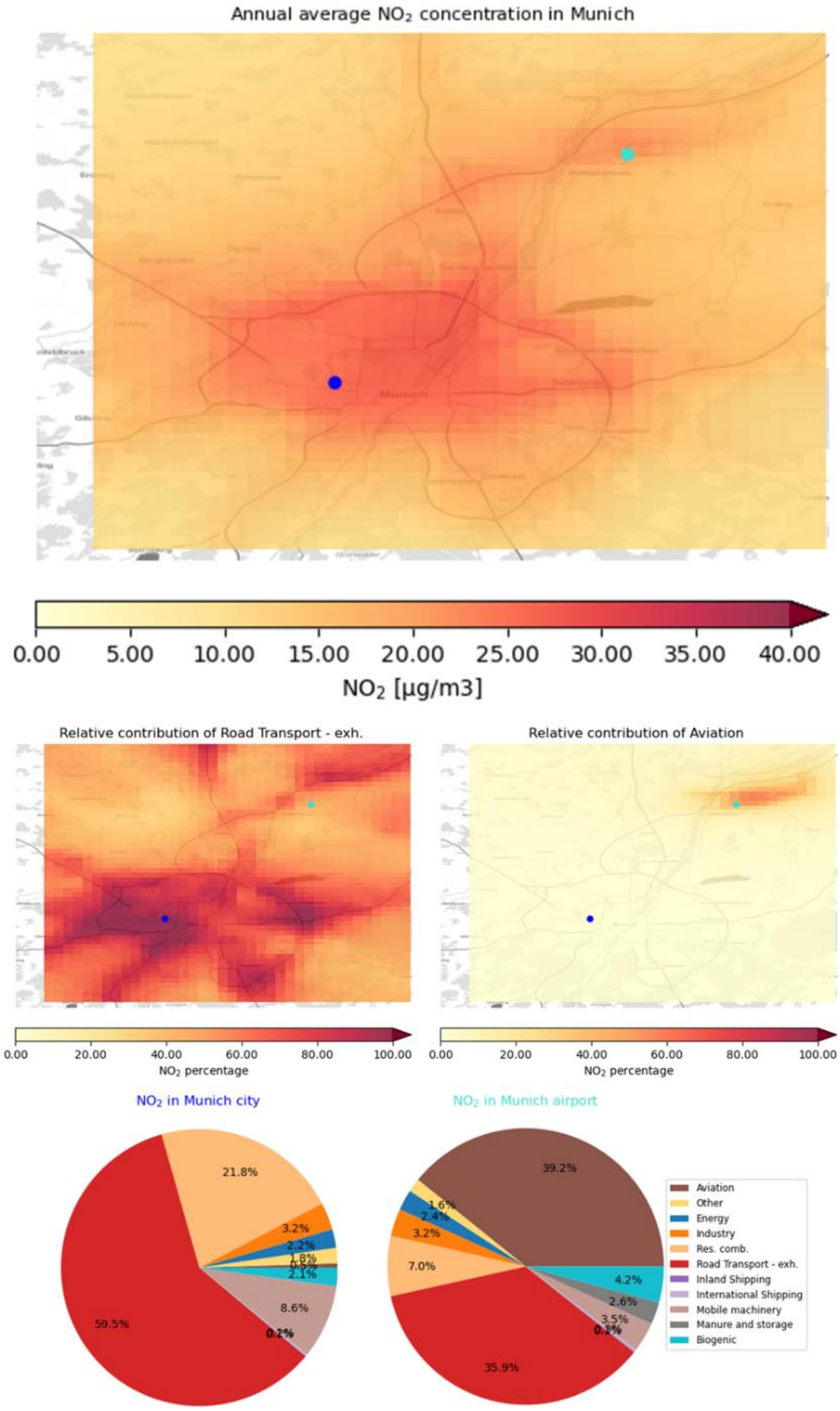

Figure 12 Predicted annual average NO_2 concentration in and around Munich (top panel) and the relative contributions of traffic (the largest contributor in the region) and aviation to this concentration in respectively the middle left and right panel. The bottom panel shows the contribution from various sectors to the NO_2 concentration in the city centre (left) and near the airport (right)

3.4.6. Brussels

Zaventem (IATA code: BRU) is Belgium's largest airport, ranking 24th in the list of largest European airports in 2018 with a total passenger count of over 25 million [*https://web.archive.org/web/20180725214651/https://www.brusselsairport.be/en/corporate/statistics/monthly-traffic-figures*]. The airport is located ~9 km north east of the city centre of Brussels. Aviation activities cause a contribution to the annual average NO_2 concentration of 26% (6.8 µg/m^3) near the airport and 1.2% (0.31 µg/m^3) near the city centre. A 63% reduction of the relative contribution is seen for every 1.8 km separation from the airport toward the city centre.

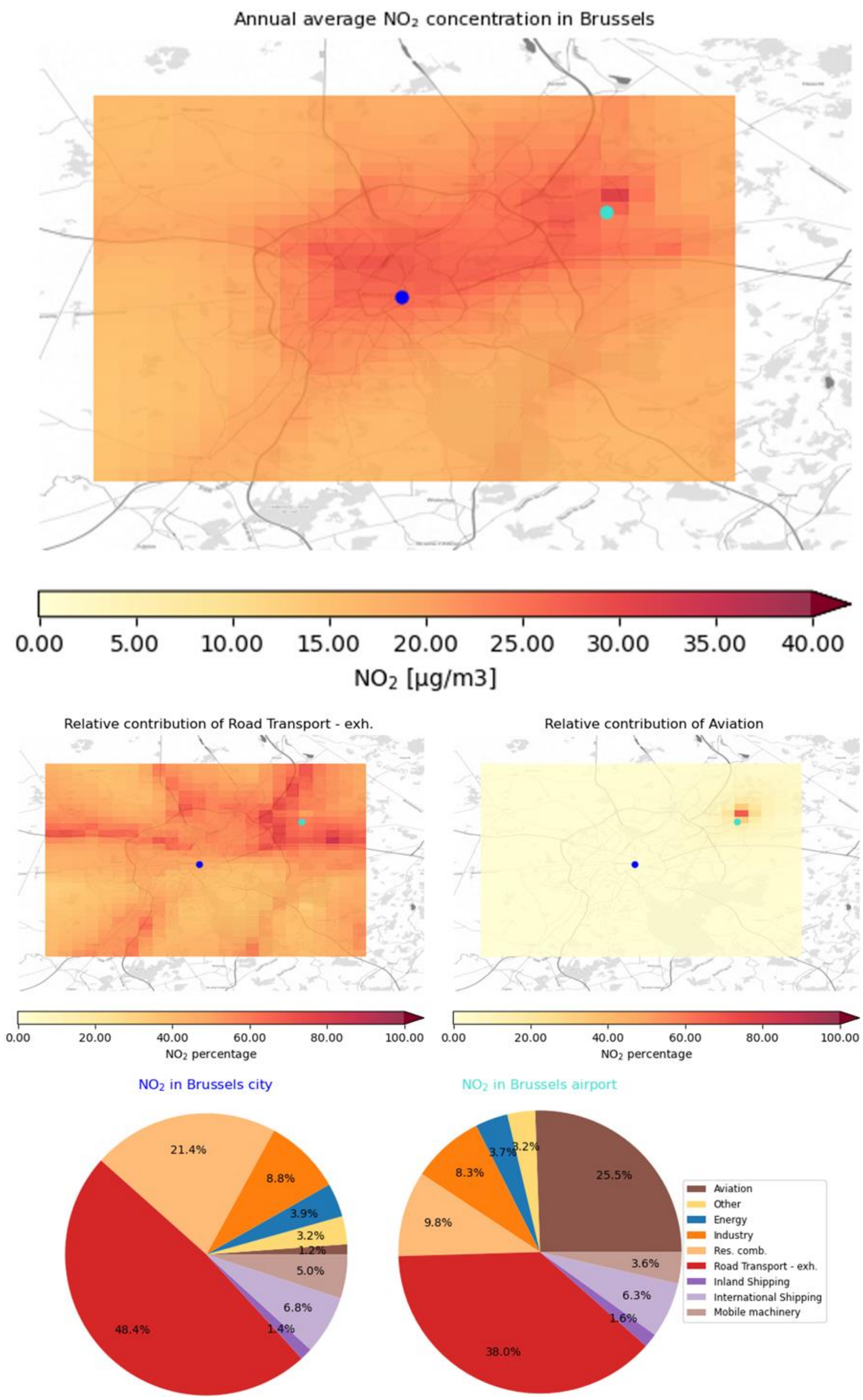

Figure 13 Predicted annual average NO_2 concentration in and around Brussels (top panel) and the relative contributions of traffic (the largest contributor in the region) and aviation to this concentration in respectively the middle left and right panel. The bottom panel shows the contribution from various sectors to the NO_2 concentration in the city centre (left) and near the airport (right)

3.4.7. Overview of all cities

The results presented above show NO_2 concentration distributions and sector contributions for all cities of interest. These results are summarized in **Table 3**. This table gives an overview of the contribution of aviation emissions to the NO_2 concentration for all city centres of interest. The average contribution from aviation to the NO_2 concentration in the respective city centres is 2.5%. Detailed results for other pollutants can be found in the **Appendix**. It is however noteworthy that for the other pollutants the relative contribution is smaller with respectively 1.9%, 0.5% and 0.3% for SO_2, $PM_{2.5}$, and PM_{10}. Near the airports, the contributions from aviation are significantly higher as can be seen in **Figure 14**.

Table 3 The relative contribution of aviation (%) to the annual average concentration of NO_2 in the city centres. ‡Simulations performed with GrETA and ER datasets. *Simulations performed with the CAMS-REG v5.1 dataset

	Annual average NO_2 concentration [µg/m³]	Aviation contribution to annual NO_2 concentration (%)	Distance from city centre to airport [km]	Airport source type
London*	27	1.6	25	Point
Paris*	30	2.3	30	Point
Amsterdam‡	26	4.6	15	Surface
Frankfurt am Main‡	29	5.0	12	Surface
Munich‡	25	0.5	35	Surface
Brussels*	27	1.2	9	Point
Average	27	2.5	-	-

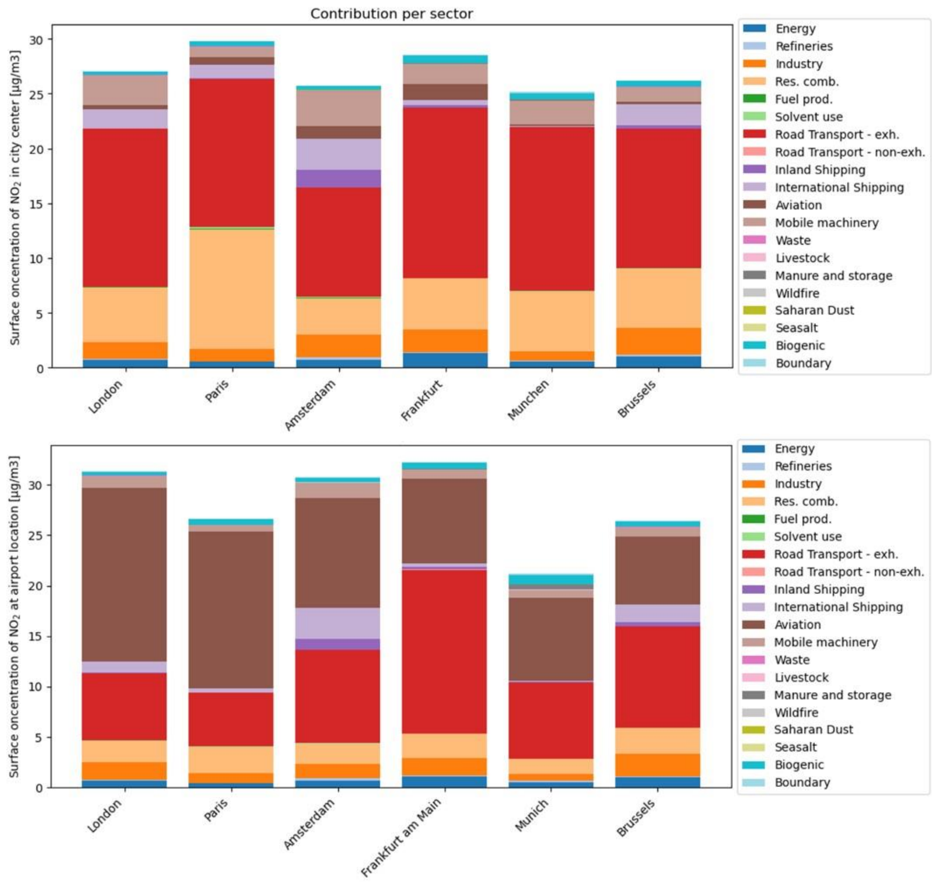

Figure 14 Stacked bar plots showing the total NO_2 concentration and how it is attributed to the various emission sources in the city centres (top) and in the vicinity of the airports (bottom)

3.5. MODEL RESULTS COMPARED TO OBSERVATIONS

An evaluation of the model results against selected measurement stations near or in cities is made to give an indication of the accuracy of the modelled concentrations. This will help put the results into perspective. A vast network of monitoring sites from which data is freely available exists in Europe as can be seen in **Figure 15**. In this figure, all EEA and EIONET stations with at least 50% temporal coverage in hourly NO_2 observations in 2018 are shown. For the evaluation of the model results a selection is made to only compare with (urban) background stations, which are representative for the resolution at which the model runs have been performed. It should be noted that the measurement results in the EEA dataset have been collected from the European Environment Agency's Air Quality e-Reporting (AQ e-Reporting) datahub, which leaves the quality assurance to individual data providers. This is also disclaimed at the website: "despite constant improvement of the quality of data collected within new reporting procedures for air quality information, still inconsistencies, incompleteness and/or errors cannot be ruled out.". So even though the data is assumed to be reliable, the measurements have an associated uncertainty. Mismatches between model results and measurements can reflect these uncertainties as well as model misrepresentations.

It should furthermore be noted that temporal profiles of emissions in the model from for example traffic and residential combustion are based on activity data but translated in a (often temperature dependent) daily, weekly and annual cycle and therefore do not reflect true activities on individual days.

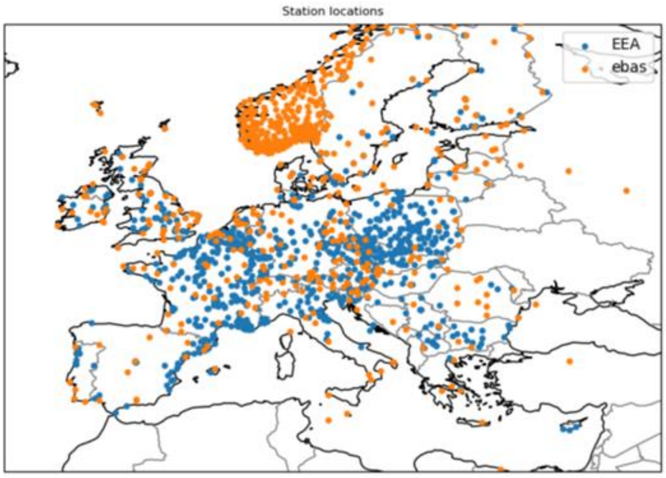

Figure 15 All the sites in the EIONET measurement network (orange) and the EEA sites (blue) with data coverage for at least 50% of the days in 2018

3.5.1. London

A comparison at the Bloomsbury Urban Centre measurement station (an urban background site) near the city centre of London shows that the model results are moderately correlated with measurements for all three resolutions (i.e., ~25x25 km, ~6x6 km and ~1x1 km). The highest resolution shows the strongest correlation but the improvement with respect to the other simulation resolutions is limited in terms of Pearson correlation coefficient (R = 0.51 for the highest resolution vs R=0.50 for the lowest resolution). The nRMSE of 0.51 is also lowest for the highest resolution model, but the best slope in the correlation plot is found for the 6x6 km simulation (0.95). For details on how the biases, correlations and RMSE are computed the reader is referred to **Appendix 7.6.1**.

In winter all model results seem to underestimate the NO_2 concentration. This potentially indicates that a temperature dependent emission source with a strong yearly variation might be slightly misrepresented. This could be the seasonal profile for residential combustion, but it is also known that during cold temperatures, vehicle emissions, especially from diesel cars, are larger (additional emissions from cold starts and inefficient engine modes) than during warm temperatures (Suarez-Bertoa and Asorga, 2018; Weilenmann et al., 2009). This temperature dependence is not taken into account in current simulations.

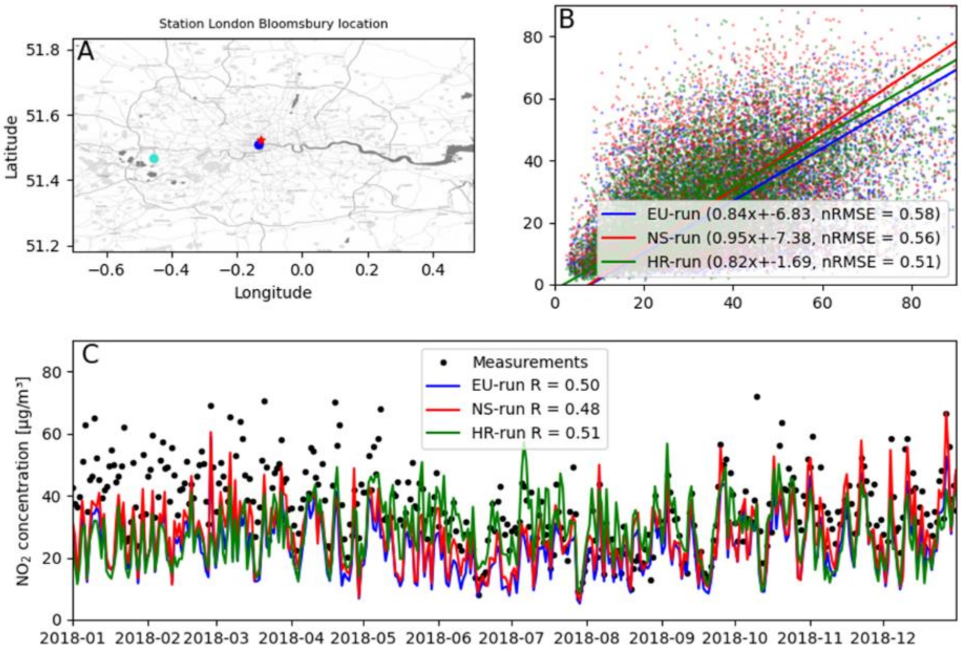

Figure 16 The location of the closest measurement station (urban background) to the city centre of London (blue dot) is depicted as a red star in the top left panel. The top right panel shows the observed hourly NO_2 concentration compared to the modelled equivalent from the ~25x25 km European simulation (blue), the ~6x6 km Northern European simulation (red) and the ~1x1 km high-resolution simulation (green). The corresponding timeseries are shown in the bottom panel

3.5.2. Paris

For Paris, a comparison at the Tremblay-en-France measurement station (rural background) shows that an improved model resolution does lead to a lower yearly averaged bias (see **Figure 17**) but does not necessarily result in a better temporal representation of the measured concentrations.

The temporal variability in NO_2 concentration is captured most accurately by the 25x25 km simulation. This seems to be a consequence of a relatively high modelled NO_2 concentration in the summer period in the high-resolution simulation compared to measurements, something which was also visible in the timeseries in London. This indicates that the cause may be found in emissions with a strong seasonal variability, e.g., residential combustion which play a dominant important role in these urbanized areas. In a 25x25 km simulation these effects will appear less clearly because in grid cells of such a size many different sectors contribute to the emissions. It is furthermore noteworthy that representing emissions sources as point sources, while in reality they are not (e.g., airports), leads to a larger misrepresentation with increasing resolution. This reasoning can however not be used to explain the summer time overestimation of NO_2 concentration in the HR simulations results because emissions from residential combustion sources are most pronounced in winter.

The NO_2 concentrations are mainly influenced by local emissions, which makes it difficult to model these concentrations in a spatial and time consistent matter.

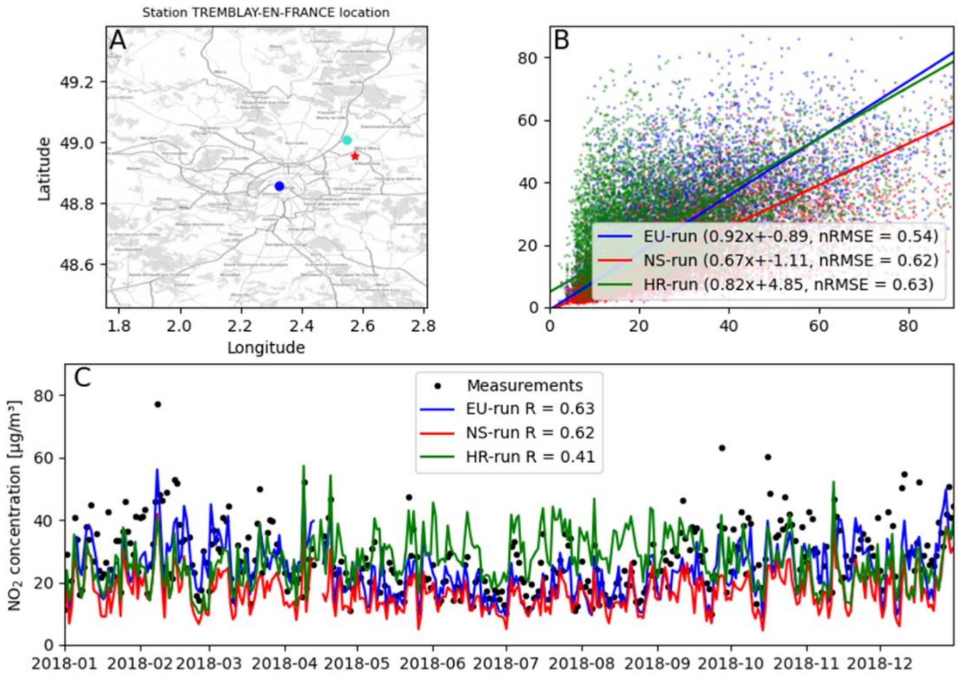

Figure 17 The location of the closest measurement station (rural background) to the city centre of Paris (blue dot) is depicted as a red star in the top left panel. The top right panel shows the observed hourly NO_2 concentration compared to the modelled equivalent from the ~25x25 km European simulation (blue), the ~6x6 km Northern European simulation (red) and the ~1x1 km high-resolution simulation (green). The corresponding timeseries are shown in the bottom panel

3.5.3. Amsterdam

A comparison at the measurement station in the Vondelpark (urban background) in Amsterdam likewise shows that an improved model resolution does not necessarily result in a better temporal correlation between model and measurement (**Figure 18**). The temporal variability in NO_2 concentration is again captured most accurately by the 25x25 km simulation which is once more caused by a high modelled NO_2 concentration in the summer period in the HR simulation compared to measurements.

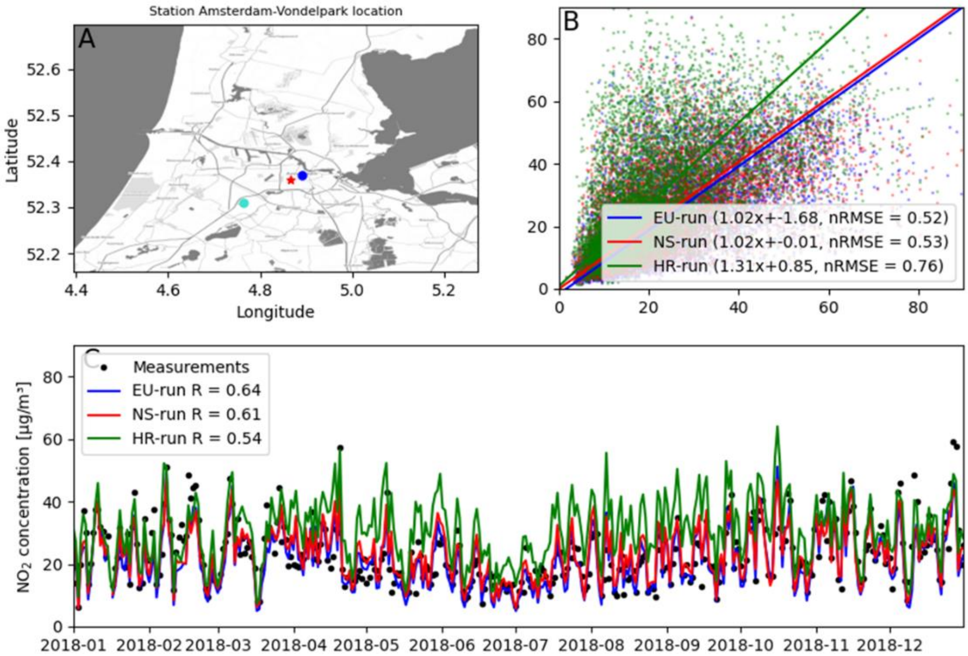

Figure 18 The measurement station (urban background) closest to the city centre of Amsterdam (blue dot) is depicted as a red star in the top left panel. The top right panel shows the observed hourly NO_2 concentration compared to the modelled equivalent from the ~25x25 km European simulation (blue), the ~6x6 km Northern European simulation (red) and the ~1x1 km high-resolution simulation (green). The corresponding timeseries are shown in the bottom panel

3.5.4. Frankfurt am Main

A comparison at a measurement station (suburban area) in the vicinity of Frankfurt am Main shows that the model results are moderately correlated with measurements for all 3 resolutions when compared at hourly time intervals (**Figure 19**). Correlations are very similar but the level of the pollutant concentration is captured most accurately by the high-resolution simulation.

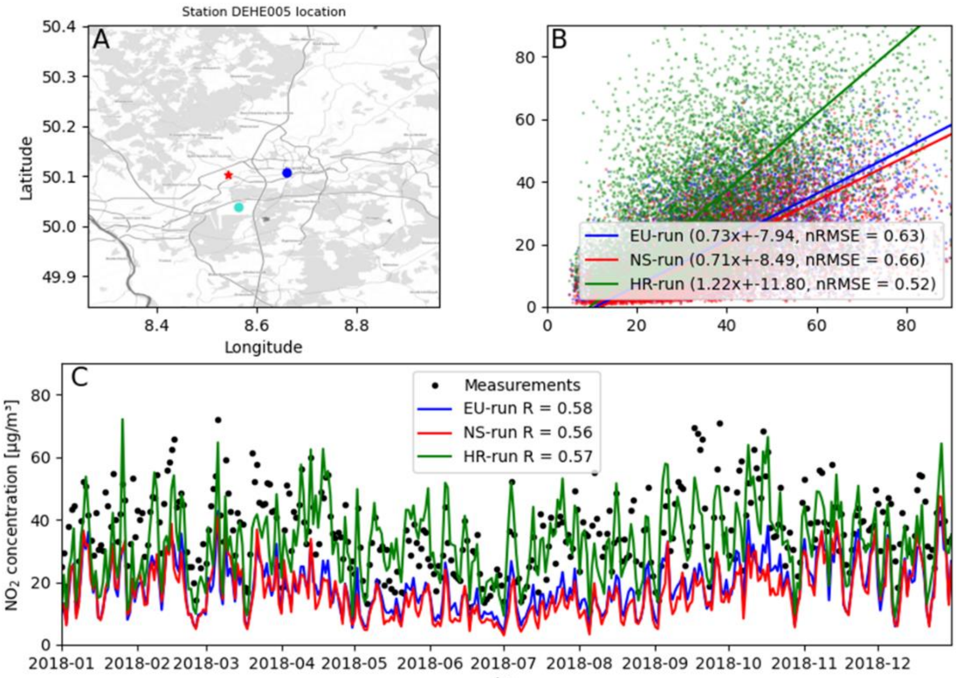

Figure 19 The measurement station (urban background) closest to the city centre of Frankfurt am Main (blue dot) is depicted as a red star in the top left panel. The top right panel shows the observed NO_2 hourly concentration compared to the modelled equivalent from the ~25x25km European simulation (blue) the ~6x6 km Northern European simulation (red) and the ~1x1 km high-resolution simulation (green). The corresponding timeseries are shown in the bottom panel

3.5.5. Munich

A comparison at an urban background measurement station at the Munich university campus shows that the model results are moderately correlated with measurements for all 3 resolutions when compared at hourly time intervals (**Figure 20**). Correlations are very similar and differences between the HR simulation and the 6x6 km resolution simulation are barely noticeable both in terms of statistical performance (bias, nRMSE) as well as temporal profile.

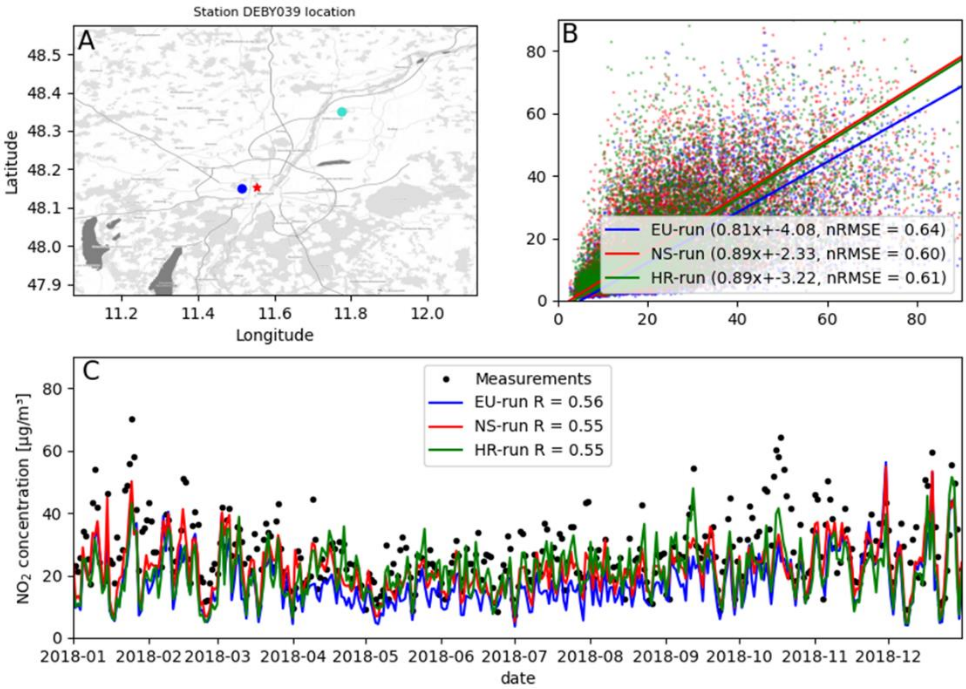

Figure 20 The measurement station (urban background) closest to the city centre of Munich (blue dot) is depicted as a red star in the top left panel. The top right panel shows the observed hourly NO_2 concentration compared to the modelled equivalent from the ~25x25 km European simulation (blue), the ~6x6 km Northern European simulation (red) and the ~1x1 km high-resolution simulation (green). The corresponding timeseries are shown in the bottom panel

3.5.6. Brussels

A comparison at a measurement station (urban background) in Brussels shows that model results are moderately correlated with measurements for the 25x25 km resolution simulation and the 6x6 km resolution simulation when compared at hourly time intervals (**Figure 21**). The results from the high-resolution simulation are strongly correlated (R = 0.71) with measurements. The bias and normalised RMSE is also lowest in the high-resolution simulation results.

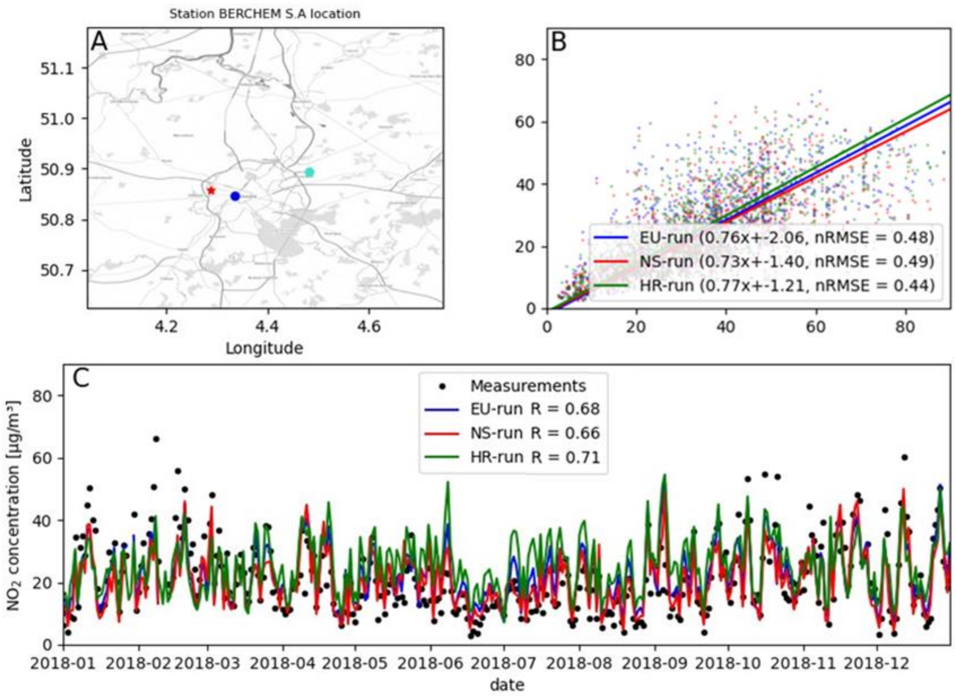

Figure 21 The measurement station (urban background) closest to the city centre of Brussels (blue dot) is depicted as a red star in the top left panel. The top right panel shows the observed hourly NO_2 concentration compared to the modelled equivalent from the ~25x25 km European simulation (blue), the ~6x6 km Northern European simulation (red) and the ~1x1 km HR simulation (green). The corresponding timeseries are shown in the bottom panel

4. DISCUSSION

In this section, some aspects which should be considered while interpreting the results of the source apportionment modelling simulations, are discussed.

When comparing the simulation results with measured pollutant concentrations, the Pearson correlations (R) vary between moderate (0.4) to strong (0.7), indicating that the model grasps the temporal variability in the NO_2 concentration reasonably well. Counterintuitively, the increased resolution does not always improve the temporal representation in the model results with respect to measurements (e.g., Paris and Amsterdam). This could be due to several factors, but some potential candidates are misrepresentations of temporal profiles or local levels of emissions. If for example roadworks, jams or alterations in the local traffic situation change the flow of cars through a city, the performance of simulations with a high resolution will be more heavily influenced than simulations with a coarser resolution. This emphasizes the fact that if modelling becomes more local, the nature of the input information (emissions, meteorology, orography, land-use, etc.) should likewise become more detailed. True activity data can overcome some of these issues, but their usage is beyond the scope of the work presented here. More importantly, given the relatively small contribution of the aviation activities at the airports to the air quality in the city centres as calculated in this study, it is questionable whether such detailed modelling exercises would add additional value to the results/conclusions from this study. Only in specific circumstances where the population density near the airports is high and coincide with high contributions from aviation, such more detailed modelling exercise could be more conclusive than the presented results from this study.

Secondly, looking at the temporal profiles of the simulated concentrations, one might notice that the increased resolution does not always lead to very strong changes in NO_2 concentrations over time. The biggest observed change is a quite pronounced wintertime concentration increase in the HR simulation. For example, the difference in the modelled NO_2 concentrations at the measurement station near Munich between the simulation at the 1x1 km and at the 6x6 km resolution are barely noticeable. Contrarily to this observation, the source apportioned annually averaged results can be quite different between the different resolutions. For example, for the city centre of London, the 6x6 km resolution simulation performed in an earlier Concawe study with focus on shipping emissions (Concawe, 2023) gives a 45% contribution from traffic and 1.9% contribution from aviation to the NO_2 concentration[4].This differs from the 53% and 1.6% contribution found at the higher resolution simulation presented here. The increased resolution allows a better representation of locally increased concentrations, such as those near the airport, where in the coarser runs the concentrations are smeared out over a larger grid cell. Therefore, the higher resolution leads to larger contributions from the local sources. This difference indicates the added benefit of looking at a higher resolution as is also seen in the lowest average bias for the six cities.

Thirdly, the difference between describing the airport as a surface source or as a point source will also influence the results, through alterations in chemistry and transport. It is more physically accurate to represent an airport as a surface source taking the exact geometry and location of the runways into account. This data is however not available outside Germany and the Netherlands. One should take this into consideration when comparing results for the simulations around Amsterdam,

[4] A more detailed discussion of the results of the 6x6 km resolution simulations (with a focus on the effect of shipping activity) can be found at Concawe (2023).

Frankfurt am Main, and Munich with results from the simulations around London, Paris and Brussels. Generally, the relative contribution in the vicinity of the airport becomes lower by spreading the emissions over an area but the extent where a significant contribution from the airport can be found increases.

Finally, the contributions at the city centre should not be seen as the only relevant location with respect to population exposure as people also live close to the airport. For example, in the case of Paris, the area between the city centre location and Charles de Gaulle airport (**Figure 9)** is completely urbanized. This also holds for London and to some extent for all other cities as well. Hence, many people in these areas will be exposed to NO_2 concentrations with a higher relative contribution from aviation than those predicted in the city centre.

For all the investigate cities an exponent is fitted to the declining contribution of aviation as function of distance from the respective airport. It is found that a 63% reduction of the relative contribution is seen on average for every 3.8 km (spread between 1.8 km and 4.9 km) separation from the airport toward the city centre. This means that at 2.6 km from the airport the relative contribution from aviation to the NO_2 concentration is halved with respect to the concentration at the airport. More details on this analysis can be found in **Appendix 7.6.2**.

5. CONCLUSION

Aviation activities result in emissions of NO_x, SO_2 and PM that can have a negative impact on air quality. To investigate the extent of the contribution from aviation to air pollution, simulations with the chemical transport model LOTOS-EUROS have been performed to model the atmospheric concentrations of NO_2, SO_2, PM_{10} and $PM_{2.5}$ in 2018. With the labelling capabilities of LOTOS-EUROS, it is possible to track emissions from various labelled sources and monitor their respective contributions to atmospheric concentrations. The concentrations of the aforementioned pollutants are modelled in higher detail for six European cities (London, Paris, Amsterdam, Frankfurt am Main, Munich, and Brussels) with large airports nearby. for the year 2018. Four of these cities are ranked as having the top four largest European airports (Heathrow, Charles de Gaulle, Schiphol and Frankfurt am Main). These four airports cumulatively had a throughput of nearly 300 million passengers (>25% of all passengers carried by air in the European Union).

An initial exploration into various emission datasets was performed from which the conclusion was drawn to use emissions at the highest available resolution for as many of the relevant pollutants as possible depending on the data availability. This prevents appearance of unrealistic patches in simulated concentrations. Therefore, for the Netherlands and Germany, the ER and GrETA emissions datasets are used respectively. These datasets contain high resolution data for all pollutants of interest and also consider airports as surface sources (i.e., more detailed representation of airports with runways) rather than point sources. However, these datasets do not cover Paris, London and Brussels. For these cities the CAMS-REG v5.1 1x1 set was used, which contains high resolution NO_x, NH_3, NMVOC emission data, but not for SO_2 and PM.

The modelled NO_2 concentrations are compared to measurements from EIONET stations. The modelled hourly NO_2 concentrations correlate moderately (0.4) to strongly (0.7) with measured pollutant concentrations for six stations in the vicinity of the cities of interest indicating that the model grasps the temporal variability in the NO_2 concentration reasonably well. In addition, reasonable biases (between 0.77 and 1.31) provide confidence in the modelled total surface concentrations. Employing a labelling approach to track emissions from various source sectors as they contribute to the atmospheric concentrations furthermore allows apportionment of these modelled concentrations to the underlying emission sources.

The source apportionment results show:

- An average contribution from aviation to the NO_2 concentration in the respective city centres of the six cities examined of 2.5%, ranging from 0.5% (Munich) to 4.6% (Amsterdam).
- For the other pollutants, the relative contribution is smaller with respectively 1.9%, 0.5% and 0.3% for SO_2, $PM_{2.5}$, and PM_{10}. This suggests that aviation is not a significant contributor to pollutants concentrations in the city centres compared to other sources, like traffic and residential combustion.
- Closer to the airports, the average relative contributions from aviation to the NO_2 concentration in the six airports examined is significantly higher with 40%, varying from 26% (Zaventem) to 58% (Charles de Gaulle).
- This also holds for the other pollutants with aviation contributing respectively 45%, 6.2% and 4.6% to the concentration of SO_2, $PM_{2.5}$, and PM_{10}.

It is important to note that densely populated areas are not restricted to what is defined as the city centre in this study. Most of the cities also have a large number of inhabitants that live closer to the airport in the extended densely populated area around the city centre and hence are exposed to NO_2 concentrations with a contribution from aviation that can reach up to 58% for locations closer to the airport (case of CDG airport).

If one looks at the example of London (the largest city considered in this study with approximately 10 million inhabitants), the results the NO_2 concentrations are elevated significantly at Heathrow (LHR) airport with a contribution of 55% (17 $\mu g/m^3$) from aviation. However, the relative contribution of aviation declines as function of distance from the airport with a reduction rate of 63% for every 2.8 km separation from the airport toward the city centre. In the city centre of London, the contribution diminishes to 1.6% (0.44 $\mu g/m^3$). Inhabitants of the densely populated region between the city centre and the airport will be exposed to NO_2 levels caused by aviation varying in this range. Paris is the second largest city considered in this study with 7.8 million inhabitants in its urbanized area, followed by Munich with 2.5 million residents. These cities as well as the smaller cities (Frankfurt am Main (2.3 million), Amsterdam (1.5 million) and Brussels (1.3 million)), all show a similar trend of decreasing pollutant concentration contributions from aviation when moving from the airport to the city centre in a comparable range.

6. REFERENCES

Banzhaf, S. (2013). Interaction of surface water and groundwater in the hyporheic zone – application of pharmaceuticals and temperature as indicators. Doktor Der Ingenieurwissenschaften - Dr.-Ing

Banzhaf, S., Schaap, M., Kerschbaumer, A., Reimer, E., Stern, R., Van Der Swaluw, E., & Builtjes, P. (2012). Implementation and evaluation of pH-dependent cloud chemistry and wetdeposition in the chemical transport model REM-Calgrid. Atmospheric Environment, 49, 378-390. https://doi.org/10.1016/j.atmosenv.2011.10.069

Beelen, R., Raaschou-nielsen, O., Stafoggia, M., Andersen, Z. J., Weinmayr, G., Hoff, B., & Wolf, K. (2014). Eff ects of long-term exposure to air pollution on natural-cause mortality : an analysis of 22 European cohorts within the multicentre ESCAPE project. 785–795. https://doi.org/10.1016/S0140-6736(13)62158-3

Colette, A., & Rouïl, L. (2020). Air Quality Trends in Europe : 2000-2017 (Issue 2)

Concawe (2023). The impact of shipping emissions to urban air quality in Europe – Detailed port-city analysis, Concawe report No. 2/23

Curier, R. L., Kranenburg, R., Segers, A. J. S., Timmermans, R. M. A., & Schaap, M. (2014). Synergistic use of OMI NO2 tropospheric columns and LOTOS-EUROS to evaluate the NOx emission trends across Europe. Remote Sensing of Environment, 149(2), 58–69. https://doi.org/10.1016/j.rse.2014.03.032

Fountoukis, C., & Nenes, A. (2007). ISORROPIAII: A computationally efficient thermodynamic equilibrium model for K+-Ca2+-Mg2+-NH4+-Na+-SO42--NO3--Cl--H2O aerosols. Atmospheric Chemistry and Physics, 7(17), 4639–4659. https://doi.org/10.5194/acp-7-4639-2007

Kaiser, J. W., Heil, A., Andreae, M. O., Benedetti, A., Chubarova, N., Jones, L., Morcrette, J., & Razinger, M. (2012). Biomass burning emissions estimated with a global fire assimilation system based on observed fire radiative power. x, 527–554. https://doi.org/10.5194/bg-9-527-2012

Keunen, J. (TNO), Dellaert, S., Visschedijk, A., Jalkanen, J. P., Super, I., & Denier van der Gon, H. (2019). Copernicus Atmosphere Monitoring Service regional emissions version 5.1 business-as-usual 2020 (CAMS-REG-v5.1 BAU 2020). https://doi.org/doi.org/10.24380/eptm-kn40, 2021

Köble, R., & Seufert, G. (2001). Novel Maps for Forest Tree Species in Europe. Proceedings of the 8th European Symposium on the Physico-Chemical Behaviour of Air Pollutants: "A Changing Atmosphere!," January 2001, 1-6

Kranenburg, R., Segers, A. J., Hendriks, C., & Schaap, M. (2013). Source apportionment using LOTOS-EUROS: module description and evaluation. Geoscientific Model Development, 6(3), 721-733. https://doi.org/10.5194/gmd-6-721-2013

Kuenen, J., Dellaert, S., Visschedijk, A., Jalkanen, J.-P., Super, I., & Denier van der Gon, H. (2021). CAMS-REG-v4: a state-of-the-art high-resolution European emission inventory for air quality modelling. Earth System Science Data Discussions, 1–37. https://doi.org/10.5194/essd-2021-242

Manders, A. M. M., Builtjes, P. J. H., Curier, L., Denier van der Gon, H. A. C., Hendriks, C., Jonkers, S., Kranenburg, R., Kuenen, J., Segers, A. J., Timmermans, R. M. A., Visschedijk, A., Wichink Kruit, R. J., Van Pul, W. A. J., Sauter, F. J., van der Swaluw, E., Swart, D. P. J., Douros, J., Eskes, H., van Meijgaard, E., … Schaap, M. (2017). Curriculum Vitae of the LOTOS-EUROS (v2.0) chemistry transport model. Geoscientific Model Development Discussions, 1–53. https://doi.org/10.5194/gmd-2017-88

Mårtensson, E. M., Nilsson, E. D., de Leeuw, G., Cohen, L. H., & Hansson, H. C. (2003). Laboratory simulations and parameterization of the primary marine aerosol production. Journal of Geophysical Research: Atmospheres, 108(9), 1–12. https://doi.org/10.1029/2002jd002263

Monahan, E. C., Spiel, D. E., & Davidson, K. L. (1986). A Model of Marine Aerosol Generation Via Whitecaps and Wave Disruption. In E. C. Monahan & G. Mac Niocaill (Eds.), Oceanic Whitecaps: And Their Role in Air-Sea Exchange Processes (pp. 167–174). Springer Netherlands. https://doi.org/10.1007/978-94-009-4668-2_16

Pommier, M. (2021). Prediction of source contributions to urban background PM 10 concentrations in European cities : a case study for an episode in December 2016 using EMEP / MSC-W rv4 . 15 – Part 2 : The city contribution. 4143–4158

Schaap, M., Apituley, A., Timmermans, R. M. A., Koelemeijer, R. B. A., & De Leeuw, G. (2009). Atmospheric Chemistry and Physics Exploring the relation between aerosol optical depth and PM 2.5 at Cabauw, the Netherlands. Atmos. Chem. Phys, 9, 909–925. www.atmos-chem-phys.net/9/909/2009/

Schaap, M., Cuvelier, C., Hendriks, C., Bessagnet, B., Baldasano, J. M., Colette, A., Thunis, P., Karam, D., Fagerli, H., Graff, A., Kranenburg, R., Nyiri, A., Pay, M. T., Rouïl, L., Schulz, M., Simpson, D., Stern, R., Terrenoire, E., & Wind, P. (2015). Performance of European chemistry transport models as function of horizontal resolution. Atmospheric Environment, 112, 90–105. https://doi.org/10.1016/j.atmosenv.2015.04.003

Schaap, M., Timmermans, R. M. A., Roemer, M., Boersen, G. A. C., Builtjes, P. J. H., Sauter, F. J., Velders, G. J. M., & Beck, J. P. (2008). The LOTOS-EUROS model: Description, validation and latest developments. International Journal of Environment and Pollution, 32(2), 270–290. https://doi.org/10.1504/IJEP.2008.017106

Schaap, M., van Loon, M., ten Brink, H. M., Dentener, F. J., & Builtjes, P. J. H. (2004). Secondary inorganic aerosol simulations for Europe with special attention to nitrate. Atmospheric Chemistry and Physics, 4(3), 857–874. https://doi.org/10.5194/acp-4-857-2004

Schneider, C., Pelzer, M., Toenges-Schuller, N., Nacken, M., and Niederau, A.: ArcGIS basierte Lösung zur detaillierten, deutschlandweiten Verteilung (Gridding) nationaler Emissionsjahreswerte auf Basis des Inventars zur Emissionsberichterstattung: Forschungskennzahl 3712 63 240 2, Texte, 71, 5, 2016

Steinbrecher, R., Smiatek, G., Köble, R., Seufert, G., Theloke, J., Hauff, K., Ciccioli, P., Vautard, R., & Curci, G. (2009). Intra- and inter-annual variability of VOC emissions from natural and semi-natural vegetation in Europe and neighbouring countries. Atmospheric Environment, 43(7), 1380–1391. https://doi.org/10.1016/j.atmosenv.2008.09.072

Suarez-Bertoa, R., Astorga, C., 2018. Impact of cold temperature on Euro 6 passenger car emissions. Environ. Pollut. 234, 318–329. https://doi.org/10.1016/J. ENVPOL.2017.10.096

Thürkow, M., Banzhaf, S., Butler, T., Pültz, J., & Schaap, M. (2023). Source attribution of nitrogen oxides across Germany : Comparing the labelling approach and brute force technique with LOTOS-EUROS. Atmospheric Environment, 292(September 2022), 119412. https://doi.org/10.1016/j.atmosenv.2022.119412

Timmermans, R., Kranenburg, R., Manders, A., Hendriks, C., Segers, A., Dammers, E., Zhang, Q., Wang, L., Liu, Z., Zeng, L., Gon, H. D. Van Der, & Schaap, M. (2017). Source apportionment of PM2 . 5 across China using LOTOS-EUROS. Atmospheric Environment, 164, 370–386. https://doi.org/10.1016/j.atmosenv.2017.06.003

Timmermans, R., Pinxteren, D. Van, Kranenburg, R., Hendriks, C., Fomba, K. W., Herrmann, H., & Schaap, M. (2022). Atmospheric Environment : X Evaluation of modelled LOTOS-EUROS with observational based PM10 source attribution. Atmospheric Environment: X, 14(January), 100173. https://doi.org/10.1016/j.aeaoa.2022.100173

Walcek, C. J., & Aleksic, N. M. (1998). A simple but accurate mass conservative, peak-preserving, mixing ratio bounded advection algorithm with FORTRAN code. Atmospheric Environment, 32(22), 3863-3880. https://doi.org/10.1016/S1352-2310(98)00099-5

Whitten, D. G. (1980). Photoinduced Electron-Transfer Reactions of Metal Complexes in Solution. Accounts of Chemical Research, 13(3), 83–90. https://doi.org/10.1021/ar50147a004

Wichink Kruit, R. J., Schaap, M., Sauter, F. J., Van Zanten, M. C., & Van Pul, W. A. J. (2012). Modeling the distribution of ammonia across Europe including bi-directional surface-atmosphere exchange. Biogeosciences, 9(12), 5261–5277. https://doi.org/10.5194/bg-9-5261-2012

Weilenmann, M., Favez, J.Y., Alvarez, R., 2009. Cold-start emissions of modern passenger cars at different low ambient temperatures and their evolution over vehicle legislation categories. Atmos. Environ. 43, 2419–2429. https://doi.org/10.1016/j.atmosenv.2009.02.005

Zanten, M. C. van, Sauter, F. J., Wichink Kruit, R. J., Jaarsveld, J. A. van, Pul, W. A. J. van, & Wichink Kruit, R. J. (2010). Description of the DEPAC module. Dry deposition modelling with DEPAC_GCN2010.
http://www.rivm.nl/Documenten_en_publicaties/Wetenschappelijk/Rapporten/2010/oktober/Description_of_the_DEPAC_module_Dry_deposition_modelling_with_DEPAC_GCN2010

7. APPENDIX

7.1. NO_2

7.1.1. Overview tables

Table 4 The absolute [µg/m^3] and relative (%) contribution of the various sectors to the NO_2 concentration in the city centres of the six cities examined in this study.

City / Sector	London		Paris		Amsterdam		Frankfurt am Main		Munich		Brussels	
	Abs.	Rel.	Abs.	Rel.	Abs.	Rel.	Abs.	Rel.	Abs.	Rel.	Abs.	Rel.
TOTAL	2.7E+1	100.0	3.0E+1	100.0	2.6E+1	100.0	2.9E+1	100.0	2.5E+1	100.0	2.7E+1	100.0
Energy	7.2E-1	2.7	5.3E-1	1.8	7.5E-1	2.9	1.3E+0	4.6	5.5E-1	2.2	1.0E+0	3.9
Refineries	4.6E-2	0.2	3.4E-2	0.1	1.7E-1	0.7	1.4E-1	0.5	1.1E-1	0.5	1.6E-1	0.62
Industry	1.5E+0	5.7	1.2E+0	3.9	2.1E+0	8.1	2.1E+0	7.2	8.0E-1	3.2	2.3E+0	8.8
Res. comb.	5.0E+0	18.6	1.1E+1	36.6	3.3E+0	13.0	4.6E+0	16.2	5.5E+0	21.8	5.7E+0	21.4
Fuel prod.	3.8E-2	0.1	7.1E-3	0.0	5.8E-2	0.2	1.9E-2	0.1	2.2E-2	0.1	2.1E-2	0.08
Solvent use	3.9E-2	0.1	1.7E-1	0.6	8.3E-2	0.3	2.1E-2	0.1	2.1E-2	0.1	4.6E-2	0.17
Road Transport - exhaust	1.4E+1	53.0	1.4E+1	45.5	1.0E+1	38.7	1.6E+1	54.4	1.5E+1	59.5	1.3E+1	48.4
Road Transport - non-exhaust	8.4E-4	0.0	8.5E-4	0.0	9.5E-3	0.0	6.8E-3	0.0	2.9E-3	0.0	3.8E-3	0.01
Inland Shipping	3.0E-2	0.1	4.9E-2	0.2	1.6E+0	6.2	2.8E-1	1.0	1.8E-2	0.1	3.7E-1	1.4
International Shipping	1.7E+0	6.4	1.3E+0	4.2	2.8E+0	10.9	4.3E-1	1.5	5.7E-2	0.2	1.8E+0	6.8
Aviation	4.4E-1	1.6	6.8E-1	2.3	1.2E+0	4.6	1.4E+0	5.0	1.2E-1	0.5	3.1E-1	1.2
Mobile machinery	2.6E+0	9.6	8.7E-1	2.9	3.2E+0	12.2	1.8E+0	6.4	2.2E+0	8.6	1.3E+0	5.0
Waste	9.9E-2	0.4	1.1E-1	0.4	4.1E-2	0.2	1.8E-2	0.1	1.7E-2	0.1	3.8E-2	0.14
Livestock	8.4E-4	0.0	8.5E-4	0.0	9.5E-3	0.0	8.5E-3	0.0	6.3E-3	0.0	3.8E-3	0.01
Manure and storage	9.2E-4	0.0	8.9E-4	0.0	9.5E-3	0.0	1.0E-1	0.4	1.4E-1	0.6	3.9E-3	0.01
Wildfire	3.9E-3	0.0	3.7E-3	0.0	2.7E-2	0.1	8.6E-3	0.0	6.8E-3	0.0	1.4E-2	0.05
Saharan Dust	8.4E-4	0.0	8.5E-4	0.0	9.5E-3	0.0	6.8E-3	0.0	2.9E-3	0.0	3.8E-3	0.01
Sea salt	8.4E-4	0.0	8.5E-4	0.0	9.5E-3	0.0	6.8E-3	0.0	2.9E-3	0.0	3.8E-3	0.01
Biogenic	3.0E-1	1.1	4.1E-1	1.4	3.8E-1	1.5	6.5E-1	2.3	5.4E-1	2.1	4.9E-1	1.85
Boundary	4.9E-2	0.2	1.2E-1	0.4	5.8E-2	0.2	8.2E-2	0.3	4.9E-2	0.2	6.0E-2	0.23

Table 5 The absolute [µg/m^3] and relative (%) contribution of the various sectors to the NO_2 concentration in the vicinity of the six airports examined in this study

Airport / Sector	London		Paris		Amsterdam		Frankfurt am Main		Munich		Brussels	
	Abs.	Rel.	Abs.	Rel.	Abs.	Rel.	Abs.	Rel.	Abs.	Rel.	Abs.	Rel.
TOTAL	3.1E+1	100.0	2.7E+1	100.0	3.1E+1	100.0	3.2E+1	100.0	2.1E+1	100.0	2.7E+1	100.0
Energy	7.3E-1	2.3	4.1E-1	1.5	7.0E-1	2.3	1.1E+0	3.4	5.1E-1	2.40	9.8E-1	3.7
Refineries	4.9E-2	0.15	3.2E-2	0.12	2.1E-1	0.7	9.1E-2	0.28	1.5E-1	0.69	1.6E-1	0.6
Industry	1.7E+0	5.5	9.9E-1	3.7	1.4E+0	4.7	1.8E+0	5.6	6.8E-1	3.20	2.2E+0	8.3
Res. comb.	2.1E+0	6.6	2.6E+0	9.8	2.0E+0	6.4	2.4E+0	7.3	1.5E+0	7.00	2.6E+0	9.8
Fuel prod.	3.2E-2	0.1	7.1E-3	0.03	5.7E-2	0.19	1.8E-2	0.06	2.1E-2	0.10	2.1E-2	0.08
Solvent use	1.5E-2	0.05	2.9E-2	0.11	7.3E-2	0.24	1.0E-2	0.03	4.6E-3	0.02	2.4E-2	0.09
Road Transport - exhaust	6.7E+0	21.0	5.3E+0	19.9	9.2E+0	29.8	1.6E+1	50.2	7.6E+0	35.9	1.0E+1	38.0
Road Transport - non-exhaust	1.1E-3	0.0	8.4E-4	0.0	1.1E-2	0.04	7.7E-3	0.02	3.8E-3	0.02	3.1E-3	0.01
Inland Shipping	2.6E-2	0.1	6.1E-2	0.2	1.1E+0	3.6	3.3E-1	1.0	2.2E-2	0.10	4.3E-1	1.6
International Shipping	1.1E+0	3.4	3.8E-1	1.4	3.1E+0	10.0	3.1E-1	0.97	6.2E-2	0.29	1.7E+0	6.3
Aviation	1.7E+1	54.9	1.6E+1	58.3	1.1E+1	35.4	8.3E+0	25.8	8.3E+0	39.2	6.8E+0	25.5
Mobile machinery	1.2E+0	3.9	6.7E-1	2.5	1.5E+0	4.6	9.2E-1	2.8	7.3E-1	3.50	9.5E-1	3.6

Waste	3.7E-2	0.12	5.2E-2	0.2	2.5E-2	0.08	1.4E-2	0.04	6.0E-3	0.03	2.4E-2	0.09
Livestock	1.1E-3	0.0	8.4E-4	0.0	1.1E-2	0.04	8.9E-3	0.03	2.5E-2	0.12	3.1E-3	0.01
Manure and storage	1.2E-3	0.0	8.9E-4	0.0	1.1E-2	0.04	9.9E-2	0.31	5.5E-1	2.60	3.2E-3	0.01
Wildfire	3.0E-3	0.01	2.6E-3	0.01	3.8E-2	0.12	1.0E-2	0.03	5.7E-3	0.03	1.3E-2	0.05
Saharan Dust	1.1E-3	0.0	8.4E-4	0.0	1.1E-2	0.04	7.7E-3	0.02	3.8E-3	0.02	3.1E-3	0.01
Sea salt	1.1E-3	0.0	8.4E-4	0.0	1.1E-2	0.04	7.7E-3	0.02	3.8E-3	0.02	3.1E-3	0.01
Biogenic	3.7E-1	1.2	5.3E-1	2.0	4.1E-1	1.3	5.7E-1	1.8	8.9E-1	4.20	5.3E-1	2.0
Boundary	4.5E-2	0.14	1.2E-1	0.44	5.9E-2	0.19	8.2E-2	0.25	4.5E-2	0.21	5.9E-2	0.22

7.2. SO_2

7.2.1. Overview tables

Table 6 The absolute [μg/m^3] and relative (%) contribution of the various sectors to the SO_2 concentration in the city centres of the six cities examined in this study

City / Sector	London		Paris		Amsterdam		Frankfurt am Main		Munich		Brussels	
	Abs.	Rel.	Abs.	Rel.	Abs.	Rel.	Abs.	Rel.	Abs.	Rel.	Abs.	Rel.
TOTAL	6.1E+0	100.0	6.1E+0	100.0	2.3E+0	100.0	3.4E+0	100.0	2.0E+0	100.0	6.0E+0	100.0
Energy	1.0E-1	1.64	1.7E-1	2.71	3.7E-1	15.92	5.9E-1	17.59	2.5E-1	12.42	3.5E-1	5.74
Refineries	1.2E-1	1.96	1.0E-1	1.71	3.3E-1	14.16	4.0E-1	11.76	1.5E-1	7.78	3.8E-1	6.32
Industry	6.2E-1	10.13	1.4E+0	23.48	1.0E+0	44.64	1.0E+0	30.36	3.8E-1	19.19	1.3E+0	21.13
Res. comb.	4.7E+0	77.8	4.2E+0	69.13	2.7E-1	11.76	1.2E+0	34.52	1.1E+0	55.05	3.8E+0	62.9
Fuel prod.	8.0E-3	0.13	9.6E-3	0.16	2.1E-2	0.89	7.9E-3	0.23	6.9E-3	0.35	6.0E-2	0.99
Solvent use	5.0E-3	0.08	5.0E-3	0.08	1.2E-2	0.53	1.6E-2	0.47	1.5E-2	0.76	7.3E-3	0.12
Road Transport - exhaust	8.7E-2	1.42	4.2E-2	0.68	3.3E-2	1.41	3.8E-2	1.13	3.3E-2	1.69	2.7E-2	0.44
Road Transport - non-exhaust	0.0E+0	0.0	0.0E+0	0.0	0.0E+0	0.0	0.0E+0	0.0	0.0E+0	0.0	0.0E+0	0.0
Inland Shipping	1.3E-5	0.0	3.7E-5	0.0	7.5E-4	0.03	6.6E-5	0.0	2.6E-5	0.0	1.4E-4	0.0
International Shipping	5.6E-2	0.92	2.2E-2	0.36	9.0E-2	3.86	8.5E-3	0.25	3.3E-3	0.17	6.7E-2	1.11
Aviation	7.2E-2	1.18	7.2E-2	1.19	1.3E-1	5.41	9.3E-2	2.78	7.2E-3	0.37	2.4E-2	0.41
Mobile machinery	2.2E-1	3.68	4.5E-3	0.07	7.0E-3	0.3	1.3E-2	0.39	2.0E-2	0.99	2.2E-2	0.37
Waste	5.1E-2	0.83	1.8E-2	0.29	1.3E-2	0.56	2.9E-3	0.09	3.3E-3	0.17	2.5E-3	0.04
Livestock	0.0E+0	0.0	0.0E+0	0.0	0.0E+0	0.0	0.0E+0	0.0	0.0E+0	0.0	0.0E+0	0.0
Manure and storage	1.0E-5	0.0	8.9E-6	0.0	1.6E-5	0.0	4.9E-5	0.0	1.0E-4	0.01	2.0E-5	0.0
Wildfire	9.0E-4	0.01	8.7E-4	0.01	3.3E-3	0.14	5.2E-4	0.02	9.6E-4	0.05	2.1E-3	0.03
Saharan Dust	0.0E+0	0.0	0.0E+0	0.0	0.0E+0	0.0	0.0E+0	0.0	0.0E+0	0.0	0.0E+0	0.0
Sea salt	0.0E+0	0.0	0.0E+0	0.0	0.0E+0	0.0	0.0E+0	0.0	0.0E+0	0.0	0.0E+0	0.0
Biogenic	0.0E+0	0.0	0.0E+0	0.0	0.0E+0	0.0	0.0E+0	0.0	0.0E+0	0.0	0.0E+0	0.0
Boundary	1.1E-2	0.18	2.2E-2	0.36	1.4E-2	0.6	2.2E-2	0.65	1.1E-2	0.55	1.9E-2	0.31

Table 7 The absolute [μg/m^3] and relative (%) contribution of the various sectors to the SO_2 concentration in the vicinity of the six airports examined in this study

Airport / Sector	London		Paris		Amsterdam		Frankfurt am Main		Munich		Brussels	
	Abs.	Rel.	Abs.	Rel.	Abs.	Rel.	Abs.	Rel.	Abs.	Rel.	Abs.	Rel.
TOTAL	9.9E+0	100.0	6.0E+0	100.0	4.2E+0	100.0	3.1E+0	100.0	1.9E+0	100.0	5.1E+0	100.0
Energy	8.3E-2	0.8	1.4E-1	2.3	3.2E-1	7.7	5.0E-1	16.0	3.1E-1	16.0	3.5E-1	6.9
Refineries	1.0E-1	1.0	1.0E-1	1.7	4.0E-1	9.5	2.1E-1	6.8	2.2E-1	11.0	3.7E-1	7.1
Industry	5.7E-1	5.8	1.1E+0	19.0	7.5E-1	18.0	8.8E-1	29.0	3.6E-1	18.0	1.3E+0	25.4
Res. comb.	1.4E+0	14.0	7.1E-1	12.0	1.9E-1	4.5	4.4E-1	15.0	3.0E-1	16.0	1.8E+0	35.5
Fuel prod.	5.9E-3	0.1	9.8E-3	0.2	2.4E-2	0.6	8.4E-3	0.3	7.4E-3	0.4	5.4E-2	1.0
Solvent use	1.3E-3	0.0	6.2E-4	0.0	2.9E-3	0.1	4.6E-3	0.2	1.8E-3	0.1	3.2E-3	0.1
Road Transport - exhaust.	3.7E-2	0.4	1.4E-2	0.2	2.9E-2	0.7	4.2E-2	1.4	1.4E-2	0.7	2.6E-2	0.5

Road Transport - non-exhaust	0.0E+0	0.0	0.0E+0	0.0	0.0E+0	0.0	0.0E+0	0.0	0.0E+0	0.0	0.0E+0	0.0
Inland Shipping	7.2E-6	0.0	1.8E-5	0.0	4.3E-4	0.0	8.5E-5	0.0	2.7E-5	0.0	1.5E-4	0.0
International Shipping	4.3E-2	0.4	2.2E-2	0.4	1.0E-1	2.4	8.2E-3	0.3	3.5E-3	0.2	6.8E-2	1.2
Aviation	7.6E+0	76.0	3.9E+0	65.0	2.4E+0	56.0	9.3E-1	30.0	6.9E-1	36.0	1.1E+0	21.3
Mobile machinery	5.5E-2	0.6	2.1E-3	0.0	3.6E-3	0.1	5.6E-3	0.2	3.0E-3	0.2	2.0E-2	0.4
Waste	1.3E-2	0.1	5.4E-3	0.1	3.8E-3	0.1	2.0E-3	0.1	1.2E-3	0.1	2.1E-3	0.0
Livestock	0.0E+0	0.0	0.0E+0	0.0	0.0E+0	0.0	0.0E+0	0.0	0.0E+0	0.0	0.0E+0	0.0
Manure and storage	1.5E-5	0.0	9.8E-6	0.0	1.6E-5	0.0	4.7E-5	0.0	1.3E-4	0.0	2.4E-5	0.0
Wildfire	4.4E-4	0.0	6.4E-4	0.0	4.8E-3	0.1	6.5E-4	0.0	5.3E-4	0.0	2.0E-3	0.0
Saharan Dust	0.0E+0	0.0	0.0E+0	0.0	0.0E+0	0.0	0.0E+0	0.0	0.0E+0	0.0	0.0E+0	0.0
Sea salt	0.0E+0	0.0	0.0E+0	0.0	0.0E+0	0.0	0.0E+0	0.0	0.0E+0	0.0	0.0E+0	0.0
Biogenic	0.0E+0	0.0	0.0E+0	0.0	0.0E+0	0.0	0.0E+0	0.0	0.0E+0	0.0	0.0E+0	0.0
Boundary	9.4E-3	0.1	2.5E-2	0.4	1.4E-2	0.3	2.2E-2	0.7	9.4E-3	0.48	1.8E-2	0.4

7.2.2. London

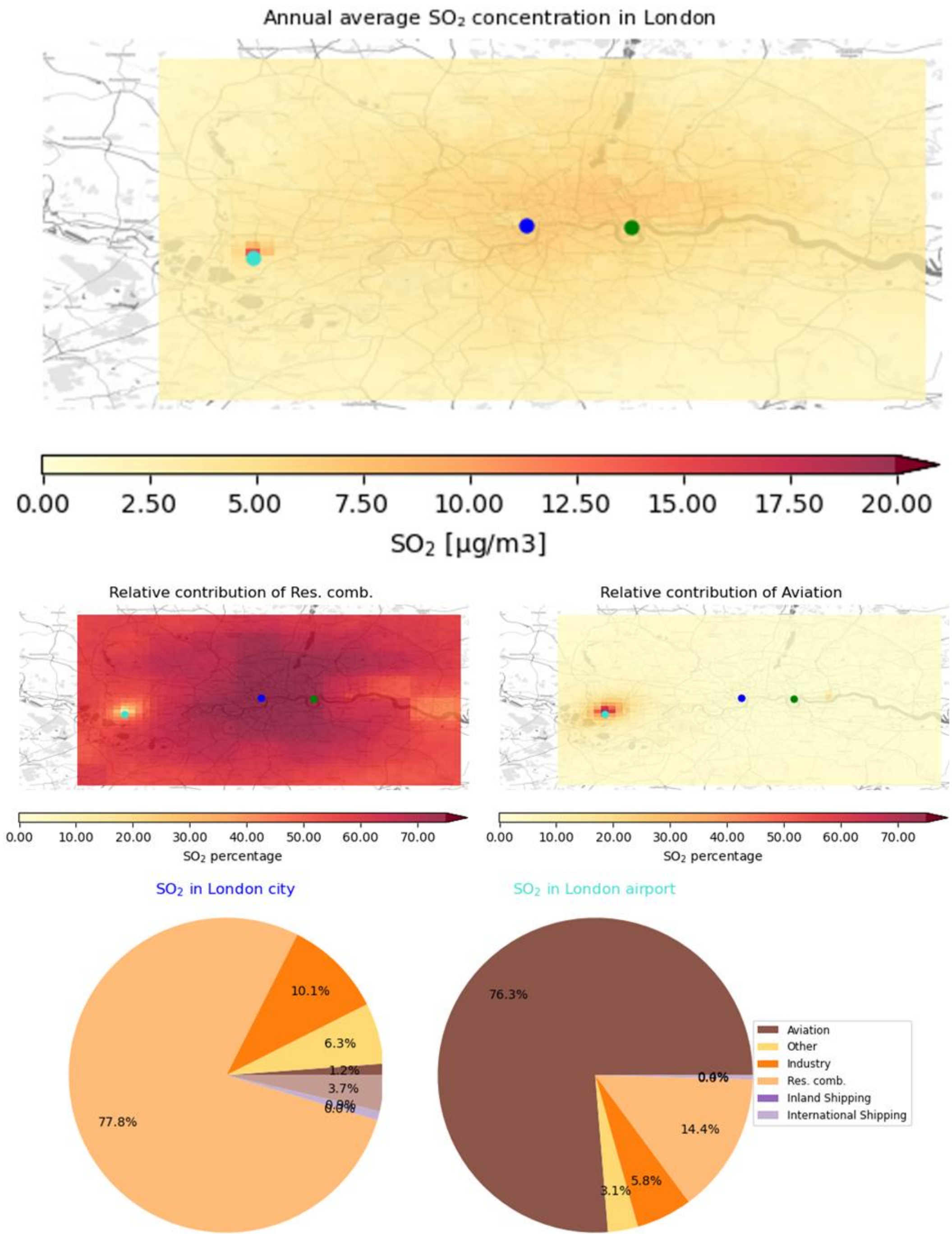

Figure 22 Predicted annual average SO_2 concentration in and around London (top panel) and the relative contributions of residential combustion (the largest anthropogenic contributor on average over the six cities) and aviation to this concentration in respectively the middle left and right panel. The bottom panel shows the contribution from various sectors to the SO_2 concentration in the city centre (left) and near the airport (right)

7.2.3. Paris

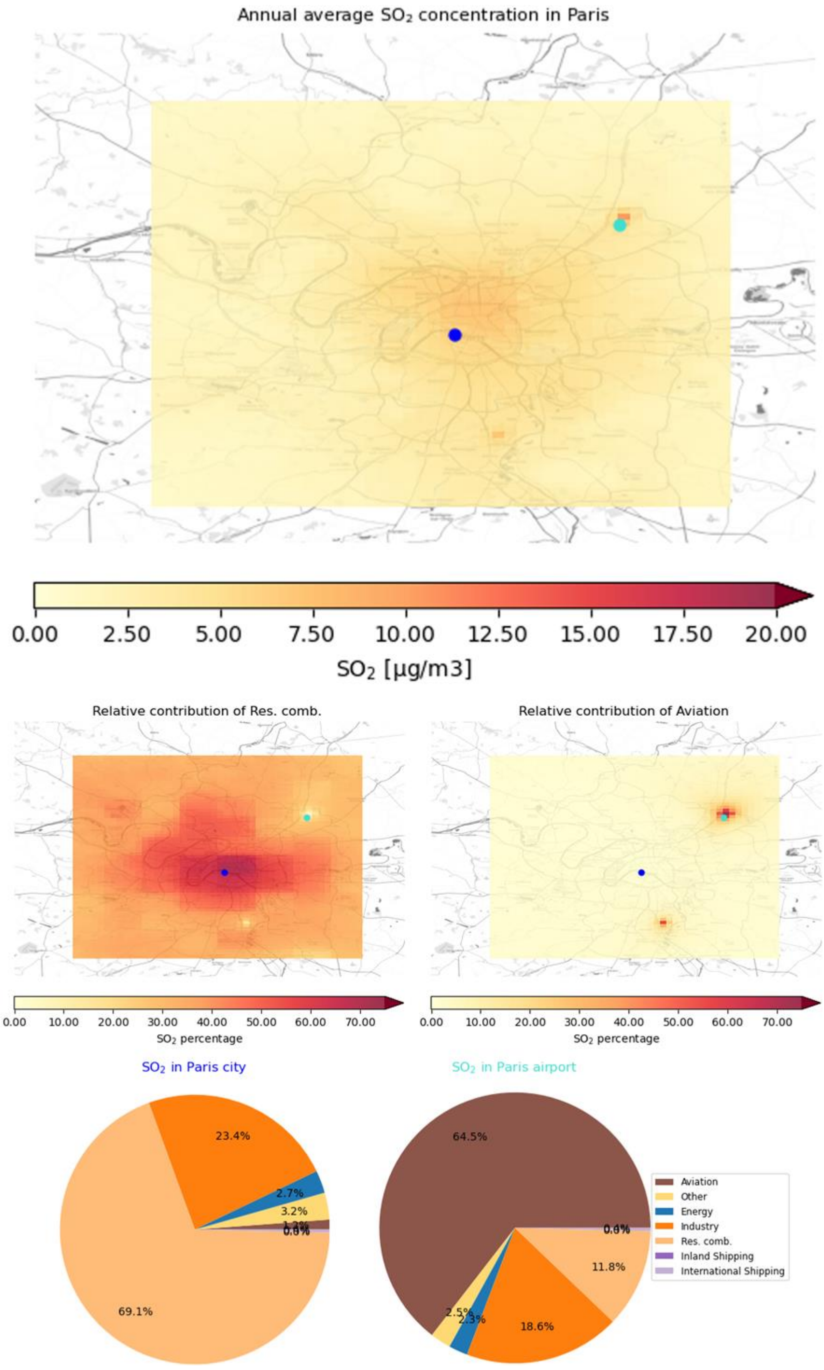

Figure 23 Predicted annual average SO_2 concentration in and around Paris (top panel) and the relative contributions of residential combustion (the largest anthropogenic contributor on average over the six cities) and aviation to this concentration in respectively the middle left and right panel. The bottom panel shows the contribution from various sectors to the SO_2 concentration in the city centre (left) and near the airport (right)

7.2.4. Amsterdam

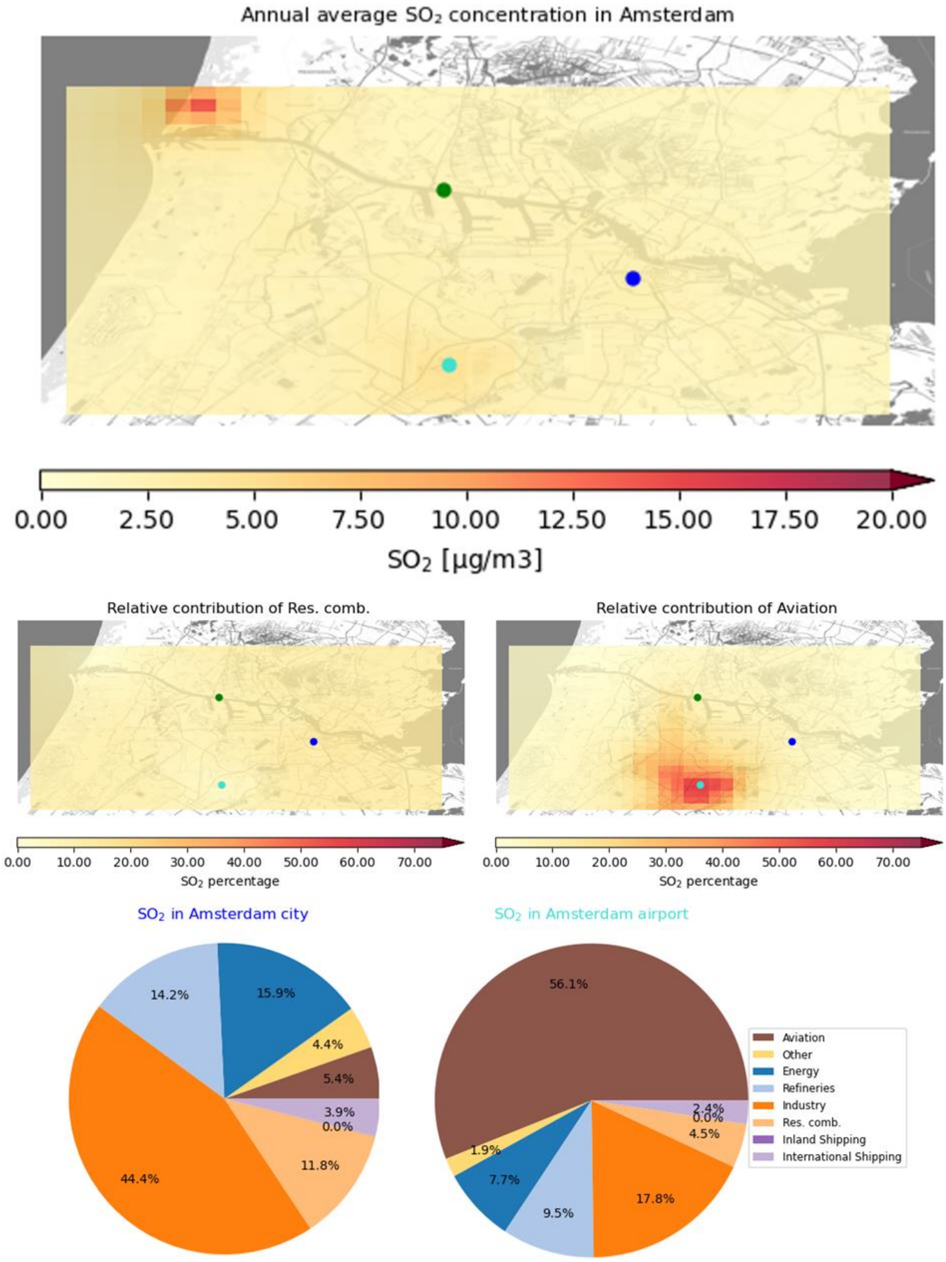

Figure 24 Predicted annual average SO_2 concentration in and around Amsterdam (top panel) and the relative contributions of residential combustion (the largest anthropogenic contributor on average over the six cities) and aviation to this concentration in respectively the middle left and right panel. The bottom panel shows the contribution from various sectors to the SO_2 concentration in the city centre (left) and near the airport (right)

7.2.5. Frankfurt am Main

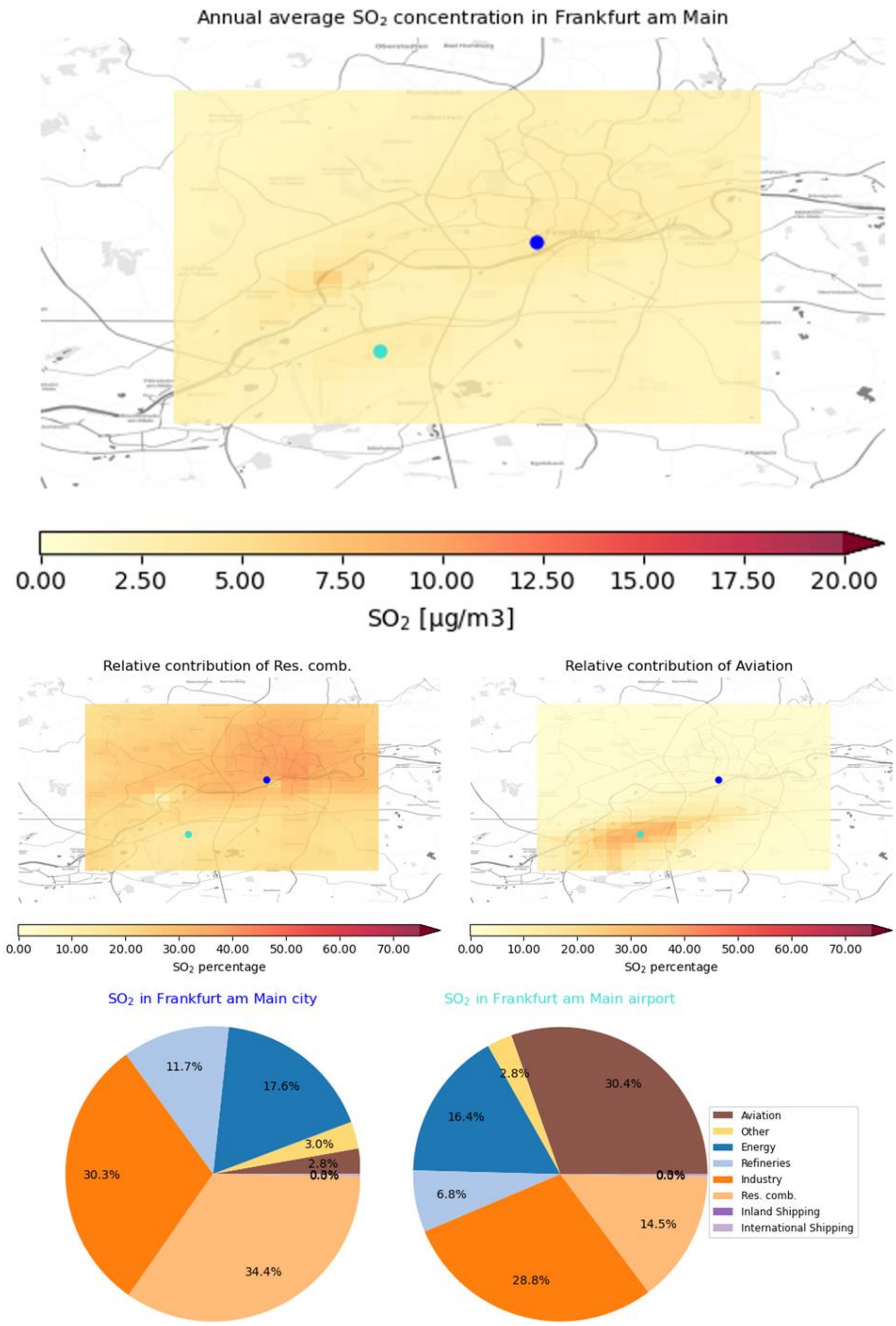

Figure 25 Predicted annual average SO_2 concentration in and around Frankfurt am Main (top panel) and the relative contributions of residential combustion (the largest anthropogenic contributor on average over the six cities) and aviation to this concentration in respectively the middle left and right panel. The bottom panel shows the contribution from various sectors to the SO_2 concentration in the city centre (left) and near the airport (right)

7.2.6. Munich

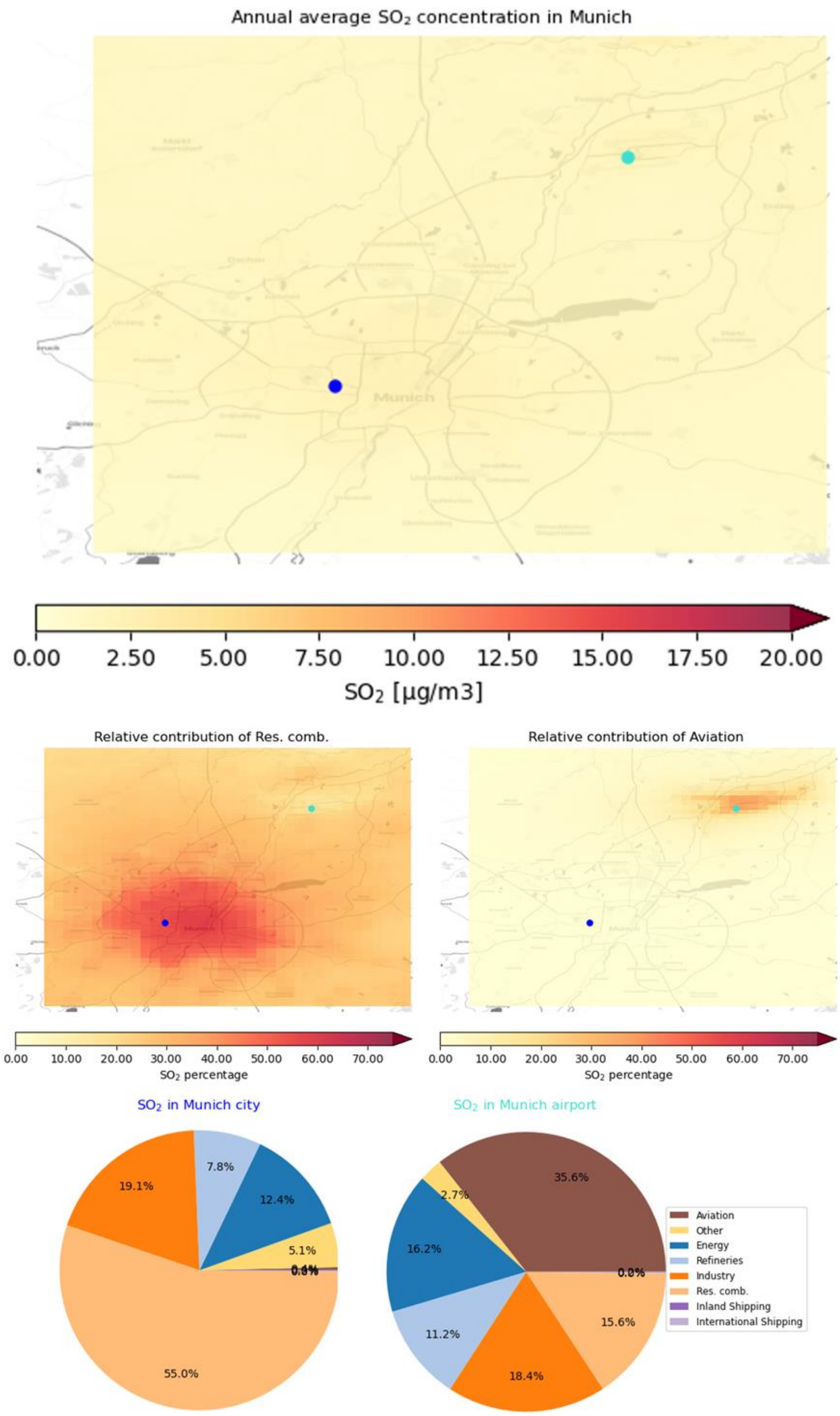

Figure 26 Predicted annual average SO_2 concentration in and around Munich (top panel) and the relative contributions of residential combustion (the largest anthropogenic contributor on average over the six cities) and aviation to this concentration in respectively the middle left and right panel. The bottom panel shows the contribution from various sectors to the SO_2 concentration in the city centre (left) and near the airport (right)

7.2.7. Brussels

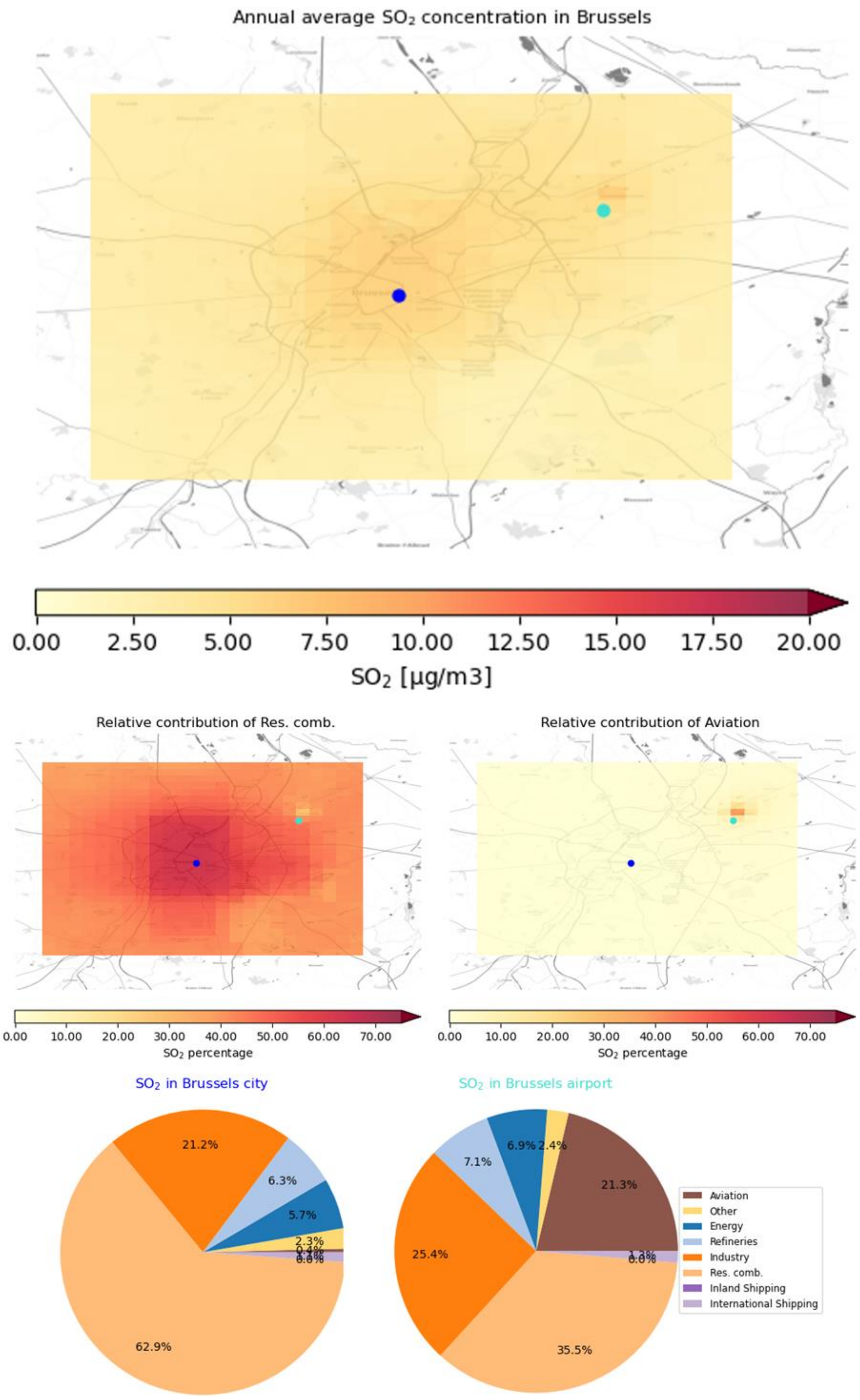

Figure 27 Predicted annual average SO_2 concentration in and around Brussels (top panel) and the relative contributions of residential combustion (the largest anthropogenic contributor on average over the six cities) and aviation to this concentration in respectively the middle left and right panel. The bottom panel shows the contribution from various sectors to the SO_2 concentration in the city centre (left) and near the airport (right)

7.3. $PM_{2.5}$

7.3.1. Overview tables

Table 8 The absolute [$\mu g/m^3$] and relative (%) contribution of the various sectors to the $PM_{2.5}$ concentration in the city centres of the six cities examined in this study

City / Sector	London		Paris		Amsterdam		Frankfurt am Main		Munich		Brussels	
	Abs.	Rel.	Abs.	Rel.	Abs.	Rel.	Abs.	Rel.	Abs.	Rel.	Abs.	Rel.
TOTAL	1.2E+1	100.0	1.9E+1	100.0	1.2E+1	100.0	1.4E+1	100.0	1.4E+1	100.0	1.4E+1	100.0
Energy	3.7E-1	3.15	3.8E-1	2.02	6.0E-1	4.99	7.2E-1	5.25	6.5E-1	4.64	5.4E-1	3.94
Refineries	1.0E-1	0.89	1.2E-1	0.62	1.5E-1	1.28	1.3E-1	0.97	1.6E-1	1.11	1.6E-1	1.17
Industry	1.6E+0	13.33	2.1E+0	11.11	1.8E+0	15.25	2.5E+0	18.54	1.8E+0	12.57	1.8E+0	13.53
Res. comb.	2.2E+0	18.63	4.0E+0	21.05	1.5E+0	12.42	3.5E+0	25.84	3.8E+0	27.14	3.4E+0	24.63
Fuel prod.	4.0E-2	0.34	2.2E-2	0.12	5.8E-2	0.48	3.5E-2	0.26	3.4E-2	0.24	4.1E-2	0.3
Solvent use	8.1E-1	6.91	3.7E-1	1.95	1.2E+0	10.17	8.9E-1	6.48	8.3E-1	5.91	4.8E-1	3.52
Road Transport - exhaust	1.2E+0	10.34	1.8E+0	9.58	1.5E+0	12.5	1.9E+0	13.94	2.5E+0	17.57	1.6E+0	11.47
Road Transport - non-exhaust	1.2E+0	9.83	1.2E+0	6.53	3.3E-1	2.78	4.1E-1	2.96	3.3E-1	2.34	8.1E-1	5.93
Inland Shipping	3.1E-2	0.27	5.3E-2	0.28	2.0E-1	1.63	7.3E-2	0.53	2.7E-2	0.19	1.2E-1	0.85
International Shipping	7.3E-1	6.22	4.7E-1	2.47	9.7E-1	8.08	2.9E-1	2.08	1.7E-1	1.21	7.4E-1	5.46
Aviation	5.0E-2	0.43	9.0E-2	0.47	6.7E-2	0.56	6.9E-2	0.51	5.6E-2	0.4	4.6E-2	0.34
Mobile machinery	4.6E-1	3.91	4.0E-1	2.13	5.5E-1	4.62	6.3E-1	4.62	8.9E-1	6.35	4.1E-1	3.04
Waste	8.3E-1	7.09	5.8E+0	30.37	4.4E-1	3.68	1.9E-1	1.35	1.5E-1	1.07	8.6E-1	6.3
Livestock	1.9E-1	1.65	3.4E-1	1.77	4.4E-1	3.68	5.4E-1	3.96	9.0E-1	6.41	6.7E-1	4.95
Manure and storage	3.3E-1	2.84	3.7E-1	1.94	4.7E-1	3.95	4.4E-1	3.22	4.5E-1	3.21	5.2E-1	3.85
Wildfire	3.3E-2	0.29	3.4E-2	0.18	1.0E-1	0.87	3.3E-2	0.24	4.3E-2	0.31	6.5E-2	0.48
Saharan Dust	7.9E-3	0.07	1.3E-2	0.07	9.4E-3	0.08	1.8E-2	0.13	3.4E-2	0.24	1.4E-2	0.1
Sea salt	7.4E-1	6.34	5.2E-1	2.74	7.2E-1	5.98	3.3E-1	2.43	1.8E-1	1.26	5.5E-1	4.04
Biogenic	1.2E-1	0.99	1.5E-1	0.81	1.7E-1	1.42	1.8E-1	1.31	2.6E-1	1.85	1.6E-1	1.21
Boundary	7.5E-1	6.4	8.3E-1	4.37	6.8E-1	5.66	7.1E-1	5.2	7.5E-1	5.35	7.1E-1	5.25

Table 9 The absolute [$\mu g/m^3$] and relative (%) contribution of the various sectors to the $PM_{2.5}$ concentration in the vicinity of the six airports examined in this study

Airport / Sector	London		Paris		Amsterdam		Frankfurt am Main		Munich		Brussels	
	Abs.	Rel.	Abs.	Rel.	Abs.	Rel.	Abs.	Rel.	Abs.	Rel.	Abs.	Rel.
TOTAL	1.1E+1	100.0	1.4E+1	100.0	1.1E+1	100.0	1.1E+1	100.0	1.1E+1	100.0	1.3E+1	100.0
Energy	3.6E-1	3.18	3.7E-1	2.61	5.8E-1	5.48	6.9E-1	6.12	7.1E-1	6.4	5.5E-1	4.19
Refineries	1.0E-1	0.89	1.2E-1	0.83	1.5E-1	1.45	1.3E-1	1.13	1.6E-1	1.48	1.5E-1	1.14
Industry	1.7E+0	14.82	1.7E+0	12.11	1.3E+0	11.89	1.8E+0	15.75	1.3E+0	11.62	1.9E+0	14.55
Res. comb.	2.4E+0	21.25	3.3E+0	23.38	1.4E+0	13.3	2.5E+0	22.39	2.3E+0	20.27	3.3E+0	25.23
Fuel prod.	3.7E-2	0.33	2.3E-2	0.16	5.5E-2	0.51	3.4E-2	0.3	4.0E-2	0.36	4.1E-2	0.31
Solvent use	3.7E-1	3.3	7.3E-2	0.51	4.3E-1	4.03	3.6E-1	3.15	1.7E-1	1.55	2.6E-1	1.94
Road Transport - exhaust	1.0E+0	9.02	1.3E+0	8.8	1.5E+0	13.87	1.9E+0	17.17	2.1E+0	19.19	1.6E+0	11.89
Road Transport - non-exhaust	6.6E-1	5.86	3.8E-1	2.7	3.0E-1	2.78	3.9E-1	3.43	2.2E-1	1.95	7.2E-1	5.47
Inland Shipping	2.8E-2	0.25	5.3E-2	0.37	1.6E-1	1.52	7.4E-2	0.65	3.3E-2	0.29	1.2E-1	0.94
International Shipping	6.6E-1	5.88	4.8E-1	3.38	9.6E-1	9.01	2.7E-1	2.4	1.8E-1	1.6	7.0E-1	5.33
Aviation	9.0E-1	8.04	2.6E+0	18.03	5.0E-1	4.75	2.7E-1	2.35	2.4E-1	2.17	2.3E-1	1.77
Mobile machinery	3.7E-1	3.29	3.2E-1	2.28	3.7E-1	3.46	4.4E-1	3.87	4.7E-1	4.21	4.1E-1	3.09
Waste	4.2E-1	3.76	8.6E-1	6.06	1.7E-1	1.61	1.7E-1	1.54	1.1E-1	1.03	4.4E-1	3.3
Livestock	2.6E-1	2.36	7.9E-1	5.57	5.3E-1	4.98	5.1E-1	4.48	1.2E+0	10.81	7.2E-1	5.47

Manure and storage	4.0E-1	3.55	4.2E-1	2.95	5.5E-1	5.2	4.3E-1	3.76	5.2E-1	4.64	5.4E-1	4.05
Wildfire	2.4E-2	0.22	2.9E-2	0.2	1.5E-1	1.37	3.7E-2	0.33	3.7E-2	0.33	6.4E-2	0.49
Saharan Dust	8.4E-3	0.08	1.3E-2	0.09	9.6E-3	0.09	1.8E-2	0.16	3.3E-2	0.3	1.4E-2	0.1
Sea salt	7.4E-1	6.64	5.1E-1	3.61	7.3E-1	6.88	3.3E-1	2.94	1.9E-1	1.72	5.4E-1	4.12
Biogenic	1.1E-1	1.02	1.8E-1	1.23	1.6E-1	1.54	1.7E-1	1.49	2.9E-1	2.59	1.7E-1	1.25
Boundary	7.5E-1	6.7	8.4E-1	5.91	6.8E-1	6.44	7.1E-1	6.3	7.5E-1	6.76	7.1E-1	5.38

7.3.2. London

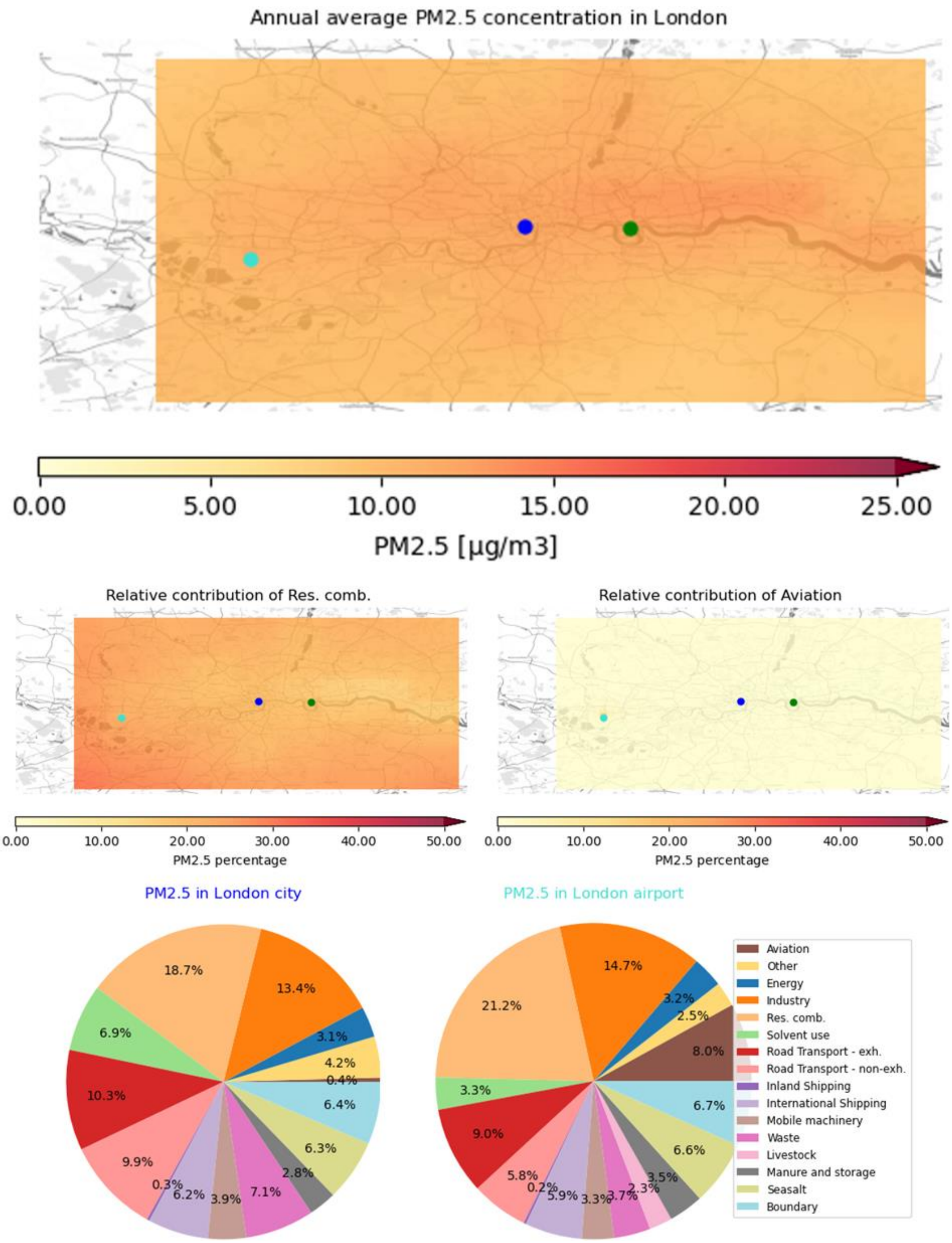

Figure 28 Predicted annual average $PM_{2.5}$ concentration in and around London (top panel) and the relative contributions from residential combustion (the largest anthropogenic contributor on average over the six cities) and aviation to this concentration in respectively the middle left and right panel. The bottom panel shows the contribution from various sectors to the $PM_{2.5}$ concentration in the city centre (left) and near the airport (right)

7.3.3. Paris

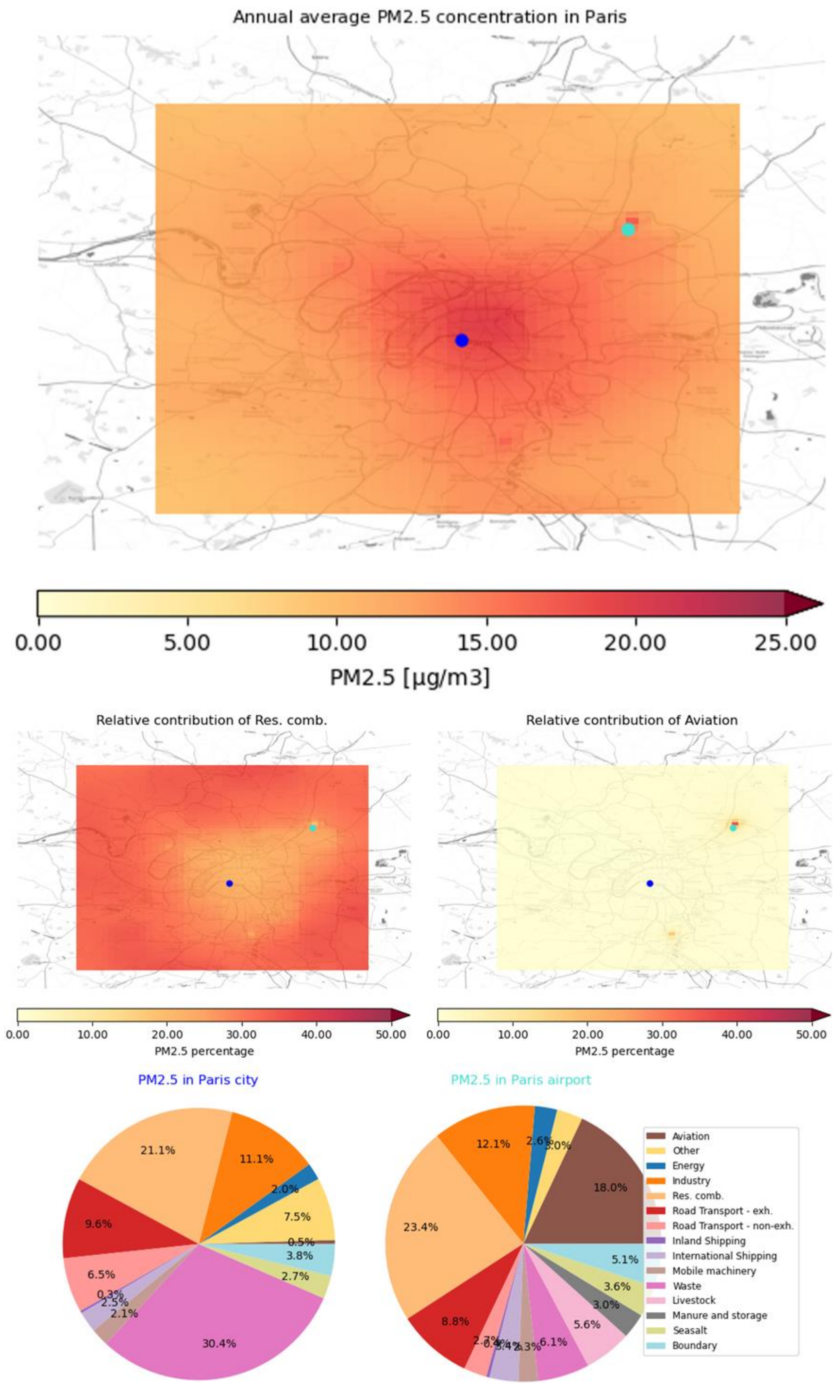

Figure 29 Predicted annual average $PM_{2.5}$ concentration in and around Paris (top panel) and the relative contributions from residential combustion (the largest anthropogenic contributor on average over the six cities) and aviation to this concentration in respectively the middle left and right panel. The bottom panel shows the contribution from various sectors to the $PM_{2.5}$ concentration in the city centre (left) and near the airport (right)

7.3.4. Amsterdam

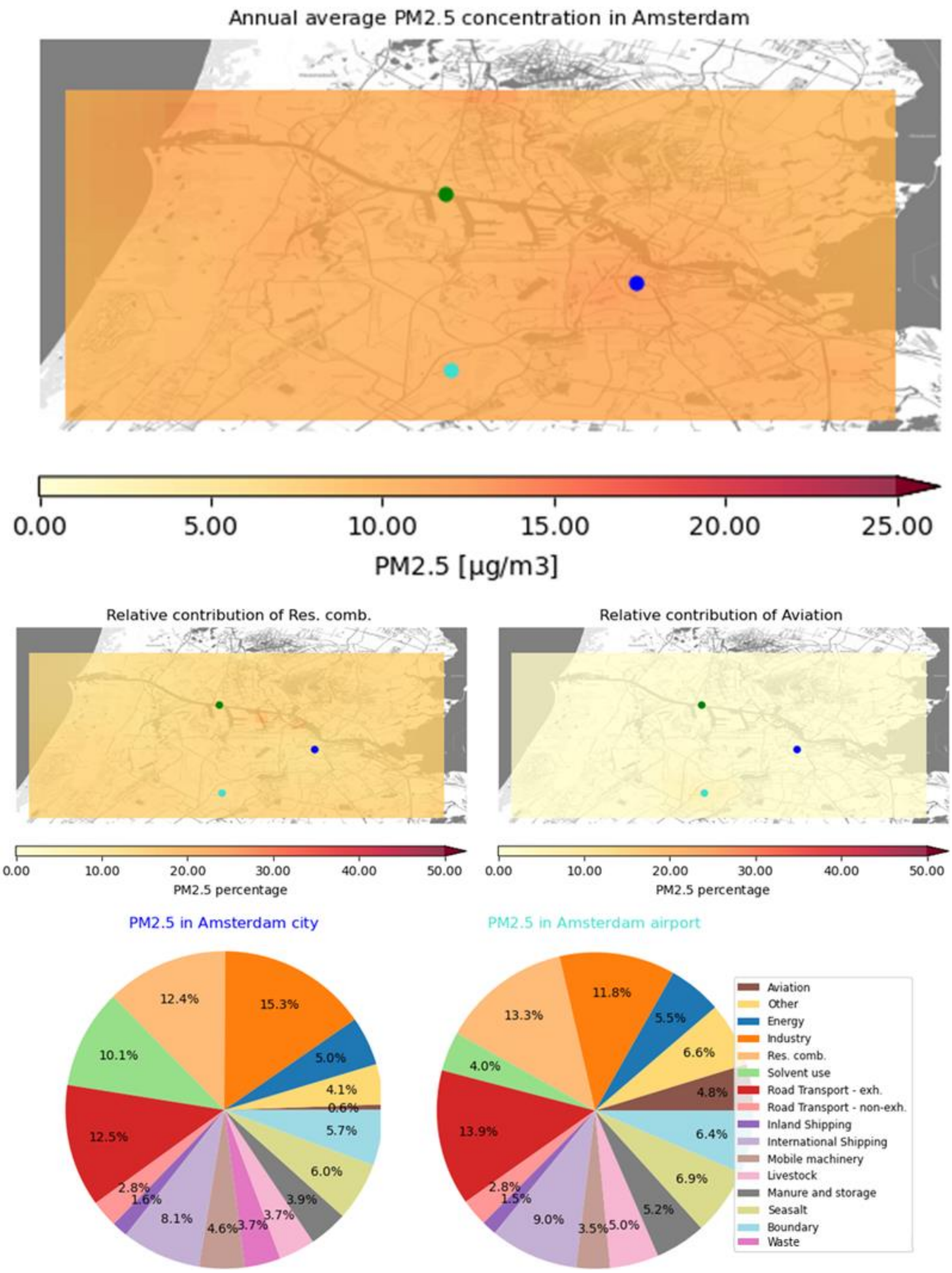

Figure 30 Predicted annual average $PM_{2.5}$ concentration in and around Amsterdam (top panel) and the relative contributions of residential combustion (the largest anthropogenic contributor on average over the six cities) and aviation to this concentration in respectively the middle left and right panel. The bottom panel shows the contribution from various sectors to the $PM_{2.5}$ concentration in the city centre (left) and near the airport (right)

7.3.5. Frankfurt am Main

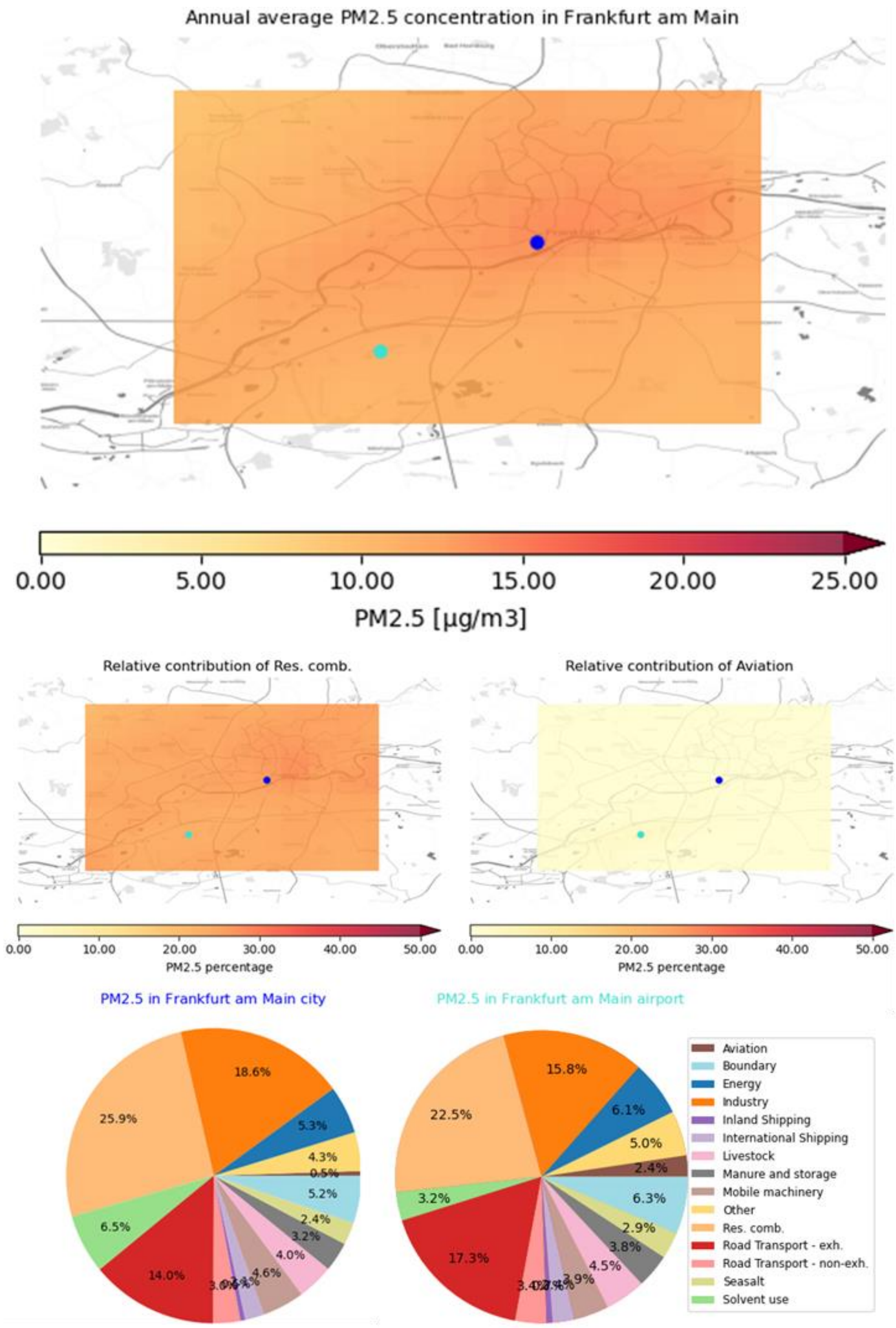

Figure 31 Predicted annual average $PM_{2.5}$ concentration in and around Frankfurt am Main (top panel) and the relative contributions from residential combustion (the largest anthropogenic contributor on average over the six cities) and aviation to this concentration in respectively the middle left and right panel. The bottom panel shows the contribution from various sectors to the $PM_{2.5}$ concentration in the city centre (left) and near the airport (right)

7.3.6. Munich

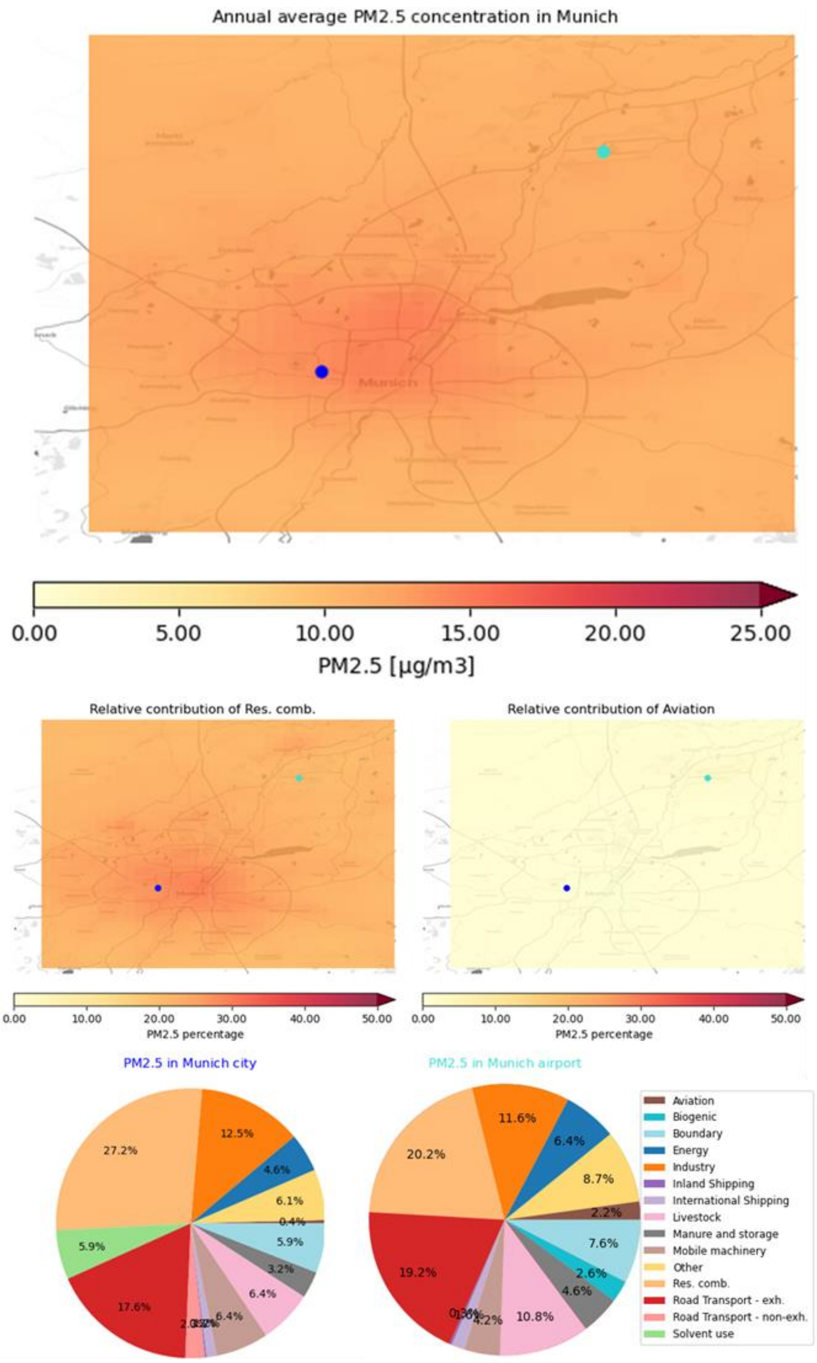

Figure 32 Predicted annual average $PM_{2.5}$ concentration in and around Munich (top panel) and the relative contributions from residential combustion (the largest anthropogenic contributor on average over the six cities) and aviation to this concentration in respectively the middle left and right panel. The bottom panel shows the contribution from various sectors to the $PM_{2.5}$ concentration in the city centre (left) and near the airport (right)

7.3.7. Brussels

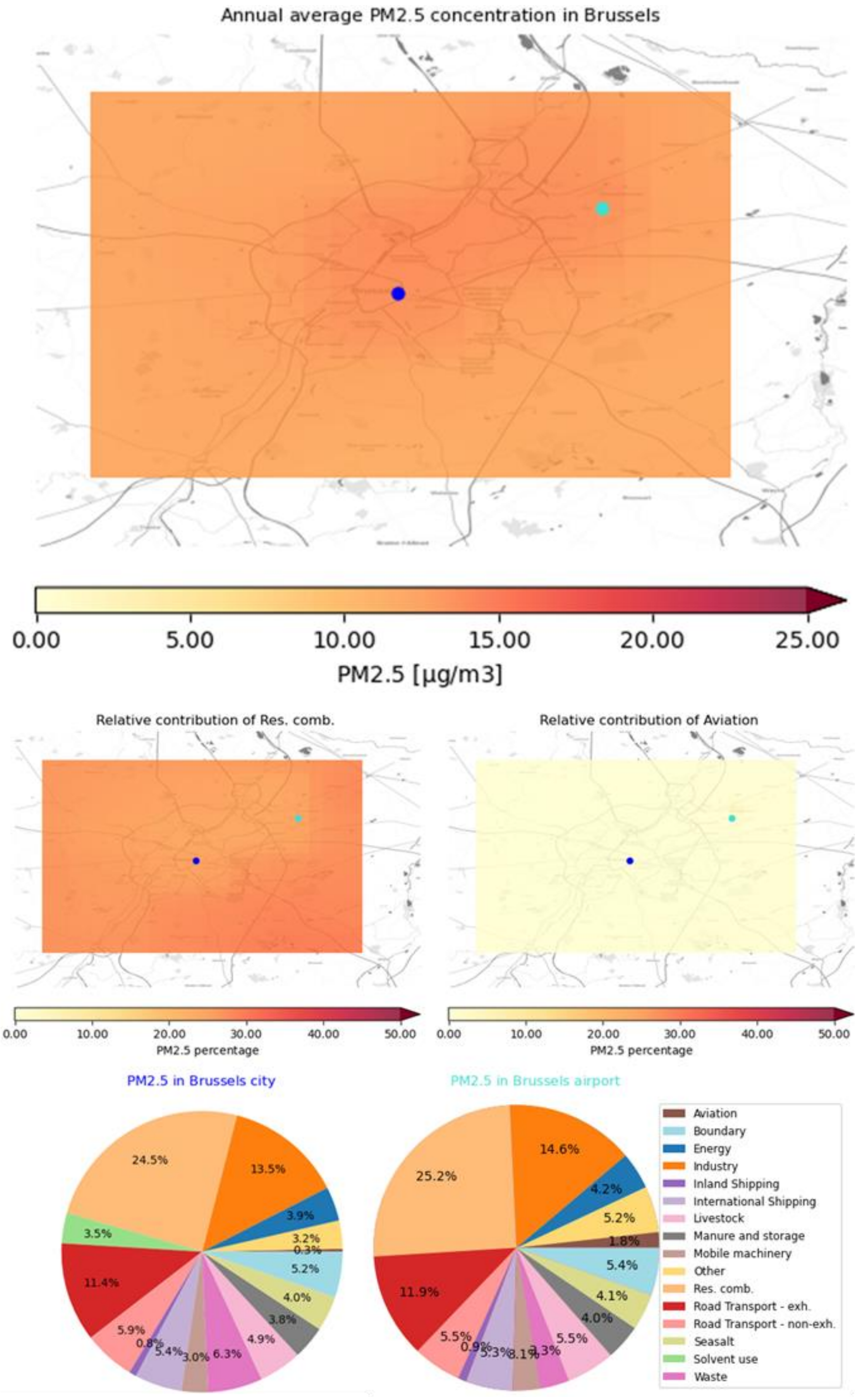

Figure 33 Predicted annual average $PM_{2.5}$ concentration in and around Brussels (top panel) and the relative contributions from residential combustion (the largest anthropogenic contributor on average over the six cities) and aviation to this concentration in respectively the middle left and right panel. The bottom panel shows the contribution from various sectors to the $PM_{2.5}$ concentration in the city centre (left) and near the airport (right)

7.4. PM_{10}

7.4.1. Overview tables

Table 10 The absolute [$\mu g/m^3$] and relative (%) contribution of the various sectors to the PM_{10} concentration in the city centres of the six cities examined in this study

City / Sector	London		Paris		Amsterdam		Frankfurt am Main		Munich		Brussels	
	Abs.	Rel.	Abs.	Rel.	Abs.	Rel.	Abs.	Rel.	Abs.	Rel.	Abs.	Rel.
TOTAL	2.4E+1	100.0	3.1E+1	100.0	2.2E+1	100.0	2.5E+1	100.0	2.1E+1	100.0	2.3E+1	100.0
Energy	4.4E-1	1.84	4.5E-1	1.44	6.9E-1	3.06	8.1E-1	3.32	7.0E-1	3.28	6.1E-1	2.64
Refineries	1.2E-1	0.49	1.3E-1	0.43	1.6E-1	0.73	1.4E-1	0.58	1.6E-1	0.76	1.7E-1	0.73
Industry	3.0E+0	12.43	3.8E+0	12.10	3.5E+0	15.45	7.5E+0	30.61	4.8E+0	22.54	3.1E+0	13.38
Res. comb.	2.3E+0	9.50	4.1E+0	13.29	1.7E+0	7.59	3.7E+0	15.14	4.0E+0	18.59	3.5E+0	14.94
Fuel prod.	7.2E-2	0.30	3.8E-2	0.12	1.1E-1	0.49	5.9E-2	0.24	4.5E-2	0.21	7.4E-2	0.32
Solvent use	9.7E-1	4.05	4.6E-1	1.47	1.2E+0	5.45	9.6E-1	3.92	8.9E-1	4.16	5.0E-1	2.17
Road Transport - exhaust	1.4E+0	5.86	2.0E+0	6.52	1.7E+0	7.63	2.1E+0	8.69	2.6E+0	12.25	1.8E+0	7.62
Road Transport - non-exhaust	3.9E+0	16.40	5.7E+0	18.39	1.5E+0	6.70	1.7E+0	6.90	1.3E+0	6.10	2.9E+0	12.47
Inland Shipping	3.7E-2	0.16	6.3E-2	0.20	2.1E-1	0.92	8.5E-2	0.35	3.2E-2	0.15	1.3E-1	0.55
International Shipping	1.0E+0	4.23	6.9E-1	2.23	1.3E+0	5.85	4.1E-1	1.67	2.2E-1	1.03	1.0E+0	4.33
Aviation	5.9E-2	0.25	1.1E-1	0.35	8.3E-2	0.37	8.9E-2	0.36	6.1E-2	0.29	5.5E-2	0.24
Mobile machinery	5.2E-1	2.18	5.2E-1	1.67	6.3E-1	2.80	8.5E-1	3.46	1.3E+0	6.06	5.3E-1	2.29
Waste	8.8E-1	3.69	5.8E+0	18.65	4.7E-1	2.10	2.2E-1	0.89	2.0E-1	0.92	8.6E-1	3.72
Livestock	2.3E-1	0.97	3.9E-1	1.25	5.3E-1	2.38	5.9E-1	2.42	9.4E-1	4.40	7.9E-1	3.43
Manure and storage	5.5E-1	2.28	7.3E-1	2.35	7.2E-1	3.21	8.4E-1	3.43	7.6E-1	3.58	9.3E-1	4.03
Wildfire	4.6E-2	0.19	4.6E-2	0.15	1.5E-1	0.66	4.1E-2	0.17	5.4E-2	0.25	8.9E-2	0.39
Saharan Dust	3.9E-2	0.16	7.5E-2	0.24	4.3E-2	0.19	8.1E-2	0.33	1.4E-1	0.67	6.0E-2	0.26
Sea salt	4.9E+0	20.54	3.1E+0	10.06	5.0E+0	22.28	1.9E+0	7.55	8.2E-1	3.83	3.4E+0	14.68
Biogenic	1.5E-1	0.64	2.0E-1	0.63	2.1E-1	0.93	2.1E-1	0.87	2.8E-1	1.33	2.0E-1	0.87
Boundary	3.3E+0	13.81	2.7E+0	8.58	2.5E+0	11.16	2.2E+0	8.98	2.0E+0	9.34	2.6E+0	11.13

Table 11 The absolute [$\mu g/m^3$] and relative (%) contribution of the various sectors to the PM_{10} concentration in the vicinity of the six airports examined in this study

Airport / Sector	London		Paris		Amsterdam		Frankfurt am Main		Munich		Brussels	
	Abs.	Rel.	Abs.	Rel.	Abs.	Rel.	Abs.	Rel.	Abs.	Rel.	Abs.	Rel.
TOTAL	2.2E+1	100.0	2.3E+1	100.0	2.0E+1	100.0	1.9E+1	100.0	1.6E+1	100.0	2.2E+1	100.0
Energy	4.3E-1	1.93	4.3E-1	1.89	6.6E-1	3.35	7.8E-1	4.08	7.7E-1	4.91	6.3E-1	2.84
Refineries	1.1E-1	0.51	1.3E-1	0.57	1.7E-1	0.83	1.4E-1	0.71	1.7E-1	1.08	1.6E-1	0.72
Industry	3.3E+0	15.07	2.9E+0	12.84	1.9E+0	9.55	4.1E+0	21.3	2.3E+0	14.68	3.3E+0	14.71
Res. comb.	2.5E+0	11.13	3.4E+0	14.85	1.5E+0	7.73	2.6E+0	13.75	2.3E+0	14.81	3.4E+0	15.52
Fuel prod.	6.7E-2	0.3	3.9E-2	0.17	1.1E-1	0.54	5.8E-2	0.3	5.2E-2	0.33	7.4E-2	0.34
Solvent use	4.3E-1	1.92	8.4E-2	0.37	4.3E-1	2.18	3.9E-1	2.03	1.8E-1	1.18	2.7E-1	1.21
Road Transport - exhaust	1.2E+0	5.43	1.5E+0	6.38	1.7E+0	8.48	2.2E+0	11.3	2.3E+0	14.68	1.8E+0	7.96
Road Transport - non-exhaust	2.1E+0	9.37	1.3E+0	5.55	1.2E+0	6.01	1.5E+0	7.92	4.5E-1	2.87	2.1E+0	9.41
Inland Shipping	3.3E-2	0.15	6.4E-2	0.28	1.7E-1	0.87	8.6E-2	0.45	3.8E-2	0.24	1.4E-1	0.62
International Shipping	9.3E-1	4.19	7.0E-1	3.05	1.3E+0	6.52	3.9E-1	2.02	2.3E-1	1.48	9.6E-1	4.33
Aviation	9.1E-1	4.12	3.3E+0	14.28	7.2E-1	3.62	4.0E-1	2.07	3.3E-1	2.14	2.9E-1	1.31
Mobile machinery	4.2E-1	1.91	4.1E-1	1.77	4.3E-1	2.18	5.6E-1	2.93	5.4E-1	3.43	5.2E-1	2.34
Waste	4.4E-1	2.0	8.7E-1	3.78	1.8E-1	0.9	2.0E-1	1.04	1.3E-1	0.83	4.4E-1	1.99
Livestock	3.1E-1	1.39	9.3E-1	4.05	6.1E-1	3.09	5.6E-1	2.89	1.3E+0	8.46	8.7E-1	3.92
Manure and storage	6.4E-1	2.9	8.9E-1	3.9	8.3E-1	4.21	8.2E-1	4.27	1.1E+0	6.86	1.0E+0	4.62

Wildfire	3.3E-2	0.15	3.8E-2	0.16	2.1E-1	1.05	4.7E-2	0.24	4.3E-2	0.28	8.8E-2	0.4
Saharan Dust	3.9E-2	0.18	7.3E-2	0.32	4.3E-2	0.22	8.3E-2	0.43	1.4E-1	0.88	6.0E-2	0.27
Sea salt	4.8E+0	21.86	3.1E+0	13.41	5.0E+0	25.2	1.8E+0	9.53	8.8E-1	5.63	3.4E+0	15.16
Biogenic	1.5E-1	0.68	2.2E-1	0.95	2.0E-1	1.02	2.0E-1	1.06	3.1E-1	2.01	2.0E-1	0.91
Boundary	3.3E+0	14.8	2.6E+0	11.5	2.5E+0	12.53	2.2E+0	11.46	2.5E+0	11.5	2.5E+0	11.49

7.4.2. London

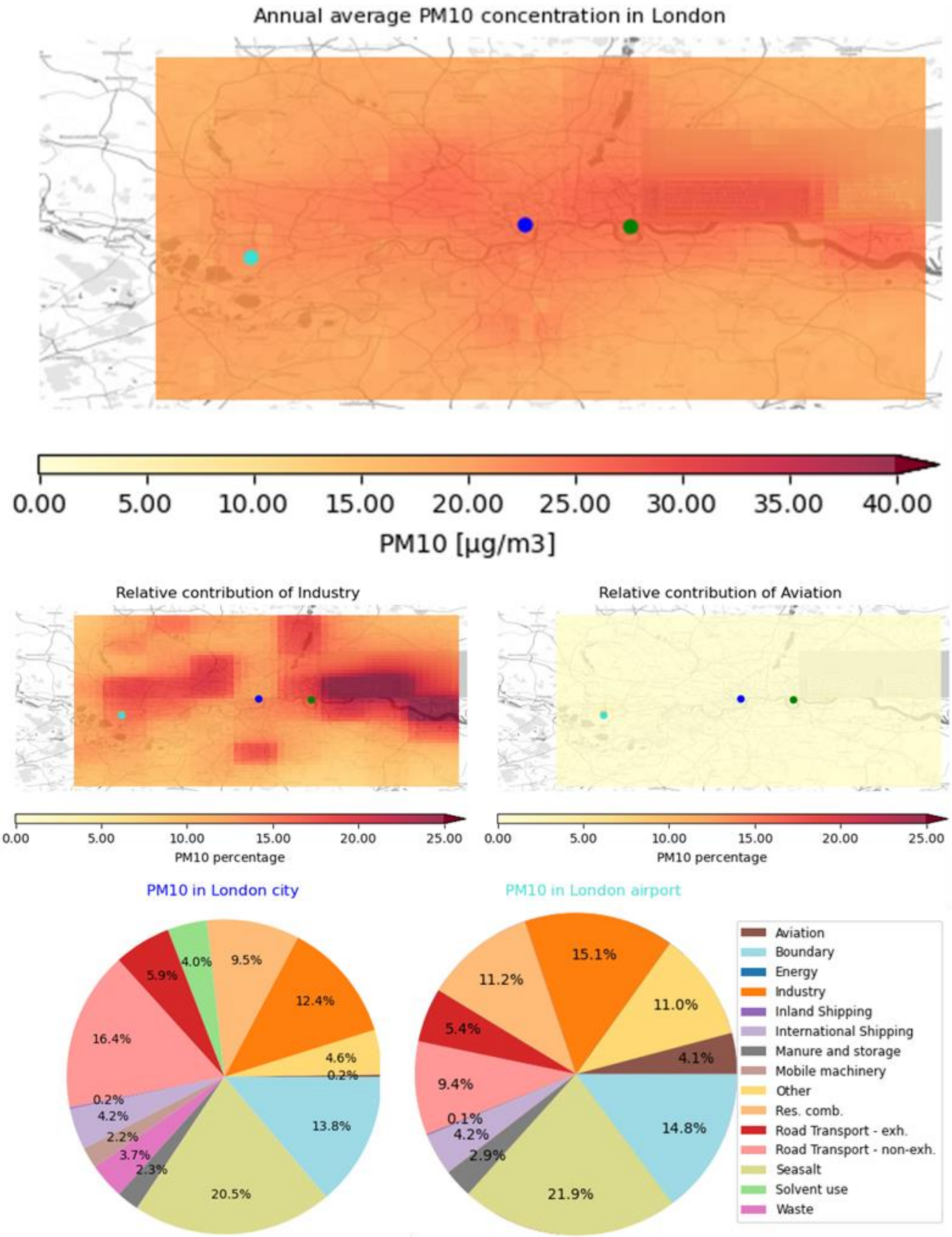

Figure 34 Predicted annual average PM_{10} concentration in and around London (top panel) and the relative contributions from industry (the largest anthropogenic contributor on average over the six cities) and aviation to this concentration in respectively the middle left and right panel. The bottom panel shows the contribution from various sectors to the concentration in the city centre (left) and near the airport (right)

7.4.3. Paris

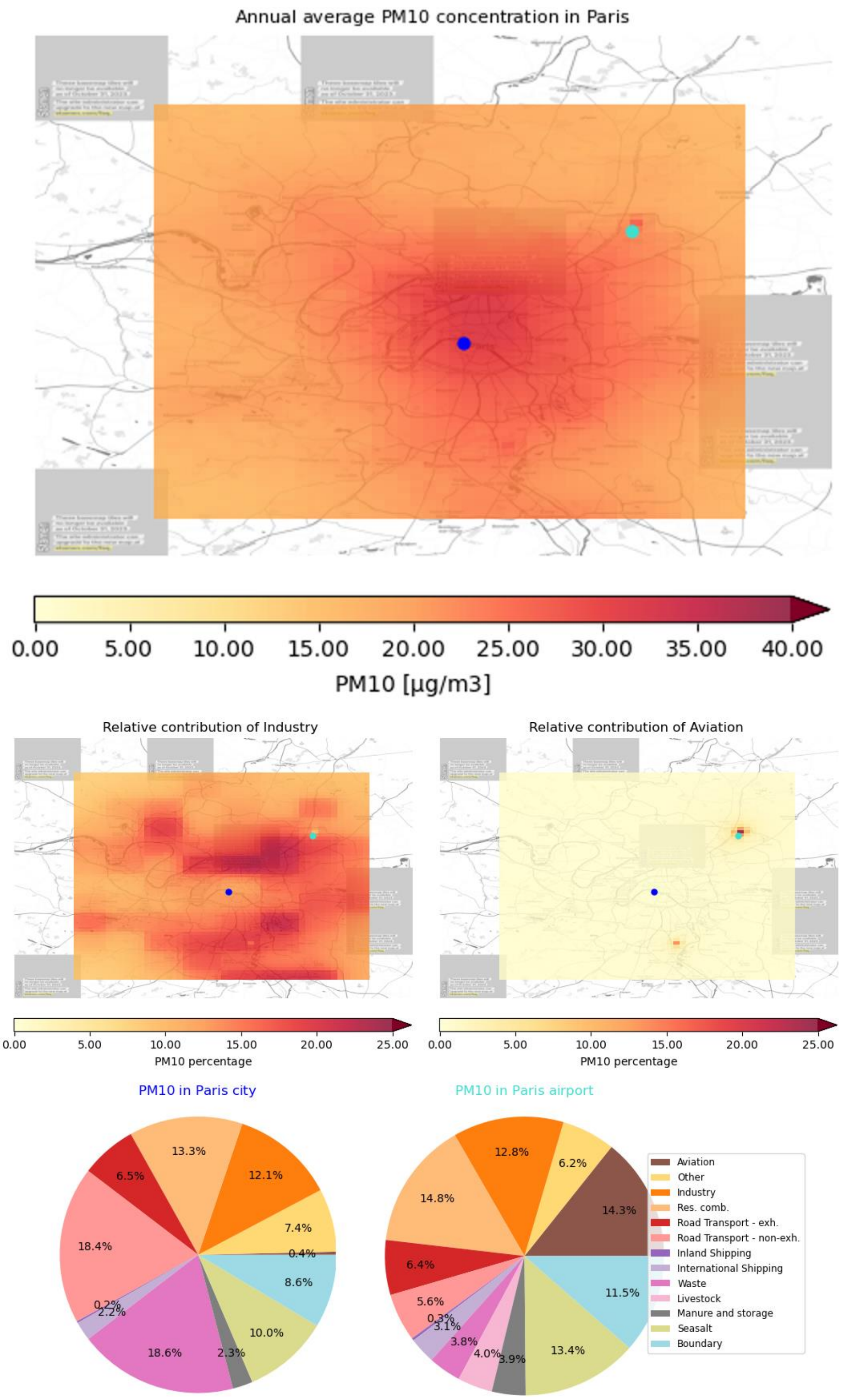

Figure 35 Predicted annual average PM_{10} concentration in and around Paris (top panel) and the relative contributions from industry (the largest anthropogenic contributor on average over the six cities) and aviation to this concentration in respectively the middle left and right panel. The bottom panel shows the contribution from various sectors to the concentration in the city centre (left) and near the airport (right)

7.4.4. Amsterdam

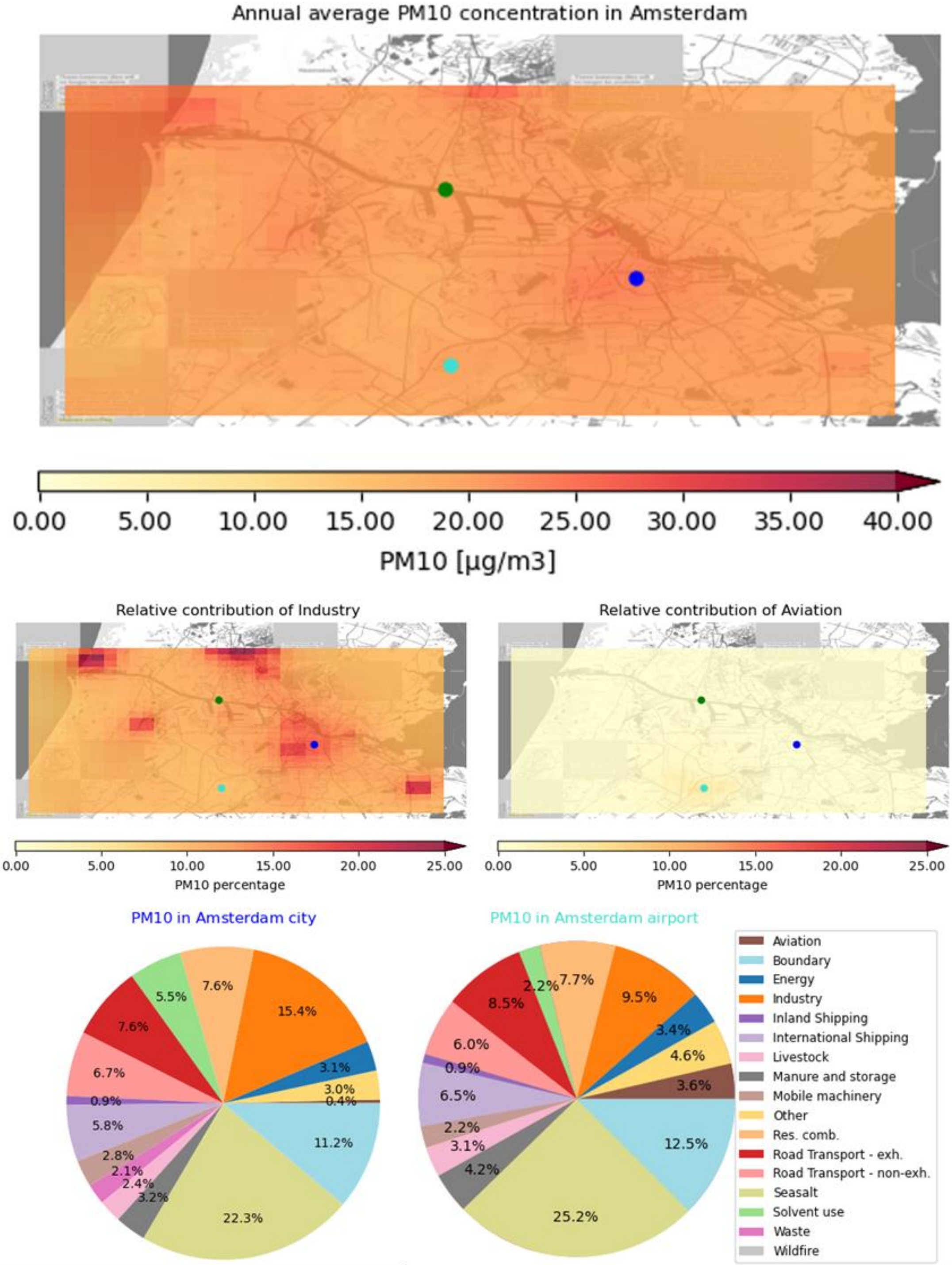

Figure 36 Predicted annual average PM_{10} concentration in and around Amsterdam (top panel) and the relative contributions from industry (the largest anthropogenic contributor on average over the six cities) and aviation to this concentration in respectively the middle left and right panel. The bottom panel shows the contribution from various sectors to the concentration in the city centre (left) and near the airport (right)

7.4.5. Frankfurt am Main

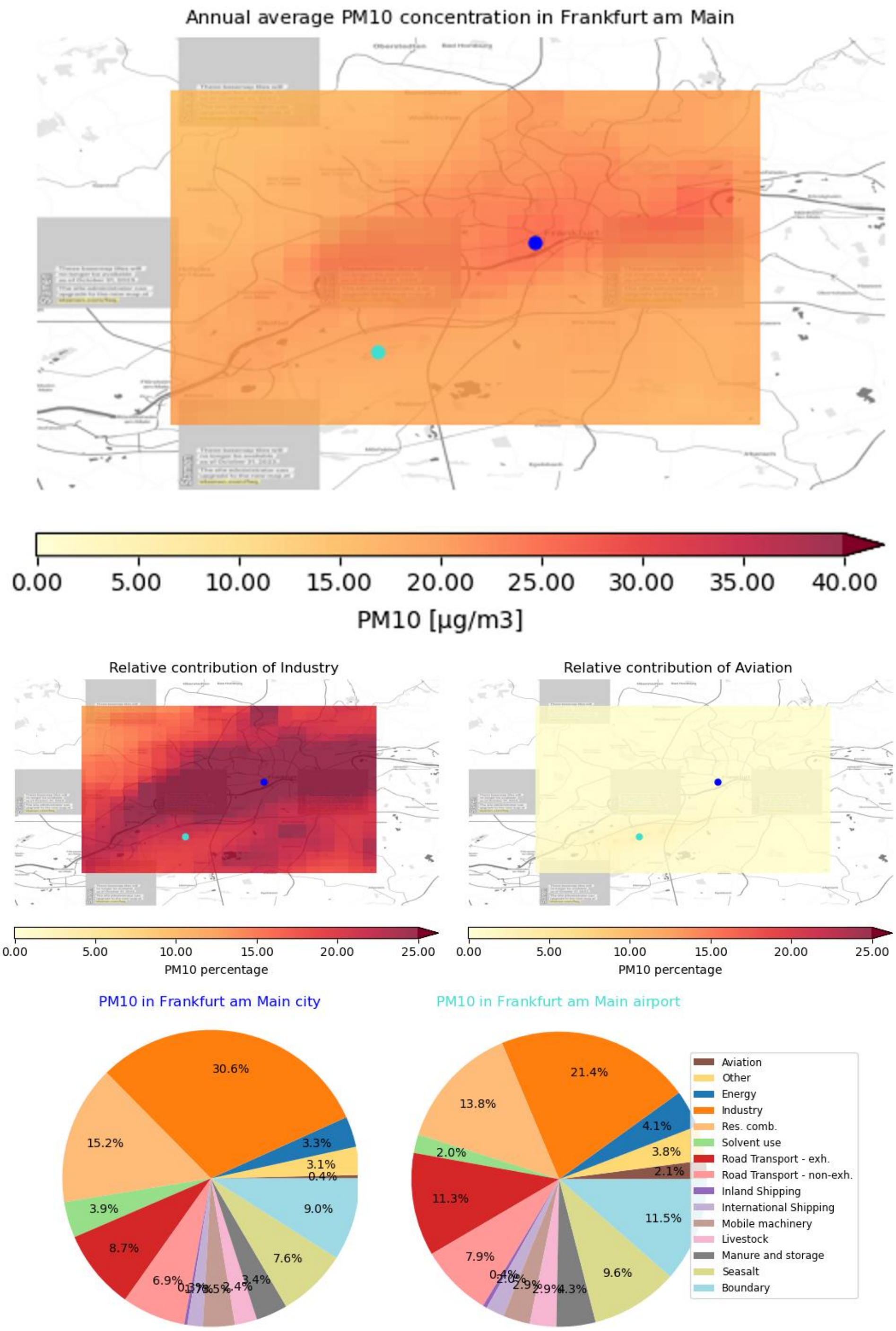

Figure 37 Predicted annual average PM_{10} concentration in and around Frankfurt am Main (top panel) and the relative contributions from industry (the largest anthropogenic contributor on average over the six cities) and aviation to this concentration in respectively the middle left and right panel. The bottom panel shows the contribution from various sectors to the concentration in the city centre (left) and near the airport (right)

7.4.6. Munich

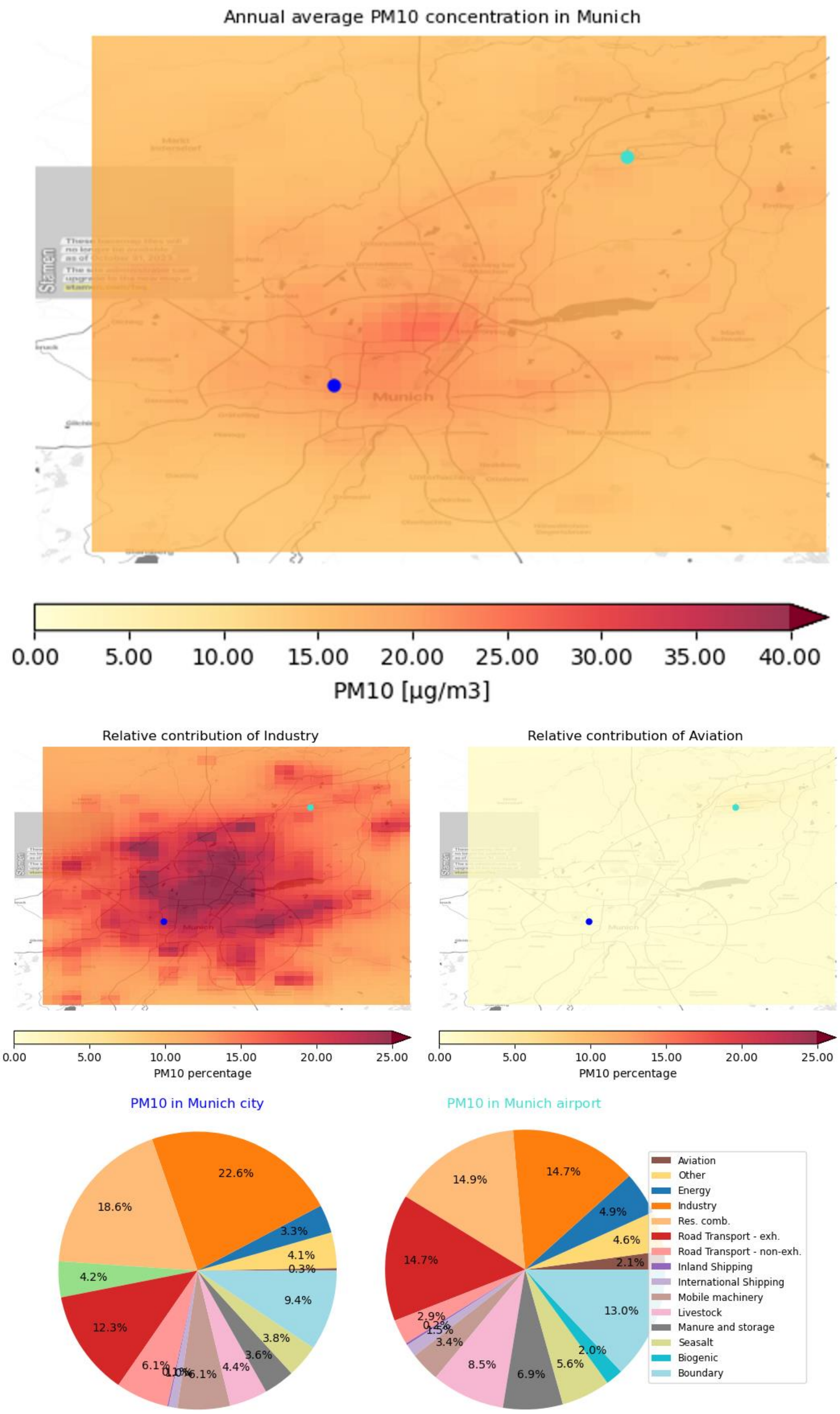

Figure 38 Predicted annual average PM_{10} concentration in and around Munich (top panel) and the relative contributions from industry (the largest anthropogenic contributor on average over the six cities) and aviation to this concentration in respectively the middle left and right panel. The bottom panel shows the contribution from various sectors to the concentration in the city centre (left) and near the airport (right)

7.4.7. Brussels

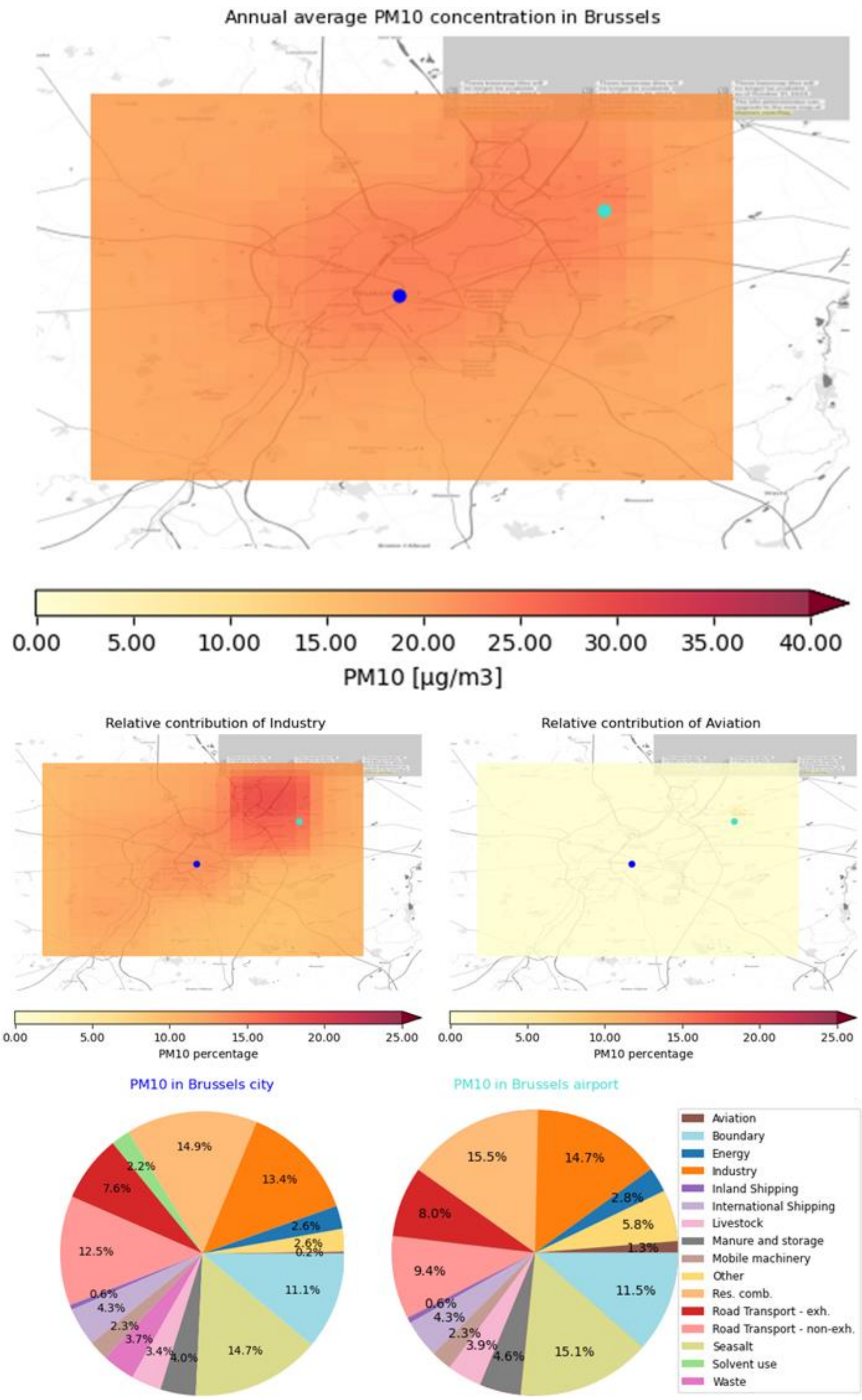

Figure 39 Predicted annual average PM_{10} concentration in and around Brussels (top panel) and the relative contributions from industry (the largest anthropogenic contributor on average over the six cities) and aviation to this concentration in respectively the middle left and right panel. The bottom panel shows the contribution from various sectors to the concentration in the city centre (left) and near the airport (right)

7.5. COMPARISON BETWEEN MODELS AND OBSERVATIONS FOR THE OTHER POLLUTANTS

The station annual mean values from observations and model results for SO_2, $PM_{2.5}$ and PM_{10} respectively are shown on the left panels and the underlying networks of stations with measurements for at least 50% of the days in 2018 on the right panels.

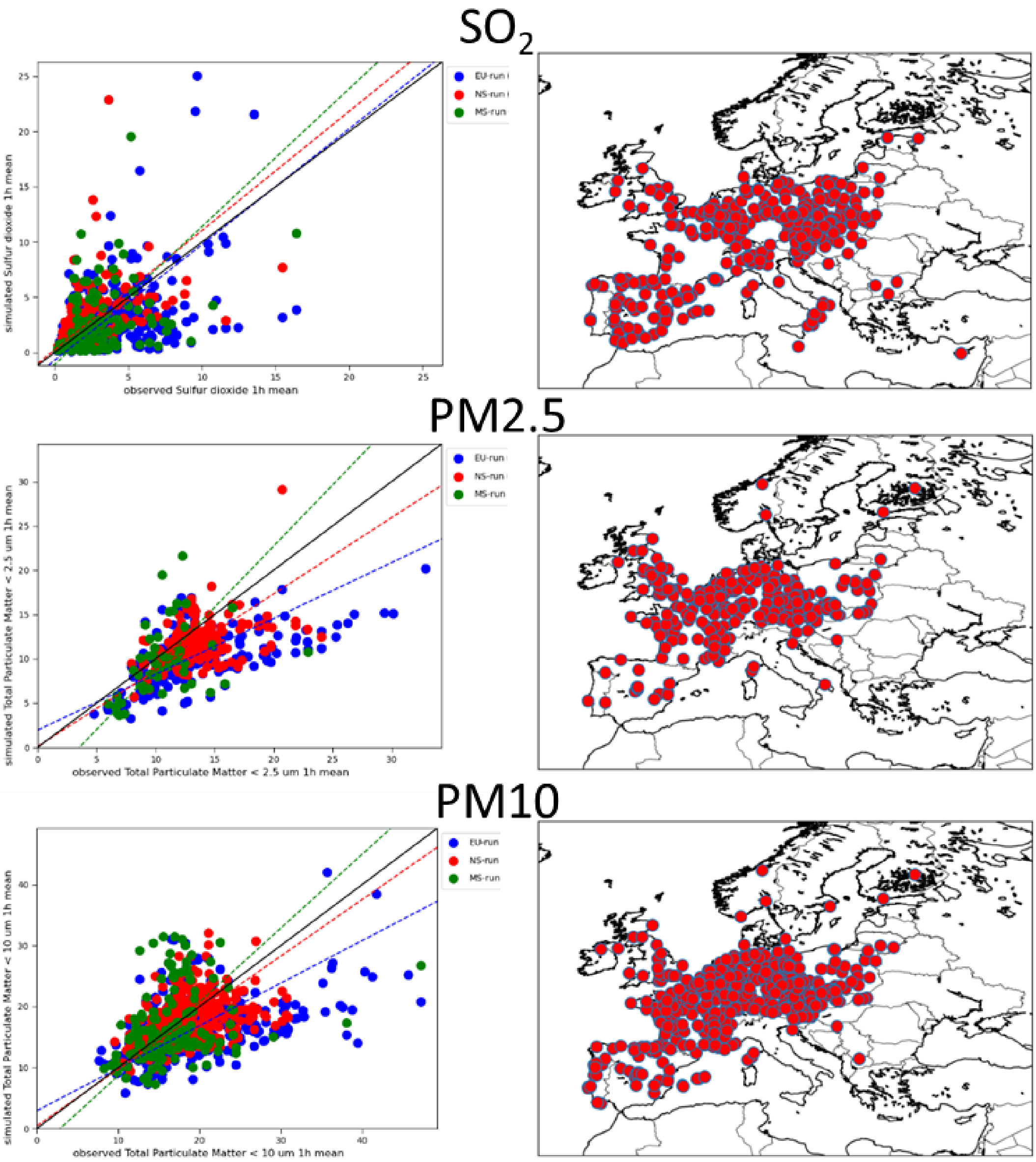

Figure 40 Observed vs modelled annual mean concentrations of SO_2 (top panel), $PM_{2.5}$ (middle panel) and PM_{10} (bottom panel) in 2018

7.6. METRICS FOR MODEL PERFORMANCE EVALUATION AND ASSESSMENT OF THE EXPONENTIAL DROP-OFF OF THE RELATIVE AVIATION CONTRIBUTION

7.6.1. Model evaluation metric

The modelled and observed concentrations are compared by multiple statistical measures. The normalized root mean square error (nRMSE) is the RMSE divided by the mean of the observations and can be interpreted as a fraction of the overall range that is typically resolved by the model. Next to this a Pearson correlation coefficient is computed to assess how well observed temporal variability in concentrations is captured by the model. Lastly, the slope of a linear regression fit of the modelled and observed concentrations is a measure of structural over- or underestimations of high or low concentrations. Ideally a 1-to-1 line is found indicating that (in combination with high correlation coefficients) the spread in measured and modelled concentrations are aligned. The mathematical formulations to compute the parameters of interest are as follows (overbars denote mean quantities):

Mean bias: $$Bias = \frac{1}{N}\sum(C_{model} - C_{observation})$$

Root mean square error‡: $$RMSE = \sqrt{\frac{1}{N}\sum(C_{model} - C_{observation})^2}$$

Temporal correlation: $$R^2 = \left(\frac{\sum(C_{model}-\overline{C_{model}})(C_{observation}-\overline{C_{observation}})}{\sqrt{\sum(C_{model}-\overline{C_{model}})^2\sum(C_{observation}-\overline{C_{observation}})^2}}\right)^2$$

In these equations C stands for the (modelled or observed) atmospheric concentration in µg/m^3 and N for the total number of data points considered.). The normalized RMSE is the RMSE divided by ($\overline{C_{observation}}$).

7.6.2. Exponential drop-off determination

To assess how far the influence of the emission from a specific airport are spread spatially, ten equidistantly spaced points were selected on a line between the airport and the cities centre. On the selected points the relative contribution from aviation was determined. This relative contribution was subsequently plotted against the distance from the airport and subsequently fitted with a single exponential decay function. The exponent indicates how quickly a reduction of e^{-1} (a reduction by 63%) of the relative contribution from aviation is reached. In the example of London in **Figure 41**, t=0.35 indicating that in ~2.8km (1/0.35) a reduction of the contribution from aviation with 63% is reached.

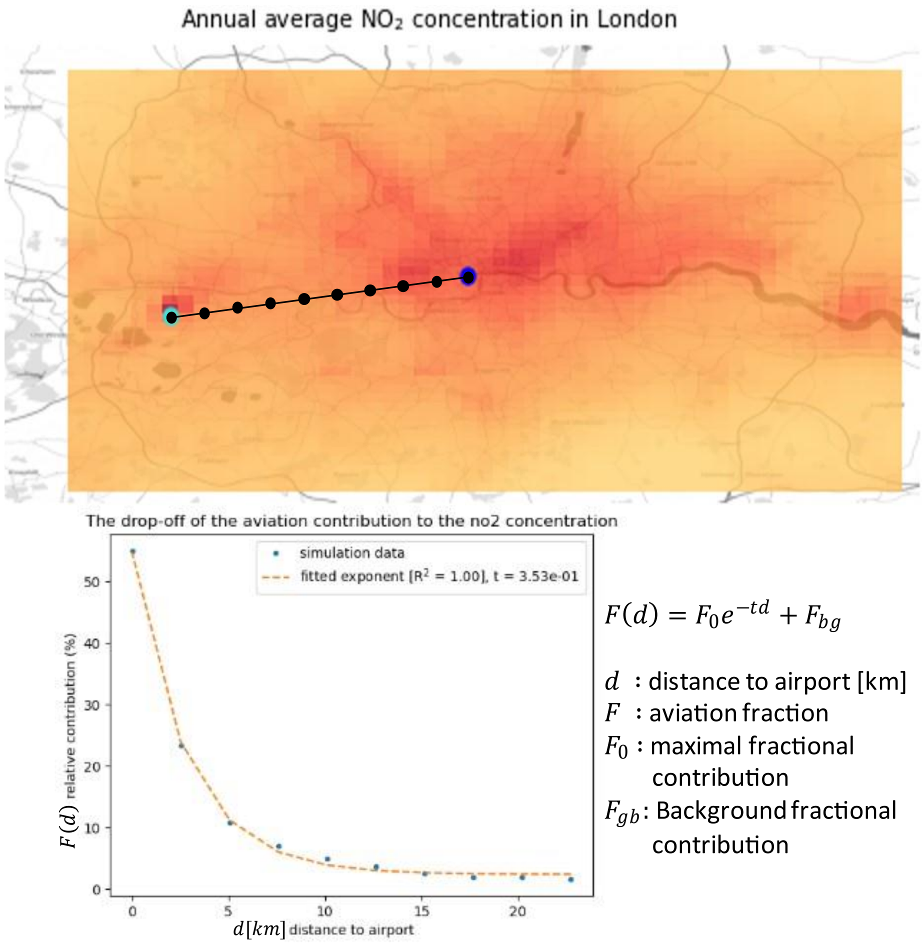

Figure 41 The exponential decay of the aviation contribution to the surface concentration as function of distance to the airport. At the 1/t distance the relative contribution from aviation is reduced by 63% with regard to its original relative contribution at the airport.

Table 12 The exponential decay fit parameters and quality for the six cities. * Refers to cities that are represented as point sources in the used emission dataset. ‡Refers to airports that are represented as surface sources taking the locations of the runways into account

	R^2 fit	t	1/t*
London*	1.00	0.353	2.8
Paris*	1.00	0.234	4.3
Amsterdam‡	1.00	0.239	4.2
Frankfurt am Main‡	0.97	0.204	4.9
Munich‡	1.00	0.204	4.9
Brussels*	1.00	0.550	1.8
Average	0.99	0.30	3.8

Environmental Science for European Refining

Concawe
Boulevard du Souverain 165
B-1160 Brussels
Belgium

Tel: +32-2-566 91 60
Fax: +32-2-566 91 81
e-mail: info@concawe.eu
http://www.concawe.eu

ISBN 978-2-87567-177-6